

EXPERIMENTAL STUDY OF THE PHENOMENON OF
LOCAL SCOUR AROUND BRIDGE PIERS

A Thesis

Submitted to

The Faculty of Graduate Studies

The University of Manitoba

In Partial Fulfillment

of the Requirements for the Degree
Master of Science in Civil Engineering

by

Nangantani Davies Godfrey Mtundu

Winnipeg, Manitoba

October, 1980

EXPERIMENTAL STUDY OF THE PHENOMENON OF
LOCAL SCOUR AROUND BRIDGE PIERS

BY

NANGANTANI DAVIES GODFREY MTUNDU

A thesis submitted to the Faculty of Graduate Studies of
the University of Manitoba in partial fulfillment of the requirements
of the degree of

MASTER OF SCIENCE

© 1980

Permission has been granted to the LIBRARY OF THE UNIVER-
SITY OF MANITOBA to lend or sell copies of this thesis, to
the NATIONAL LIBRARY OF CANADA to microfilm this
thesis and to lend or sell copies of the film, and UNIVERSITY
MICROFILMS to publish an abstract of this thesis.

The author reserves other publication rights, and neither the
thesis nor extensive extracts from it may be printed or other-
wise reproduced without the author's written permission.

ABSTRACT

The purpose of this study was to investigate the phenomenon of local scour around bridge piers and to develop functional relationships between the various parameters that influence the phenomenon. All the data used in the study were obtained from experiments conducted in a laboratory flume.

The study was limited to rectangular piers of length to width ratio of 5.3. All the piers essentially behaved as blunt-nosed and were in all tests aligned parallel to the flow. Subcritical, unidirectional and uniform flow conditions were maintained at Froude numbers ranging from 0.12 to 0.23. Only non-cohesive bed material (sand) was used and clear-water scour conditions were maintained by keeping the flow velocity below the threshold value for the initiation of sediment movement.

The results of this study indicated that a reduction of the bluntness of the pier nose reduces the scour potential when compared to a square-nosed pier which causes the deepest scour depths. The depth of flow was found to have negligible influence except for depths less than 2.6 pier widths. The depth of scour was found to vary linearly with the mean approach flow velocity.

ACKNOWLEDGEMENTS

The author is greatly indebted to Dr. Luis Magalhaés for his supervision and advice throughout this study and for his critical review of the manuscript. The critical comments and valuable suggestions for improvement of the thesis received from Professors Cass Booy and Jeffrey Tinkler are gratefully acknowledged.

The technical assistance of Mr. Stanley Kaskiw is acknowledged with the warmest appreciation. The author is also greatly indebted to Ms. Eileen Repeta for her support and utmost patience in the typing of this manuscript. The assistance of these people greatly facilitated the completion of this work. The inspirational support of Mr. Bruce Webb is also appreciated.

The author would also like to express his gratitude to the World Meteorological Organisation who, in conjunction with the Malawi Government, sponsored the author's five-year fellowship at this University.

Lastly, but certainly not least, I would like to express my utmost gratitude to my parents: to my father, Godfrey, for instilling in me the spirit to accomplish all my undertakings and to my mother, Evelyn, for her unfailing patience during my long absence from my homeland.

TABLE OF CONTENTS

<u>Chapter</u>		<u>Page</u>
	ABSTRACT	ii
	ACKNOWLEDGEMENTS	iii
	TABLE OF CONTENTS	iv
	LIST OF FIGURES	vi
	LIST OF TABLES	viii
	LIST OF PLATES	ix
	NOMENCLATURE AND DIMENSIONS	x
I	INTRODUCTION	1
	1.1 General Aspects of the Problem of Local Scour	1
	1.2 Purpose and Scope of Study	2
II	CATEGORIES OF SCOUR AT BRIDGE PIERS	4
	2.1 Scour and Degradation of Channel Bed	4
	2.2 Local Scour Due to Bridge Piers	5
III	MECHANISM OF LOCAL SCOUR AND THE SCOURING PROCESS	8
	3.1 Interaction Between Pier and Flow Field	8
	3.2 Blunt-Nosed Piers and the Horseshoe-Vortex System	8
	3.3 Sharp-Nosed Piers	9
	3.4 Other Vortex Systems	10
IV	EVALUATION OF LOCAL SCOUR	12
	4.1 General	12
	4.2 Analysis of Local Scour Parameters	12
	4.2.1 Variables Affecting Local Scour	12
	4.2.2 Dimensional Analysis	13
V	REVIEW OF PREVIOUS STUDIES ON LOCAL SCOUR	17
	5.1 General	17
	5.2 Experimental Studies	18
	5.3 Analytical Studies	21

<u>Chapter</u>		<u>Page</u>
VI	EXPERIMENTAL PROCEDURE AND OBSERVATIONS	26
	6.1 Experimental Apparatus	26
	6.2 Geometrical Characteristics of the Piers	27
	6.3 Bed-Material Characteristics	27
	6.4 Experimental Procedure	27
	6.5 Observations	29
VII	CORRELATION OF DATA AND DISCUSSION OF RESULTS	32
	7.1 Experimental Results	32
	7.2 Influence of Pier Shape	33
	7.3 Influence of the Depth of Flow	34
	7.4 Influence of the Mean Approach Flow Velocity	34
	7.5 Comparison with Previous Studies	38
	7.5.1 Influence of the Pier Shape	38
	7.5.2 Influence of the Depth of Flow	38
	7.5.3 Influence of the Mean Approach Flow Velocity	39
	7.6 Influences of the Pier Reynolds Number and the Pier Froude Number	41
VIII	PROTECTION AGAINST SCOUR	42
	8.1 General	42
	8.2 Rip-Rap Mats	42
	8.3 Foundation Caissons	45
	8.4 Piles Placed Upstream of Pier	45
IX	CONCLUSIONS AND RECOMMENDATIONS	46
	9.1 Limitations	46
	9.2 Influences of the Parameters Affecting Local Scour	46
	9.2.1 Pier Shape	46
	9.2.2 Depth of Flow	46
	9.2.3 Mean Approach Flow Velocity	47
	9.3 Recommendations for Future Studies	47
	BIBLIOGRAPHY	49
	APPENDIX A	51
	APPENDIX B	101
	APPENDIX C	106

LIST OF FIGURES

<u>Figure</u>		<u>Page</u>
2.1	Cross-Section at a Bridge Waterway Opening, Illustrating Scour Terminology	52
2.2	Variation of Scour Depth With Time	53
3.1	Horseshoe-Vortex on a Flat Bed	54
3.2	Features of Flow Around a Blunt-Nosed Pier	55
3.3	Flow Around a Sharp-Nosed Pier	56
5.1	Hincu's Experimental Results for Circular Piers	57
5.2	Experimental Results for a Circular Pier Presented by Alvarez and Bribiesca	57
5.3	Results of Equilibrium Scour Study	58
5.4	Scour Depth Versus Time for a Vertical Cylinder	58
5.5	Ratio of Maximum Depth of Scour to Average Depth of Flow Versus a Flow Parameter	59
5.6(a)	Euler-Reynolds Relations	60
5.6(b)	The Euler-Froude Function	60
5.6(c)	The Scour-Hole Depth Function	60
5.7	Experimental Results of Baker and Chabert and Engeldinger for Clear-water Scour	61
6.1	Geometrical Characteristics of Piers	62
6.2	The Particle Size Distribution Curve	63
6.3	Definition Sketch for Flow Around a Rectangular Pier	64
6.4	The Variation of Scour Depth with Time for Different Pier Shapes	65
7.1	Velocity Profiles at the Threshold of Sediment Movement	68
7.2	The Variation of Scour Depth with Time for Different Flow Conditions	69
7.3	The Influence of the Pier Shape	72
7.4	The Variation of Scour Depth with Time for Different Flow Depths	73
7.5	The Influence of the Depth of Flow	74

<u>Figure</u>		<u>Page</u>
7.6	The Influence of Velocity for the Round-Nosed Pier	75
7.7	The Influence of Velocity for the Square-Nosed Pier	79
7.8	The Influence of Velocity for the Triangular-Nosed Pier	83
7.9	Comparison of the Linear Regression Lines for the Different Pier Shapes	87
7.10	The 5-Hour Scour Depth Versus Longitudinal Extent of Scour for the Different Pier Shapes	90
7.11	Influence of the Mean Approach Flow Velocity: Square-Nosed Pier	93
7.12	Influence of the Mean Approach Flow Velocity: Triangular- Nosed Pier	96
7.13	Influence of the Mean Approach Flow Velocity: Round-Nosed Pier	97
8.1	Recommended Design Curve for Pier Rip-Rap	98
8.2	The Effect of Pier Footings on Local Scour	99
8.3	Piers Placed Upstream of Pier	100

LIST OF TABLES

<u>Table</u>		<u>Page</u>
7.1	Summary of Collected Data for the Round-Nosed Pier	102
7.2	Summary of Collected Data for the Square-Nosed Pier	103
7.3	Summary of Collected Data for the Triangular-Nosed Pier	105

LIST OF PLATES

<u>Plate</u>		<u>Page</u>
1(a)	View of the Scour Pattern from Upstream (TEST No. RN006)	107
1(b)	View of the Scour Pattern from Downstream (TEST No. RN006)	107
2(a)	View of the Scour Pattern from Upstream (TEST No. TN002)	108
2(b)	View of the Scour Pattern from Downstream (TEST No. TN002)	108
2(c)	View of the Scour Profile (TEST No. TN002)	109

NOMENCLATURE AND DIMENSIONS

<u>Symbol</u>	<u>Dimensions</u>	<u>Definition</u>
a_1, a_2, a_3	-	Coefficients in Scour-Depth Equation 5.9
a	L	$b/2$
b	L	Width of Pier (equivalent to diameter of pier in the case of a circular pier)
c	-	Pier Shape Factor
D	L	Characteristic Size of Sediment
DG	L	Equivalent to D_{50}
D_{15}	L	Sediment Size of Protective Layer of Rip-Rap at Which 15% by Weight is Finer (in Eq. 8.2)
D_{50}	L	Mean Grain Diameter of Sediment (sediment size at which 50% of material by weight is finer)
D_{50}	L	Sediment Size of Protective Layer of Rip-Rap at Which 50% by Weight is Finer (in Eq. 8.2)
d_0	L	Depth of Approach Flow
d_s	L	Depth of Scour
d_{se}	L	Equilibrium Depth of Scour
d_{sm}	L	Maximum Depth of Scour
d_{s3}	L	Depth of Scour After 3 Hours of Test Run
d_{s4}	L	Depth of Scour After 4 Hours of Test Run
d_{s5}	L	Depth of Scour After 5 Hours of Test Run

<u>Symbol</u>	<u>Dimensions</u>	<u>Definition</u>
d_{15}	L	Sediment Size of Protected Layer Under Rip-Rap at Which 15% by Weight is Finer (in Eq. 8.2)
d_{50}	L	Sediment Size of Protected Layer Under Rip-Rap at Which 50% by Weight is Finer (in Eq. 8.2)
d_{85}	L	Sediment Size of Protected Layer Under Rip-Rap at Which 85% by Weight is Finer (in Eq. 8.2)
Eu^*	-	Scour Euler Number ($= U/\sqrt{2gd_s}$)
F	-	Equivalent to Fr
FRD	-	Equivalent to Fr
Fr	-	Froude Number of Approach Flow ($= U/\sqrt{gd_0}$)
Fr^*	-	Pier Froude Number ($= U/\sqrt{gb}$)
G	-	$\frac{\left[\left(\frac{\rho_s}{\rho} \right) - 1 \right] g D_{50}^3}{v^2}$
G_s	-	Specific Gravity of Sediment
g	$\frac{L}{T^2}$	Acceleration Due to Gravity
H	L	Equivalent to d_0
h_0	L	Equivalent to d_0
k	L	Equivalent Sand Roughness Size
k	-	A Constant in Equation 5.2
Le	L	Longitudinal Extent of Scour Hole
l	L	Length of Pier

<u>Symbol</u>	<u>Dimensions</u>	<u>Definition</u>
N_s	-	Sediment Number $(= \frac{U}{\sqrt{(s-1)gD_{50}}})$
N_{sc}	-	Lowest Value of the Sediment Number for Which Scour Will Occur
Q_s	L^3	Solid Volume of Sediment Removed From Scour Hole
q_{s1}	$\frac{L^3}{T}$	Capacity of Flow to Transport Sediment Out of Scour Hole
q_{s2}	$\frac{L^3}{T}$	Rate of Sediment Supply to Scour Hole
Re^*	-	Pier Reynolds Number $(= \frac{Ub}{\nu})$
RNP	-	Round-Nosed Pier
SG	-	Equivalent to S
SNP	-	Square-Nosed Pier
S_0	-	Slope of Channel Bed
s	-	Ratio of Solids Density to Fluid Density $(= G_s)$
TNP	-	Triangular-Nosed Pier
t	T	Time
U	$\frac{L}{T}$	Mean Velocity of Undisturbed Approach Flow
U_c	$\frac{L}{T}$	Threshold or Critical Velocity for Initiation of Movement of Undisturbed Bed Material
VMC	$\frac{L}{T}$	Mean Velocity of Approach Flow at the First Displacement of a Grain or Grains on Rip-Rap Around the Pier
Y	L	Equivalent to d_0

<u>Symbol</u>	<u>Dimensions</u>	<u>Definition</u>
y	L	Equivalent to d_s
z	L	Equivalent to b
α	-	Angle of Attack
β	-	Wedge Angle of a Sharp-Nosed Pier
γ	$\frac{F}{L^3}$	Specific Weight of Fluid
γ'_s	$\frac{F}{L^3}$	Submerged Specific Weight of Sediment Grains
μ	$\frac{FT}{L^2}$	Dynamic Viscosity of Fluid
ν	$\frac{L^2}{T}$	Kinematic Viscosity of Fluid
ρ	$\frac{FT^2}{L^4}$	Density of Fluid
ρ_s	$\frac{FT^2}{L^4}$	Density of Sediment
ϕ	-	Angle of Repose

CHAPTER I

INTRODUCTION

1.1 General Aspects of the Problem of Local Scour

Local scour is defined as the abrupt lowering of the streambed in the vicinity of a hydraulic structure. In the specific case of a bridge pier, the scour is due to the erosion of the bed material by the local flow structure induced by the pier. The flow structure itself consists of eddies which are generated by the significant changes in the direction of the flow caused by the pier.

Many of the bridge failures in the past were largely attributed to the undermining of the foundations of piers and/or abutments by scour holes created by the flowing water. Consequently, early bridge designers often over-designed their bridge foundations to circumvent this hydraulically related problem. Common methods of design often comprised erecting massive piers and abutments, aligned across long-crossings, usually with very short spans, and selecting bridge sites in relatively straight reaches with stable banks. However, a lot of these early methods of combating the scour problem met with only limited success. One major flaw was failure to recognise the fact that any obstruction placed in a stream modified the flow pattern in the vicinity of that obstruction, thereby causing severe scour to occur, and pier massiveness only contributed to an enhancement of the problem. Additionally, but not as severe, scour occurred when the designers placed the piers at such a spacing as to cause extreme contractions to the flow sections, resulting in streambed scour due to higher induced velocities.

A pier will obviously have an increased factor of safety from scour if it is based on a firm bedrock. However, such a foundation, albeit

desirable, is not often economically feasible, particularly in alluvial streams where access to a solid geological formation may require unjustifiably excessive excavations. It is clear, therefore, that in order to avoid over- or under-design of the foundations of piers in an erodible bed, it is necessary to know the maximum depth which will be reached by the scouring process. This, in turn, requires the understanding of the mechanism of local scour. Clearly, this understanding will not only facilitate the evaluation of potential scour depths, but will, in addition, lead to the development of methods to be adopted in the design of pier foundations to accommodate the scour, to reduce its magnitude, or to eliminate it completely; the choice as to what extent this is carried out will undoubtedly be dictated by economic analyses.

1.2 Purpose and Scope of Study

The phenomenon of local scour is among the many fields of sediment transport where the processes of water and sediment movement are very complicated. Given the overall complexity and multiplicity of the factors influencing local scour, it is not surprising that no entirely satisfactory theoretical solution of the scour problem has yet evolved. One obvious approach to the evolution of predictive principles is to conduct an experimental study. This has the advantage of exercising separate control over each of the individual factors affecting the phenomenon, once they have been recognised. The influence of each of the various factors is, therefore, sorted out from the total phenomenon.

Many studies of local scour have been conducted by various investigators previously. The results from these studies, however, have not always been in complete agreement. Experimental data have, in some cases,

been regarded as inadequate and data from different sources have, many times, been in conflict. The present trend, however, appears to be in the direction of unanimity as regards the important parameters governing local scour.

The object of this research reflects a continuing effort in the attempts to provide more experimental data on local scour, with the hope that, coupled with certain theoretical approximations, functional relationships between the various parameters might be developed.

This study was limited to the following conditions:

- (i) rectangular piers with length to width ratio of 5.33; for each pier both the nose and the tail were of the same shape; three shapes were investigated, namely round, square and triangular; the length and width dimensions were the same for all piers.
- (ii) subcritical, unidirectional and uniform flow conditions.
- (iii) non-cohesive granular bed material (sand).
- (iv) clear-water scour which, herein, refers to the condition in which the bed material upstream of the pier is undisturbed and, therefore, the flow of sediment into the scour hole is zero; in other words, movement of sediment begins in the vicinity of the pier and proceeds downstream therefrom.
- (v) zero angle of attack; each pier had its major axis aligned with the main direction of flow.

CHAPTER II

CATEGORIES OF SCOUR AT BRIDGE PIERS

2.1 Scour and Degradation of Channel Bed

General degradation of an alluvial channel bed is usually a combination of local scour and other forms of scour. The term "scour", by itself, is used to mean

'a lowering by erosion of the channel bed below an assumed natural level or other appropriate datum, tending to expose or undermine foundations that would otherwise remain buried' (Neill, 1973).¹

There are several interrelated factors which may lead to the lowering of the channel bed at a bridge pier site leading, therefore, to the following categorization of scour:

- (i) Degradation, Temporary or Progressive is associated with a change of river regimes due to natural geological processes or induced by man's activities either upstream or downstream from the bridge site; thus, a river may change from a meandering to a braided one.
- (ii) Natural Scour in alluvial channels is associated with variations in flow conditions and changes in sediment supply. This results in temporary or progressive shifting of the thalweg (the deepest flow depth in a river section), bed-form migration and channel shifting. Thus a small channel within the main channel that shifts its course closer to a pier will lower the bed elevation adjacent to the pier.
- (iii) General Scour is associated with the constriction of the flow section. Bridge piers contract the width of the channel, hence reducing the net waterway area. This results in an increase in

¹ All the technical literature is listed in the Bibliography at the end of the main text.

the flow velocity under the bridge and hence the scouring capability of the flow.

- (iv) Local Scour around the piers is caused by local flow disturbances (vortices or eddies) induced by the piers themselves. These disturbances are a result of the abrupt change in the direction of flow caused by the piers.

The progressive or temporary degradation and the natural scour usually occur over relatively long reaches and over long time spans. The first three factors may cause the elevation of the entire bed to be lowered. Local scour, however, is confined only to the vicinity of a pier and may occur in conjunction with or in the absence of any one, two or all the other factors. General and local scour are illustrated in Fig. 2.1.¹

Inasmuch as the four forms of scour described in the preceding paragraph are caused by entirely different phenomena, it is virtually impossible to single out the influence of each of the various factors from the total scour phenomenon. By the same token, it is prohibitive to find a single criterion to predict the magnitude of the scour due to their combined effect near each pier. However, by carefully studying each factor, estimates of their contributions to the total scour can be made. This study is restricted to the phenomenon of local scour only.

2.2 Local Scour Due to Bridge Piers

Local scour is, as defined in an earlier section, the abrupt decrease in bed elevation in the immediate vicinity of a pier due to erosion of bed material by the local flow structure induced by the pier. Local scour

¹ All figures are to be found after the main text.

is the most important cause of a decrease in bed elevation and has been extensively studied both in the past and recently, and is still being investigated upon today. Besides its severity, another reason why it has received the most attention is that it is most conveniently studied with the aid of hydraulic models. The other forms of scour, on the other hand, are more complex in nature and difficult to model for the purposes of laboratory study; it is also apparent that their severity is not significant enough to warrant the often expensive model studies.

Three classes of local scour may be identified by considering the amount of sediment transported into and out of the scour hole:

- (i) Stable Scour: The local disturbances caused by the pier result in a scour hole of a certain magnitude, after which there is no additional scour, a condition which is established when the sediment discharge into the hole is equal to the sediment discharge out of the hole. The condition of "no scour", whereby both sediment discharges are zero may also be classified as stable scour.
- (ii) Clear-water Scour: The rate at which sediment is supplied to the scour hole by the approach flow is zero, but the capacity of the flow to transport sediment out of the hole is greater than zero. The flow then continues to erode the scoured zone, increasing the depth of scour with time until a limiting rate of scour is approached asymptotically.
- (iii) Scour with Continuous Sediment Supply: The inflow of sediment from upstream may be smaller or greater than the rate of sediment removal from the scour hole. If the sediment supply discharge is greater than the amount being eroded away from the scour hole

the depth of scour will decrease with time. Conversely, the reverse situation will occur when the supply rate is less than the erosion rate and the depth of scour will increase, reach a maximum and eventually vary aperiodically with time about an equilibrium value due to the passage of dunes through the scoured zone.

The distinction between Cases (ii) and (iii) is shown in Fig. 2.2.

The scouring processes described above are conveniently represented by the following relationship suggested by Laursen (1952):

$$[2.1] \quad \frac{dQ_s}{dt} = q_{s1} - q_{s2}$$

wherein $\frac{dQ_s}{dt}$ is the rate of local scour in volume per unit time; q_{s1} is the capacity of the flow to transport sediment out of the scour hole in volume per unit time; and q_{s2} is the rate at which sediment is supplied to the scour hole by the undisturbed flow. With this relationship the three cases are then summarized as follows:

- (i) $q_{s1} = q_{s2} = C$ represents stable scour. When $C = 0$ there is no scour.
- (ii) $q_{s1} \gg q_{s2} \approx 0$ represents clear-water scour.
- (iii) $q_{s1} \geq q_{s2} > 0$ or $q_{s1} \leq q_{s2} > 0$ represents scour with continuous sediment supply.

This study was limited to case (ii) of clear-water scour.

CHAPTER III

MECHANISM OF LOCAL SCOUR AND THE SCOURING PROCESS

3.1 Interaction Between Pier and Flow Field

Local scour at a bridge pier is caused by a system of vortices or eddies which develop around the pier. Depending on the type of pier and free-stream conditions, the eddy-structure near a pier can be composed of any, all, or none of the following three basic systems: the horseshoe-vortex system, the wake-vortex system and the trailing-vortex system (Roper et al, 1967). The so-called "horseshoe" vortex system is, however, the dominant cause of scour at the nose of a bridge pier. The axis of this vortex is horizontal and the term "horseshoe" is derived from the shape that the vortex system takes as it wraps around the upstream base of the pier and tails downstream (see Fig. 3.1).

The magnitude of a locally scoured hole depends, among other factors, on the shape of the pier as it reflects the strength of the horseshoe-vortex at the base of the pier. Depending on the geometry and the angle of attack of the undisturbed flow piers are, therefore, classified as either blunt-nosed or sharp-nosed (Breusers et al, 1977). The three pier shapes investigated in this study all behaved as blunt-nosed in this sense.

3.2 Blunt-Nosed Piers and the Horseshoe-Vortex System

A blunt-nosed pier causes the greatest scour depth as it induces a horseshoe-vortex of the greatest strength. Tison (1961) attributed the formation of the horseshoe-vortex to the downward flow in the front of the pier; he showed that this vertical velocity component existed as a result of the horizontal curvature of the streamlines in front of the pier and the reduced velocity near the bed by friction. Shen and others (1966), however, have stated that the mechanism which forms the horseshoe

vortex system is a pressure field induced by the pier. If the pressure field is sufficiently strong the approaching boundary layer separates ahead of the pier and rolls up to form the horseshoe-vortex, as illustrated in Fig. 3.1 for a circular pier. A sufficiently large pressure gradient is required to initiate this process and a blunt-nosed pier is defined as one capable of inducing such a pressure field.

In the vicinity of a blunt-nosed pier scour begins when the horseshoe-vortex system develops enough shear stress to dislodge and suspend the bed material. The combined actions of the vortex and the convergence of streamlines due to increased horizontal velocity near the pier then carries the scoured material a short distance downstream with the flow, that is, until the action of viscosity and/or adverse pressure gradients sufficiently dissipate the vortex system.

As the scouring process continues, the material adjacent to the scour hole starts to slide into the hole as a result of reduced lateral support. With time, the scour hole extends both downwards and outwards due to the complementary processes of material removal and sliding. Eventually the whole process tends to equilibrium.

At equilibrium the shear stress developed in the scoured zone is no longer sufficient to move the bed material. In cases where there is general sediment movement on the bed (live-bed situations) the equilibrium condition would be characterized by equal rates of sediment supply to and sediment removal from the scour hole.

3.3 Sharp-Nosed Piers

A sharp-nosed pier is defined as one which causes only a weak separation of the boundary layer on approaching the pier, and hence prevents the formation of a strong horseshoe-vortex system. This type of

pier is illustrated in Fig. 3.3. The curvature of the flow streamlines near the upstream end of the pier is said to be the major factor that determines the magnitude and, also, the location of maximum scour when the major axis of the pier is aligned with the flow (Shen et al, 1966). Thus streamlining the front end of the pier reduces the strength of the horseshoe-vortex, thereby reducing the scour. However, a sharp-nosed pier in straight flow could behave like a blunt-nosed pier if the flow is at an angle of attack. For instance, a sharp-nosed pier aligned at a skewed angle with the flow has been observed by Roper et al (1967) to induce a strong horseshoe-vortex system and develop a large scour hole at the nose of the pier as a result.

3.4 Other Vortex Systems

The wake-vortex system has a vertical axis and develops because of partial blockage of the flow by the pier (Simons and Şentürk, 1977). As outlined by Roper and others (1967) the wake-vortex system is formed by the rolling up of the unstable shear layers generated at the surface of the pier. These shear layers are then shed alternately from the pier and convected downstream. The strength of the wake-vortex system depends on the pressure gradients over the rear whose strength is in turn dependent on the shape of the tail of the pier. The wake system suspends the scoured material which is then carried a limited distance downstream from the pier. For most piers, however, very little additional scouring is caused by wake vortices.

The other type of vortex system is called the trailing-vortex system.

'The trailing-vortex system usually occurs only on completely submerged piers and is similar to that which occurs at the tips of finite lifting surfaces in finite wing theory. It is composed of one or

more discrete vortices attached to the top of the pier and extending downstream. These vortices form when finite pressure differences exist between two surfaces meeting at a corner, such as at the top of the pier.'

(Breusers et al, 1977)

Again, this system of vortices contributes little or no scouring in addition to that caused by the horseshoe-vortex system.

CHAPTER IV

EVALUATION OF LOCAL SCOUR

4.1 General

Local scour is a function of a multiple of interrelated factors involving complex water and sediment movement processes. The number and complexity of these factors is such that prediction of the value of potential scour continues to defy rigorous mathematical analysis. A satisfactory theoretical analysis would probably have to await the development of a model for computing the velocity field and the related local sediment-transport phenomena in the scour hole. As of yet the attempts that have been made in this direction are, at best, explanatory only in view of the underlying assumptions.

Inasmuch as an exhaustive theoretical solution seems illusory under the above circumstances, present knowledge of the scour problem appears to be limited to experimental observations and theoretical approximations. Dimensional analysis, complemented with correlation of experimental data, seems therefore, to provide the only avenue leading to the derivation of pertinent local scour relationships.

4.2 Analysis of Local Scour Parameters

4.2.1 Variables Affecting Local Scour

There are many parameters which may influence the scouring phenomenon. For the purposes of this study, in which the assumption of steady and uniform flow is perfectly valid and in which consideration is limited to the case of an isolated bridge pier, the following parameters may be listed:

- (i) Characteristics of the fluid:
 - a. - density, ρ
 - b. - kinematic viscosity, ν
- (ii) Characteristics of the bed material:
 - a. - density of sediment, ρ_s
 - b. - size distribution
 - c. - grain form
 - d. - cohesion
- (iii) Characteristics of the flow:
 - a. - approach flow depth, d_0
 - b. - mean velocity of undisturbed flow, U
 - c. - roughness of channel bed, k
 - d. - slope of channel bed, S_0
- (iv) Characteristics of the pier:
 - a. - shape, c
 - b. - dimensions, b and l
 - c. - surface condition
 - d. - angle of attack or position of pier in relation to the direction of flow, α
- (v) Other Characteristics:
 - a. - acceleration due to gravity, g
 - b. - time, as it reflects the stage of scour, t

4.2.2 Dimensional Analysis

For purposes of analysis, certain restrictive conditions have to be imposed on some of the variables and consideration has to be limited to the quantifiable variables. Under such restrictive conditions the pertinent variables may be reduced to the following:

- (i) fluid density, ρ
- (ii) fluid kinematic viscosity, ν
- (iii) acceleration due to gravity, g
- (iv) density of sediment, ρ_s
- (v) mean size of sediment, conveniently represented by the mean grain diameter, D_{50}
- (vi) depth of approach flow, d_0
- (vii) mean velocity of approach flow, U
- (viii) width of pier, b
- (ix) shape of pier, c

In addition, the bed material was restricted to non-cohesive sediment, and the flow to a flat bed without dunes or ripples (fixed-bed condition).

The piers studied were all rectangular with smooth or smoothed surfaces.

The shapes of pier noses and tails were rounded, square and triangular.

The variable which is of paramount interest in the study of local scour is the depth of scour, d_s . When the significant variables are included in a functional relationship, we have:

$$[4.1] \quad d_s = f_1 (\rho, \nu, g, D_{50}, \rho_s, d_0, U, b, c)$$

where the force, length and time dimensions are listed in the nomenclature (pages x to xiii).

The Buckingham Π theorem then permits us to reduce the number of separate variables of Eq. 4.1 to a smaller number of dimensionless groups in the following systematic manner:

Eliminating the force and time dimensions leads to:

$$[4.2] \quad d_s = f_2 \left(\frac{\rho_s}{\rho}, \frac{U}{\nu}, \frac{U}{\sqrt{g}}, D_{50}, d_0, b, c \right) .$$

Without any loss of generality the specific density term, ρ_s/ρ can be replaced by the relative submerged density, $(\rho_s/\rho) - 1$, which arises frequently in sediment transport phenomena when the equilibrium of forces on sediment particles is considered. Hence,

$$[4.3] \quad d_s = f_3 \left(\frac{\rho_s}{\rho} - 1, \frac{U}{v}, \frac{U}{\sqrt{g}}, D_{50}, d_0, b, c \right) .$$

The most usual and appropriate way to non-dimensionalize the scour depth is through the use of the ratio $\frac{d_s}{b}$; this ratio permits one to establish the stage of the scour-hole development. Hence,

$$[4.4] \quad \frac{d_s}{b} = \phi \left(\frac{\rho_s}{\rho} - 1, \frac{Ub}{v}, \frac{U}{\sqrt{gb}}, \frac{D_{50}}{b}, \frac{d_0}{b}, c \right) .$$

The use of the variable b in non-dimensionalising the scour depth might appear arbitrary since the variable d_0 , for instance, could have been selected without any loss of generality. However, a number of arguments might be raised in favour of the selection of the variable b . Firstly, of the non-dimensional groups used to describe scour at least one group must contain a parameter or parameters describing the interaction of the pier and the flow. The use of the variable b duly satisfies this requirement. The use of the depth variable d_0 would, on the other hand, lead to the parameters $\frac{U}{\sqrt{gd_0}}$ and $\frac{Ud_0}{v}$ which are respectively the Froude and Reynoldsnumbers characterizing the flow only. Furthermore, the relative importance of the parameters $\frac{b}{d_0}$ and the Froude number (Fr) of flow in the equation that would result through the use of d_0 would be vulnerable to criticism due to the confounding of the two effects by the common dependence on the upstream depth (Henderson, 1966). Inasmuch

as a rational functional relationship must of necessity contain independent dimensionless groups of variables, the effect of $\frac{b}{d_0}$ and Fr would not be considered independent since the parameters would tend to vary simultaneously in a correlated manner when the depth was varied.

In the present study, an attempt was made to correlate, using experimental data, the parameters indicated in Eq. 4.4. The parameters $\frac{U_b}{\nu}$ and $\frac{U}{\sqrt{gb}}$ are herein, subsequently, referred to as the pier Reynolds number (Re*) and the pier Froude number (Fr*) respectively.

CHAPTER V

REVIEW OF PREVIOUS STUDIES ON LOCAL SCOUR

5.1 General

There are literally hundreds of references pertaining either directly or indirectly to the basic understanding of local scour phenomena. For instance, a comprehensive list of assorted references (more than three hundred), each with a brief abstract were published by Karaki and Haynie (1963). Most of these studies were confined to laboratory experiments, where the velocities were, for the most part, below or at the critical velocity for initiation of sediment motion (clear-water scour). However, due to the complex nature of local scour phenomena, experimental data from different sources have often been either incomplete or conflicting and to date no generally accepted criteria for predicting local scour are existent.

Despite the necessity of field data to augment the knowledge gained from small-scale experiments, it is, perhaps, very unfortunate that the availability of such data is still limited. However, this limitation is not entirely regrettable since even well-documented data that have been collected from prototype studies are often difficult to analyze due to the manifold variation exhibited by the flow of individual streams, variability of bed material and complicated geometrical pier shapes. Another complication arises from the fact that a scour hole that rapidly develops during a flood may fill up again as the flood waters recede; therefore post-flood-recession data might not necessarily reflect the maximum scour depth reached during the scouring process.

The review on prototype studies will not be presented herein as the main concern in this study is on model studies. However, excellent reviews can be found in the publications by Breusers et al (1977) and Neill (1964).

5.2 Experimental Studies

The influence of velocity has been reported by a good number of previous investigators on local scour. For instance, Tison (1961), in summarizing his results, mentioned that the velocity profile exerted some influence on the maximum local scour depth and that the curvature of flow streamlines at the upstream end of the pier was responsible for causing secondary vertical currents and local scour.

Breusers et al (1977) have cited the work of Chabert and Engeldinger who distinguished two regimes in their study on the influence of flow velocity: for velocities at or below the threshold velocity for the initiation of movement of bed material the depth of scour approached a limit asymptotically, as illustrated in Fig. 2.2(a), whereas for velocities above the threshold value the scour depth oscillated aperiodically due to the passage of dunes through the scoured zone (Fig. 2.2(b)). Chabert and Engeldinger also observed that scouring started at about one-half the threshold velocity and that maximum scour was obtained at velocities near the threshold value.

Laursen and Toch (1953, 1956) concluded from their studies that there was no systematic influence of velocity on local scour in the range studied. Their studies must have been conducted at velocities above the threshold value since they observed that the depth of scour varied with time due to the aperiodic dumping of sediment into the scour holes by dunes moving past the scoured zones.

Breusers et al (1977) have also reported the work done by Hincu who found that the scour depth was constant ($d_s = d_{sm}$) above a certain velocity (U_c). At lower velocities the following linear relationship was obtained:

$$[5.1] \quad \frac{d_s(U)}{d_{sm}} = \left(\frac{2U}{U_c} - 1 \right)$$

as shown in Fig. 5.1. As reported by Breusers et al (1977), a linear increase of scour depth with velocity for velocities below the threshold value was also observed by Alvarez and Bribiesca, as shown in Fig. 5.2. Breusers et al (1977) also cite the results found by Nicollet on the velocity for the initiation of scour, whose ratio to the threshold velocity (U_c) was observed to be 0.42 to 0.53 for a circular pier and 0.50 to 0.65 for round-nosed piers.

In most reported studies on the influence of shape, a well-streamlined pier was always found to reduce scour. In the comprehensive list of abstracts compiled by Karaki and Haynie (1963) it is mentioned that Flamant discussed the experimental work on local scour by Durand-Claye who compared the scour for square-nosed, round-nosed and triangular-nosed rectangular piers. The experiments indicated that the square-nosed pier caused the deepest scour whereas the triangular-nosed pier resulted in a comparatively most reduced depth of scour.

Tison (1961) found that a lenticular pier whose thickness was gradually increased from 5.3 cm at the water surface to 8.1 cm near the bed resulted in a reduction in the depth of scour of 2.5 cm, whereas a flared pier with a wide base gave very little scour under the same conditions. The maximum scour depth was observed to occur at the upstream nose for the rectangular pier and at the sides for the streamlined shapes.

The length of a rectangular pier at zero angle of attack was found to have an insignificant influence.

In the extensive programme of study by Chabert and Engeldinger, another aspect of local scour that was investigated on was the effect of pier width (Breusers et al, 1977). Experiments showed that the depth of scour increased with the width of the pier as b^α in which $\alpha \leq 1$. Other results showed that at zero angle of attack, streamlining the pier reduced the potential depth of scour, but that this advantage could no longer be capitalized at angles of attack above 10° .

Laursen and Toch (1956) concluded from their studies that the depth of scour depended on the depth of flow (d_0), the shape (c) and the width (b) of the pier, and that the influences of grain size and velocity were insignificant, as shown in Fig. 5.3.

The conclusion drawn from the experimental results obtained by Varzeliotis, cited by Neill (1964), was that, in the range of mean velocity used (0.40 to 0.58 m/s) the depth of scour increased slowly with depth of flow up to $\frac{d_0}{b}$ equal to 2 to 3. The length of a round-nosed pier was also observed to exert no influence on the scour depth for zero angle of attack and length/width (l/b) ratios of 1 to 20.

Tarras analyzed the data obtained by Chabert and Engeldinger (quoted from Breusers et al, 1977), and concentrating on the maximum scour depth near the threshold velocity of the undisturbed bed material, the following relationship was derived:

$$[5.2] \quad d_{sm} = 1.05 kb^{0.75} \quad (\text{S.I. units})$$

in which $k = 1.0$ for a circular pier and 1.4 for a rectangular pier.

Tables were also given showing the influence of pier shape, and using a

circular pier as a basis, it was found that lenticular shapes produced a relative scour depth of 0.75, elliptical shapes 0.85, rounded piers 1.0 and rectangular piers 1.1 to 1.4 at zero angle of attack.

The report by Breusers et al (1977) also indicates that Hincú found that the influence of the depth of flow was negligible for $\frac{d_0}{b} > 1$ and that d_{sm} increased with grain size. In this case the results were correlated with the expression:

$$[5.3] \quad \frac{d_{sm}}{b} = 2.42 \left(\frac{U_c^2}{gb} \right)^{1/3} \quad \text{for } 0.05 \leq \frac{U_c^2}{gb} \leq 0.6 .$$

With a relation given for U_c as a function of g , D , ρ_s , ρ , and d_0 , Breusers et al (1977) have stated that, for natural sands, the relation may be converted into:

$$[5.4] \quad \frac{d_{sm}}{b} = 3.3 \left(\frac{D_{50}}{b} \right)^{0.2} \left(\frac{d_0}{b} \right)^{0.13} .$$

5.3 Analytical Studies

Cartsens (1966) developed similarity criteria for localized scour. The approach adopted in this study involved, firstly, the formulation of sediment-transport functions of localized scour which were then integrated to obtain scour-depth functions. The principal assumption in the derivation of the scour-depth functions was that the velocity and velocity distribution in areas of active local scour were functions only of the geometry of the obstruction and the scour hole. Analysis was made for flow situations free from gravity waves, sediment inflow from upstream and extraneous influences on the flow pattern such as dunes passing through the scour hole. For scour around a vertical cylinder the following scour-depth function was derived:

$$\begin{aligned}
 [5.5] \quad & 4.14 \times 10^{-6} (N_s^2 - N_{sc}^2)^{5/2} \left(\frac{D_{50}}{b}\right) \left(\frac{Ut}{b}\right) = \\
 & \frac{(d_s/b)^5}{\tan\phi} + \frac{(d_s/b)^4}{16} - \frac{\tan\phi (d_s/b)^3}{24} + \frac{\tan\phi (d_s/b)^2}{32} \\
 & - \frac{\tan^3\phi (d_s/b)}{32} + \frac{\tan^4\phi}{64} \ln \left(\frac{2(d_s/b)}{\tan\phi} + 1\right)
 \end{aligned}$$

where $N_s = \frac{U}{\sqrt{(s-1)gD_{50}}}$.

N_s , defined as the sediment number, was derived from a consideration of the forces acting on a typical particle on the bed surface (drag and lift forces versus the stabilizing force of the effective weight of the particle).

N_{sc} was then defined as the lowest value of the sediment number for which scour would occur. The scour-depth function, Eq. 5.5, as well as some experimentally-determined results are shown in Fig. 5.4. Eq. 5.5 is valid for clear-water scour conditions only.

Shen et al (1966) investigated the magnitude of maximum scour analytically using the momentum principle, by attempting to integrate the Navier-Stokes equation in the boundary layer in the scour hole, and by attempting to specify the relation between the strength of the horseshoe-vortex and local scour. This analysis led to the conclusion that the circulation of the horseshoe-vortex was proportional to $\frac{Ub}{2}$. Further analytical consideration of the behaviour of flow in the vicinity of the pier led to the conclusion that the strength of the vortex could be expressed as a function of the pier Reynolds number (Re^*). From the hypothesis that the maximum scour depth was related to the vortex strength, the conclusion was made that the maximum scour depth could be expressed

as a function of the pier Reynolds number. From a combination of experimental data from a number of sources, the following regime-type relation, shown in Fig. 5.5, was deduced:

$$[5.6a] \quad \frac{d_{sm}}{d_0} = 2 \left[Fr^2 (b/d_0)^3 \right]^{0.215}$$

Eq. 5.6(a) can alternatively be written as:

$$[5.6b] \quad \frac{d_{sm}}{b} = 2Fr^{0.43} (d_0/b)^{0.355} .$$

Coleman (1971) analyzed laboratory data under conditions of continuous sediment transport from experiments conducted on a circular cylinder. From these data the conclusion was made that the scour Euler number (Eu^*) was a parametric function of the pier Reynolds number, as in the following equation:

$$[5.7a] \quad \frac{U}{(2gd_s)^{1/2}} = A \left(\frac{\rho Ub}{\mu} \right)^{9/10}$$

where the parameter of the function was written in terms of the fluid properties, the pier diameter and the gravity field strength, as in the equation:

$$[5.7b] \quad A = 0.6 \left(\frac{\mu}{\rho g^{1/2} b^{3/2}} \right)^{9/10}$$

The introduction of the value of A into Eq. 5.7(a) enabled the Euler-Reynolds functions to be collapsed into a single function relating the scour Euler number and the pier Froude number, as in the equation:

$$[5.8a] \quad \frac{U}{(2gd_s)^{1/2}} = 0.6 \left[\frac{U}{(gb)^{1/2}} \right]^{9/10} .$$

By solving Eq. 5.8(a) for d_s , the following equation resulted:

$$[5.8b] \quad d_s = 1.49 b^{9/10} \left(\frac{U^2}{2g} \right)^{1/10} .$$

This correlation reduces to

$$[5.8c] \quad \begin{aligned} \frac{d_s}{b} &= 1.49 \left(\frac{U^2}{2gb} \right)^{1/10} \\ &= 1.39 (Fr^*)^{1/5} \end{aligned}$$

The relations found by Coleman (1971) are summarized in Fig. 5.6.

Baker (1980) recently developed a theoretical model which provides a basis for semi-empirical correlation of the variation of the equilibrium scour depth upstream of a circular cylinder in a bed of sand, with the various flow parameters for clear-water scour. His derivations were based on assumptions made about the size, shape and strength of the horseshoe-vortex responsible for the scouring process and about the forces on particles within the scour hole. The following formula was arrived at for clear-water scour:

$$[5.9] \quad \frac{d_{se}}{b} = (a_1 N - a_2) \tanh \left(a_3 \frac{d_0}{b} \right)$$

where

$$N = \frac{U}{\left[\left(\frac{\rho_s}{\rho} - 1 \right) g D_{50} \right]^{1/2}}$$

and

$$a_1, a_2, a_3 = f(d_0/b, G)$$

where

$$G = \frac{\left[\left(\frac{\rho}{\rho_s} \right) - 1 \right] g D_{50}^3}{v^2} .$$

Good agreement was found between this formula and the experimental results of Baker (1980) and those from another source, as indicated in Fig. 5.7.

CHAPTER VI

EXPERIMENTAL PROCEDURE AND OBSERVATIONS

6.1 Experimental Apparatus

A steel flume 14.0 m long, 0.91 m wide and 0.76 m deep was used for conducting the local scour tests for this study. The floor of the flume, with an average slope of 0.002 was deliberately modified by constructing a wooden floor that raised the original floor by about 17 cm. This construction permitted the provision of a recess section, 2 m long and 17 cm deep, located approximately 5.70 m downstream from a baffled section. At this location the walls of the testing section were made of glass which, therefore, facilitated observations of the scour phenomena. All the piers that were tested were set in the recess section such that the nose of the pier was 1 m from the upstream edge of the section, to minimize the effects of transition from a wooden bed to a bed consisting of the sand which filled the recess section.

Water flow was recirculated through the flume by a centrifugal pump. The flow rate was measured either volumetrically by a collecting sump or by means of a water-mercury manometer connected to a Venturi meter in the supply line or by both methods, depending on the pumping system in operation. The pumping system was able to provide controlled discharges of up to $0.085 \text{ m}^3/\text{s}$ (3 cfs). The depth of flow in the flume was controlled by a tailgate.

In order to reduce the turbulence of the water gushing into the headbox from the supply pipes, a baffled section was installed in the headbox consisting of plastic pipes each about 35 cm long and 5 cm in diameter. These were stacked ahead of a screen configuration which assisted in uniformly distributing the flow and calming surface waves.

The flume was provided with level rails and a gauge carriage. A point gauge was used to measure the depth of flow, water surface slopes and bed configurations before and after each test run.

6.2 Geometrical Characteristics of the Piers

All the piers tested were rectangular and basically of the same length (40.6 cm) and width (7.6 cm). Two of the piers, the round-nosed and the triangular-nosed (with their corresponding tails similarly constructed) were made of wood and their surfaces were smoothed. The third pier, with square nose and tail, was constructed from plexiglass, to enable provision of piezometer taps on the nose, tail and sides. The relevant geometrical characteristics of the piers are shown in Fig. 6.1.

6.3 Bed-Material Characteristics

A well-graded sand with a median diameter (D_{50}) of 0.37 mm was used as bed material during the course of the study. The sand had a density of 2680 kg/m^3 , a coefficient of uniformity (C_u) of 2.2, and a coefficient of curvature (C_c) of 1.5. The particle size distribution curve for the sand is shown in Fig. 6.2. Results from all test runs indicated an average submerged angle of repose of 40° .

6.4 Experimental Procedure

Each pier was fixed to a wooden baseboard approximately 91 cm wide and 60 cm long so that upon placement into the recess section the pier was centrally located across the section and was also aligned at zero angle of attack relative to the direction of flow. The testing section was then filled with the bed-material flush with both the upstream and downstream edges of the recess.

Before each test run, the surface of the bed was carefully levelled to a flat configuration, and the mean bed elevation was determined. The following procedure was then adopted for all test runs. With the tailgate completely lowered, the flume was nearly filled with water at a rate that induced no perceptible movement of bed-material anywhere on the bed surface. The tailgate was then raised and the supply valves were adjusted until a preselected depth of flow and discharge and hence, the required approach velocity, were achieved. Timing of the progression of scour at the nose of the pier was begun immediately after the scouring action was observed regardless of whether or not the preselected equilibrium flow conditions were established. Attainment of equilibrium flow conditions in general required a time passage of 15 to 30 minutes. At equilibrium the water surface slope was determined and always found to be equal to the slope of the flume floor, thus satisfying one of the criteria for uniform flow.

Each run was terminated when the point-gauge measurements indicated that the limiting scour depth was being approached asymptotically at a slow rate. In general, this required a running time of five hours or more.

At the completion of each run the flume was slowly drained, usually overnight, in order to preserve the configuration or scour pattern established by the flow. This configuration was then mapped by taking point-gauge measurements at preselected points in the neighbourhood of the pier. Photographs of the scour patterns were also taken. In addition, the angle, ϕ , the scour hole made with the horizontal and the longitudinal extent, L_e , of the scour hole along the main axis of the pier were measured (see Fig. 6.3 for the definition of the above variables).

The density and kinematic viscosity of the water were also determined indirectly for each test run by measuring the water temperature. The density was also measured directly using a hydrometer.

In a separate run, the bed surface was levelled in the absence of any pier and the threshold velocity for the initiation of bed material was determined by the following procedure. The flume was filled with water as in the case of other test runs. With an appropriately selected pump discharge set, the depth of flow was very slowly lowered until the threshold of sediment motion was observed. The flow depth was arrested at this point and allowed to run to equilibrium, making certain that the threshold condition was not exceeded. The velocity was then determined in the usual way, and the velocity profile was also determined both at an upstream section where the undisturbed depth of flow was measured in the other test runs and in the location where the piers were set in the recess section. Measurements of the point velocities were, in this case, made by a current meter.

6.5 Observations

For each pier, the scouring process was initiated near the corners B and B' (see Fig. 6.1). Breusers et al (1977) attribute this phenomenon to the greater stretching of the horseshoe-vortex near the corners B and B' and hence sufficiently increasing the rotational velocity in the vortex core to overcome the particles' resistance to motion.

In the case of the round-nosed pier, the vortex appeared to grow rapidly in both size and strength, as evidenced by the uniformly scoured hole at all stages of the scour process. The progression of scour with time for the round-nosed pier is shown in Fig. 6.4(a).

For both the square-nosed and triangular-nosed piers scour was initiated at the corners B and B' by what appeared to be an eddy with a vertical axis, as material was observed to be swirled up in suspension on a periodic basis. The periodicity of this action was, however, observed to decrease with time as the horseshoe-vortex system appeared to be spreading around the entire nose and growing in strength. In the case of the square-nosed pier, the scouring action, initially greater at corners B and B', eventually became uniform at later stages of the process (see Fig. 6.4(b)). On the other hand, the strength of the vortex at corners B and B' for the triangular-nosed pier continued to be greater than at corner A, as evidenced by the higher scour depth at any time during any individual test run (see Fig. 6.4(c)).

As the scouring activity continued the material adjacent to the scoured zone was observed to slide into the scour hole as a result of loss of lateral support. It was also observed that at some stage in the scouring process the horseshoe-vortex had apparently a little more difficulty with dislodging larger particles that had slid into the scour hole. Consequently, a transition armour coat was formed in the hole which tended to limit, at least transiently, continued erosion. Subsequently, of course, these larger particles were rolled out of the hole on an intermittent basis. This is reflected in the time-progression curves in Fig. 6.4 by the small fluctuations of the scour depth. In clear-water scour, any apparent oscillations of the depth of scour are, therefore, not due to the passage of dunes through the scoured zone as would be observed in the case of a live-bed situation (see Section 2.2).

During the initial stages of the scour process the action of the wake-vortex system was observed as bursts of sediment were thrown up

vertically by some swirling action and swept downstream - much like the whirlwind effect on dust and other debris. Large scour holes were observed to start to develop downstream from the piers on either side of a centreline ripple but these were later filled in by mounds formed by material eroded from the scour hole around the nose of the pier. The mounds progressing from either side of the pier subsequently coincided into one at the tail of the pier; this larger mound, illustrated in Fig. 6.3, was then progressively flattened and extended downstream.

The scour pattern that eventually developed at the end of each run was markedly similar from one pier shape to another, even at different flow conditions. The shape of the scour hole was somewhat conical, deepest close to the nose of the pier, and tapering off downstream. The general plan of all the scour holes was approximately horseshoe-shaped. In general the sides of the scour hole were resting at an angle $\phi = 40^\circ$ (roughly equal to the angle of repose of the saturated sediment) to the horizontal except for the portion of the scour hole nearest to the pier (zone YZ in Fig. 6.3). Sediment was observed to be removed, in intensive sweeping actions, from this zone by the horseshoe-vortex system. Typical scour patterns are shown in Plates 1 and 2 (Appendix C).

CHAPTER VII

CORRELATION OF DATA AND DISCUSSION OF RESULTS

7.1 Experimental Results

The threshold velocity for the initiation of bed material movement was, for the sediment used in this series of local scour experiments, found to be 0.28 m/s. Fig. 7.1 shows the velocity profiles of the threshold condition. Fig. 7.1(a) shows the velocity profile obtained at an upstream section where the depth of flow for all subsequent test runs on the piers was measured, whereas Fig. 7.1(b) shows the profile above the sand bed obtained in the recess section where the piers were located in subsequent runs. The greater velocity gradient above the sand bed is apparent in the second profile, obviously induced by the roughness elements of the bed material in comparison to the smooth wooden board serving as the bed in the upstream section.

The important experimental data collected in this study are duly summarized in Tables 7.1, 7.2, and 7.3 (Appendix B) for the round-nosed, square-nosed, and triangular-nosed piers respectively. Some of the time-progression curves for each pier are shown in Figures 7.2, 7.3 and 7.4 for the round-nosed, square-nosed and triangular-nosed piers respectively. The effect of velocity is clear in these graphs. In particular, the effect of a velocity higher than the threshold value is depicted, for the round-nosed pier, in Fig. 7.2(a), where the fluctuations of the scour depth with time due to the passage of dunes are evident.

In Section 4.2 the important variables which may influence local scour were listed and summarized in the following functional relationship:

$$[4.1] \quad d_s = f_1 (\rho, \nu, g, D_{50}, \rho_s, d_0, U, b, c) .$$

In the sections that follow, the influence of the parameters that were varied in this study are going to be examined, in turn, on the basis of the non-dimensional functional relationship that was developed in Section 4.2, namely

$$[4.4] \quad \frac{d_s}{b} = \phi \left(\frac{\rho_s}{\rho} - 1, \frac{Ub}{v}, \frac{U}{\sqrt{gb}}, \frac{D_{50}}{b}, \frac{d_0}{b}, c \right) .$$

Only one type of sediment was used in this study and, therefore, the relative submerged density, $(\rho_s/\rho) - 1$ and the parameter $\frac{D_{50}}{b}$, were essentially constant parameters.

In correlating the parameters defined in Eq. 4.4 there arises the problem of selecting the pertinent value of the scour depth, d_s , since, as has already been observed, the depth of scour approaches a limiting value asymptotically. To facilitate the correlation analysis in this study, the scour depth obtained after a certain amount of time had elapsed was determined by drawing smooth curves through the experimental points. This resulted in the variables d_{s3} , d_{s4} and d_{s5} which respectively represent the scour depths after the passage of 3, 4 and 5 hours from the time scour was first observed. These variables are subsequently referred to as the three-hour, four-hour and five-hour scour depths respectively.

7.2 Influence of the Pier Shape

The effect of the pier shape (parameter c) is clearly demonstrated in Fig. 7.3, which shows the variation of scour depth with time for different pier shapes under the same flow conditions. The square-nosed pier caused the deepest scour whereas the triangular-nosed pier resulted in a comparatively most reduced scour depth. This, naturally, leads

to the conclusion that the more pointed the nose shape, the more efficient the pier will be at reducing the depth of scour around the pier.

7.3 Influence of the Depth of Flow

The square-nosed pier was used to investigate the influence of the depth of flow on scour depth. The variation of scour depth with time for different flow depths but under the same velocity conditions is shown in Fig. 7.4. It was apparent from this set of runs that the limiting depth of scour approached the same value for depths equal to or greater than 20 cm, whereas for depths less than 20 cm a higher limiting scour depth was approached.

From the non-dimensional plot of the depth of scour against the flow depth shown in Fig. 7.5, there does not appear to be any systematic influence of the depth of flow on scour depth. However, there is a characteristic jump in behaviour around $\frac{d_0}{b} = 2.6$ which probably implies that free surface effects are significant for $\frac{d_0}{b} < 2.6$. On the basis of the observations from the experiments of this study it may be concluded that the depth of flow has no significant influence on the depth of scour except for relative depths of less than 2.6.

7.4 Influence of the Mean Approach Flow Velocity

That the higher velocities cause the deeper scour depths is evident from Fig. 7.2(a), (b), and (c). What is not so obvious from this figure is that there apparently exists a linear relationship between the depth of scour and the flow velocity. These relationships are shown for the three-, four- and five-hour scour depths for the round-nosed pier in

Fig. 7.6, the square-nosed pier in Fig. 7.7, and the triangular-nosed pier in Fig. 7.8. In each of these figures, points were plotted for different flow conditions and the line of best fit through these points was determined by linear regression analysis. This also applies to all subsequent linear relationships postulated in this chapter.

In the case of the round-nosed pier there is a considerable scatter of the data points, an indication, probably, of poor quality data. There is less scatter in the data for the triangular-nosed pier, whereas the data pertaining to the square-nosed pier shows the least scatter. The inconsistency of the results is revealed in Fig. 7.9 where a comparison of the linear regression lines for the different pier shapes is made. Inasmuch as the round-nosed pier caused a comparatively intermediate depth of scour between that caused by the square-nosed (deepest) and that caused by the triangular-nosed pier (shallowest) for the same flow conditions the expected result would be for slope in Fig. 7.9 to be intermediate between the slopes obtained for the square- and triangular-nosed piers. On the contrary, Fig. 7.9 depicts the round-nosed pier to be the most efficient at reducing scour depths.

One method of verifying the validity of the scour-depth data is to use the additional information obtained at the end of each of the five-hour test runs, namely the longitudinal extent, L_e , of the scour hole and the angle of repose, ϕ , of the scour hole to the horizontal. This assumes, of course, that these parameters were more accurately determined than the scour depth, which they were since they were measured under more stable conditions after the flume was completely drained. The $d_{s5} - L_e$ plots are presented in Fig. 7.10.

The angle of repose, averaged over approximately forty measurements, was, as already indicated in an earlier section, 40° . Fig. 7.10(a) shows that the slope of the linear regression line, which should be equal to the angle of repose, for the round-nosed pier is 32° , a value low enough to warrant suspicion of the validity of the scour-depth data. The data pertaining to the triangular-nosed pier depict an angle of repose of 34° , indicating better data but still not good enough, whereas the square-nosed data indicate an angle of repose of 39° , which obviously explains the least scatter in the linear relationships in question.

Whereas the verification above seems to indicate that the data pertaining to the round-nosed pier were the poorest, the difference in quality indicated by these data in comparison to those obtained for the triangular-nosed pier is low enough to contradict the conclusion drawn about the accuracy of the slope indicated in Fig. 7.9 for the round-nosed pier. Therefore, the information depicted in Fig. 7.3 pertaining to the round-nosed and triangular-nosed piers is not sufficient to permit the conclusion that the round-nosed pier causes the worse scour to be drawn. Moreover, the behaviour of the scour depths after five hours of test run (shown in Fig. 7.3) seems to indicate that the scour curves would eventually coincide with or even cross each other.

Despite the foregoing shortcoming of the other data correlation analysis was proceeded with the original untransformed data for all the piers. The dimensionless plots of the influence of velocity are given in Figures 7.11, 7.12, and 7.13 for the square-, triangular- and round-nosed piers respectively. Only the 4-hour scour depth relationships are shown for the latter two pier shapes. The resulting linear relationships are summarized by the following linear regression equations.

For the square-nosed pier:

$$[7.1a] \quad \frac{d_{s3}}{b} = 3.94 \frac{U}{U_c} - 2.17$$

$$[7.1b] \quad \frac{d_{s4}}{b} = 4.17 \frac{U}{U_c} - 2.30$$

$$[7.1c] \quad \frac{d_{s5}}{b} = 4.40 \frac{U}{U_c} - 2.43 .$$

For the triangular-nosed pier:

$$[7.2a] \quad \frac{d_{s3}}{b} = 3.16 \frac{U}{U_c} - 1.81$$

$$[7.2b] \quad \frac{d_{s4}}{b} = 3.33 \frac{U}{U_c} - 1.89$$

$$[7.2c] \quad \frac{d_{s5}}{b} = 3.45 \frac{U}{U_c} - 1.94 .$$

For the round-nosed pier:

$$[7.3a] \quad \frac{d_{s3}}{b} = 1.40 \frac{U}{U_c} - 0.245$$

$$[7.3b] \quad \frac{d_{s4}}{b} = 1.65 \frac{U}{U_c} - 0.393$$

$$[7.3c] \quad \frac{d_{s5}}{b} = 1.78 \frac{U}{U_c} - 0.472 .$$

7.5 Comparison with Previous Studies

7.5.1 Influence of the Pier Shape

It has been observed (Figures 7.3 and 7.9) that the square-nosed pier caused the deepest scour to occur and that comparatively reduced scour depths were noted for the other two shapes. This is in agreement with the observation made by Durand-Claye as early as 1873 (cited by Karaki and Haynie, 1963) and also by Varzeliotis (cited by Neill, 1964).

It has also been observed from Fig. 7.3 and 7.9 that the results for the round-nosed pier and the triangular-nosed pier were contradictory. The results obtained in this study are inconclusive in this sense but Varzeliotis (cited by Neill, 1964) found that the triangular-nosed pier caused the worse scour to occur than the round-nosed pier.

7.5.2 Influence of the Depth of Flow

The results of this study show a small dependence of the depth of scour on the depth of flow, especially for relative depth ratios ($\frac{d_0}{b}$) greater than 2.6. Below this value the scour depth increases the shallower the water layer. The results found by Varzeliotis (cited by Neill, 1964) are contradictory in that the opposite was found to be true. However, there is agreement among many of the previous investigators as regards the negligible influence of the depth of flow after the relative depth ratio exceeds a certain value. Hincu (cited by Breusers et al, 1977), for instance, found negligible influence of the depth of flow for $\frac{d_0}{b} > 1$ whereas this study indicated that there was negligible influence for $\frac{d_0}{b} > 2.6$.

7.5.3 Influence of the Mean Approach Flow Velocity

The linear relationship between the depth of scour and the mean approach flow velocity found in the present study has also been reported previously by investigators like Hincú and Alvarez and Bribiesca (both studies cited by Breusers et al, 1977) for velocities below the threshold value for the initiation of sediment motion. However, comparison with Hincú's results is made difficult due to the fact that the data obtained in the present study do not seem to indicate that there is a definite constant scour depth which can appropriately be labelled as the maximum depth of scour. The author also feels that above the threshold velocity the scour depth would not be constant but would oscillate aperiodically, as indicated in Section 2.2.

A comparison with the results of Alvarez and Bribiesca is indicated in Fig. 5.2 where the present results have been added to the graph. Reasonable agreement is depicted in this case, but it must be noted that the depth of scour used by Alvarez and Bribiesca was not clearly defined. The inserted data points from this study are those of the 5-hour scour depths obtained from tests on the round-nosed pier whose nose is identical to that of the circular pier used.

The results for clear-water scour reported by Baker (1980) also reduce to a linear relationship between the depth of scour and the mean approach velocity. However not enough information has been provided to allow comparison. If, on the other hand, it is assumed that $\rho_s/\rho = 2.65$, $\nu = 1 \times 10^{-6} \text{ m}^2/\text{s}$ and $\rho = 9.81 \text{ m/s}^2$, then the value of D_{50} that was used can be inferred from the given value of $G = 1.47 \times 10^3$. From this information the equation given by Baker (1980) for the plot in Fig. 5.7(a) reduces to

$$[7.4a] \quad \frac{d_s}{b} = 14.1U - 2.2$$

whereas that for the plot in Fig. 5.7(b) reduces to

$$[7.4b] \quad \frac{d_s}{b} = 11.7U - 1.9 .$$

The value of D_{50} that was inferred from Baker's results was 0.45 mm which is almost equal to that used in the present study, namely 0.37 mm. The threshold velocity of such sediment would, therefore, not be expected to differ very much from that found for the sand used in this study, namely 0.28 m/s. Introducing this velocity in Equations 7.4(a) and (b) we obtain:

$$[7.5a] \quad \frac{d_s}{b} = 3.94 \frac{U}{U_c} - 2.2 \quad \text{and}$$

$$[7.5b] \quad \frac{d_s}{b} = 3.28 \frac{U}{U_c} - 1.9 .$$

The coefficients in these equations compare well with those in Equations 7.1 and 7.2 obtained for the square-nosed and triangular-nosed piers respectively. However, they differ substantially from those in Eq. 7.3 obtained for the round-nosed pier which approximates most to the cylindrical pier used by Baker. Nevertheless, there is reasonable agreement between the two sets of results. Again it must be borne in mind that the depth of scour, as used by Baker (1980), was not clearly defined.

Further comparisons with other scour studies were rendered inappropriate because they were either conducted in live-bed situations or were carried out in both fixed- and live-bed conditions without a clear distinction between the two flow regimes.

7.6 Influences of the Pier Reynolds Number and the Pier Froude Number

In this study, the pier Reynolds number and the pier Froude number were not varied independently. Therefore, the question of whether either of the numbers plays an important role in local scour or both are significant has not been explored by the present study. However, some important remarks can be made regarding the influence of these parameters in light of some of the results obtained in this study.

Inasmuch as open channel flow is a free surface phenomenon, the Froude number is expected to play an important role in local scour. On the other hand, if free surface effects are insignificant, as observed for $\frac{d_0}{b} > 2.6$ in the present study, then it seems reasonable to infer that the Froude number will not play a significant role in the phenomenon. Furthermore, previous research seems to point to the fact that local scour is mobilized by a vortex system (Shen, 1966 and Baker, 1980) and the action of this vortex is indeed apparent when one observes the sweeping action on the sediment near the nose of a pier. That vorticity is of appreciable magnitude only within the boundary layer, where viscous forces predominate, is a well-documented fact. If viscous forces are important in local scour, then it seems reasonable to infer that the Reynolds number will, in fact, be the more significant parameter than the Froude number, as long as free surface effects do not interfere with the boundary layer. However, this conclusion would have to await future studies in order to be substantiated.

CHAPTER VIII

PROTECTION AGAINST SCOUR

8.1 General

As an addendum to this thesis, this chapter discusses the additional arrangements that have to be considered, once the potential scour depth is estimated, to accommodate, eliminate, or minimize the scour magnitude. Tests of scour protection for bridge piers were not conducted as part of this research. Nevertheless, the importance of developing acceptable and proven methods of scour protection cannot be over-emphasized and, therefore, it seems fitting to include a discussion of its subject matter.

As the first statement implies, the protection methods should really be in addition to the best selection of a pier shape and geometry that will minimize the scour. A review of literature on scour problems reveals that the main scour protection systems that have successfully been used are mats of rip-rap or a caisson placed around the pier both with top surfaces situated under the average level of the streambed; another arrangement involves placing additional structures such as small piles upstream from the pier.

8.2 Rip-Rap Mats

The armouring effect due to large sediment particles has already been noted in Section 6.5. This effect has, obviously, been long recognized by bridge designers as is evident from the frequent reference to the use of rip-rap mats in most scour protection systems. This method is undoubtedly the most usual and probably the most economical method of precluding erosion around a bridge pier. However, before one can capitalize on the armouring effect of large sediment particles it is necessary or

worthwhile to know the type, gradation, thickness and size of the rip-rap necessary to effect a good armour plate at an appropriately selected depth. Unfortunately, the evolution of rational design criteria is, perhaps not too surprisingly, in the early stages yet.

Cartsens (1966) suggested that the flow velocity giving rise to initial scour at the base of the pier was only one-half of that corresponding to general bed movement. Breusers et al (1977) also reported tests which have shown that, regardless of the pier diameter, initial scour at the base of a circular pier occurs, for a given sediment, at a flow equal to one-half the critical velocity. Using this information, they suggested that the weight and hence the diameter of rip-rap capable of restraining scour can be determined from an equation of the form:

$$[8.1] \quad U_c = k \left[2g \left(\frac{\rho_s - \rho}{\rho} \right) D \right]^{1/2}$$

where k is a constant. Furthermore, Breusers et al (1977) suggested that the horizontal dimensions of the protected zone should be at least twice the pier width measured from the face of the pier and should have a thickness equal to or greater than three times the diameter of the rip-rap.

The design of an effective rip-rap mat requires that, in addition to other considerations, fine material should not be washed up through the voids of the mat, an action usually referred to as "leaching". The interstices in the protective mat should, therefore, be small enough to prevent the finer material below from escaping but large enough to permit the upward flow of water without creating an excessive lift force. This problem is solved by the use of an inverted filter. Posey (1974)

reported that experiments conducted by the U.S. Waterways Experimental Station indicated that the following specifications produced a leach-proof filter:

$$[8.2a] \quad D_{15} < 5d_{85}$$

$$[8.2b] \quad 4d_{15} < D_{15} < 20d_{15}$$

$$[8.2c] \quad D_{50} < 25d_{50}$$

where 15% by weight of the protective layer is finer than the size indicated by D_{15} and 85% by weight of the layer being protected is finer than the size identified as d_{85} , and so on. Posey (1974) concluded that scour could be prevented by no more than two layers of an inverted filter extending out a distance of 1.5 to 2.5 pier diameters in all directions from the face of the pier.

Quazi and Peterson (1973) derived design criteria for loose-stone pier rip-rap based on the results of a laboratory study. Their starting point was the derivation of non-dimensional functional relationships, one form of which was:

$$[8.3] \quad f \left[\frac{\rho U^2}{\gamma'_s D}, \frac{\gamma'_s D^3}{\rho v^2}, \frac{D}{d_0}, \frac{b}{D} \right] = 0 \quad .$$

From a combination of their data and that obtained from other sources, they developed a design curve for sizing pier rip-rap which is shown in Fig. 8.1.

In all cases of rip-rap mat design, the top surface of the protection should be at some distance below the normal bed level to prevent excessive exposure.

8.3 Foundation Caissons

The effect of pier footings on local scour is illustrated in Fig. 8.2. As this figure shows, the founding of a pier on a caisson of larger dimensions requires that the top elevation of the caisson be located below the estimated lowest scour levels. Breusers et al (1977) have reported on experimental tests conducted by Chabert and Engeldinger from which they concluded that a caisson having a diameter of three times the pier diameter and a top elevation of about one-half the diameter of the pier below the natural bed reduced scour to one-third of that reached with pier alone. Reduction of scour depths of up to 50% can also be obtained by placing a horizontal flat plate or collar (Fig. 8.2(e)) with a diameter of at least three times the pier diameter some distance below the undisturbed bed level.

8.4 Piles Placed Upstream of Pier

This method is illustrated in Fig. 8.3. The objective in this method is to break the incident current ahead of the pier and hence weaken the vortex generating scour at the pier. The main problem with this method lies in the fact that a large number of parameters are required to define such a structure: number of piles, n ; pile diameter, δ ; pile spacing, e ; angle of opening, α ; and distance from pier, L . The number of parameters, thus, prevents the formulation of general criteria for designing such a protective system, but it has been observed from laboratory tests that such systems can reduce scour depths by as much as 50% (Breusers et al, 1977).

CHAPTER IX

CONCLUSIONS AND RECOMMENDATIONS

9.1 Limitations

The conclusions drawn from this study are limited to the following conditions:

- (i) rectangular piers of length to width ratio of 5.3 and which practically behaved as blunt-nosed piers
- (ii) subcritical, unidirectional and uniform flow conditions; the Froude number of the flow varied from 0.12 to 0.23.
- (iii) non-cohesive granular bed material (sand)
- (iv) clear-water scour; the threshold velocity for the initiation of bed material movement (0.28 m/s) was not exceeded
- (v) zero angle of attack; the main axis of the pier was always aligned parallel to the flow.

9.2 Influences of the Parameters Affecting Local Scour

9.2.1 Pier Shape

A well-streamlined pier reduces the scour potential. A square-nosed pier causes the deepest scour depths in comparison with a triangular-nosed pier. A round-nosed pier results in scour depths intermediate between that caused by the former two shapes. The last statement of this conclusion is, however, not well substantiated by the results obtained in this study.

9.2.2 Depth of Flow

There is no systematic influence of the depth of flow on scour depth as long as the ratio $\frac{d_0}{b} > 2.6$. When $\frac{d_0}{b} < 2.6$ surface effects become significant enough to affect the scour depths.

9.2.3 Mean Approach Flow Velocity

For clear-water scour, and as long as $U < U_c$, the scour depth varies linearly with velocity.

9.3 Recommendations for Future Studies

The role of the flow Froude number and the effects of the free surface require a more thorough investigation whereby the depth of flow is varied over a wider range than was possible in this study. These effects should also be investigated for different pier shapes.

The influences of the pier Froude number and the pier Reynolds number could also be investigated by varying these parameters independently. For instance, if the velocity was doubled from one test to the next, the relationship between the depth of scour and the pier Reynolds number obtained at a constant value of the pier Froude number would require that the pier width be quadrupled. Whereas this would affect the ratio $\frac{D_{50}}{b}$ somewhat, it is expected that the influence of such changes would be small provided $D_{50} \ll b$. If the effect of the relative depth of flow, $\frac{d_0}{b}$, is indeed negligible above a certain value then the change in b would not cause problems in the resulting relationship. However, if it does then $\frac{d_0}{b}$ could be kept constant by quadrupling the depth of flow as well.

The effect of sediment size also requires consideration in future studies. There exists considerable disagreement regarding the influence of this parameter. Whereas some maintain that the depth of scour is independent of the sediment size, others contend that the opposite is true. According to Henderson (1966), however, the depth of scour is independent of the sediment size only in live-bed cases and that in

clear-water scour the scour depth will be greater for fine sediments than coarse. Some interesting arguments have been made to support this contention.

The use of a point gauge in measuring the level of the scour hole is discouraged due to the problems it introduces. It was observed that probing of the gauge into the scour hole initiated additional localized scour around the point gauge. The use of sonic, optical or electronic devices such as depth echo-sounders, light-reflecting devices and laser beams is, therefore, recommended.

It was mentioned that the square-nosed pier was provided with piezometer taps to permit the determination of the pressure distribution around the pier. However, no further reference to these piezometers was made. The reason for this was that the measured piezometer levels resulted in inconsistent pressure differences from one measurement to the next, which had to do with the insensitivity of the apparatus. Inasmuch as the pressure differences being sought are very small, of the order of 1 mm, considering the scale of the experimental set up, the use of sensitive pressure transducers is highly recommendable.

There exists a possibility that compaction of the bed material could have an effect on the rate of scour. For comparison purposes, therefore, it is advisable to flatten the bed under submerged conditions, allow to drain overnight and proceed with the next test the following day. The free-drainage is expected to induce similar starting compaction conditions from one test to the next.

BIBLIOGRAPHY

- Baker, C. J. (1980), "Theoretical Approach to Prediction of Local Scour Around Bridge Piers", Journal of Hydraulic Research, Vol. 18, No. 1, pp. 1-12.
- Breusers, H. N. C., G. Nicollet and H. W. Shen (1977), "Local Scour Around Cylindrical Piers", Journal of Hydraulic Research, Vol. 15, No. 3, pp. 211-252.
- Cartsens, M. R. (1966), "Similarity Laws for Localised Scour", Proc. ASCE, Vol. 92, No. HY3, pp. 13-36.
- Coleman, N. L. (1971), "Analyzing Laboratory Measurements of Scour at Cylindrical Piers in Sand Beds", Proc. 14th IAHR Congress, Vol. 3, Paris, pp. 307-313.
- Henderson, F. M. (1966), "Open Channel Flow", Macmillan Publishing Co., Inc., New York.
- Karaki, S. S. and R. M. Haynie (1963), "Mechanics of Local Scour, Part II, Bibliography", Prepared for U.S. Department of Commerce, Bureau of Public Roads, Colorado State University Report No. CER63SSK46, Fort Collins, Colorado.
- Laursen, E. M. (1952), "Observations on the Nature of Scour", Proc. Fifth Hydraulics Conference, State University of Iowa, Iowa City, Iowa, pp. 179-197. (Original not seen, cited by Shen and Schneider, 1969.)
- Laursen, E. M. and A. Toch (1956), "Scour Around Bridge Piers and Abutments", Bull. No. 4, Iowa Highway Research Board.
- Neill, C. R. (1964), "Local Scour Around Bridge Piers", Research Council of Alberta, Highway and River Engineering Division, Edmonton, Alberta.
- Neill, C. R. (editor) (1973), "Guide to Bridge Hydraulics", Roads and Transportation Association of Canada, University of Toronto Press, Toronto, Ontario.
- Posey, C. J. (1974), "Tests of Scour Protection for Bridge Piers", Proc. ASCE, Vol. 100, No. HY12, pp. 1773-1783.
- Quazi, M. E. and A. W. Peterson (1973), "A Method for Bridge Pier Rip-Rap Design", Proc. of the First Canadian Hydraulics Conference, University of Alberta, Edmonton, Alberta.
- Roper, A. T., V. R. Schneider and H. W. Shen (1967), "Analytical Approach to Local Scour", Proc. 12th IAHR Congress, Vol. 3, Fort Collins, Colorado, pp. 151-161.

- Shen, H. W., V. R. Schneider and S. S. Karaki (1966), "Mechanics of Local Scour", Prepared for U.S. Department of Commerce, Bureau of Public Roads, Colorado State University Report No. CER66HWS22, Fort Collins, Colorado.
- Shen, H. W. and V. R. Schneider (1969), "Local Scour Around Bridge Piers", Proc. ASCE, Vol. 95, No. HY6, pp. 1919-1940.
- Simons, D. B. and F. Şentürk (1977), "Sediment Transport Technology", Water Resources Publications, Fort Collins, Colorado.
- Tison, L. J. (1961), "Local Scour in Rivers", Journal of Geophysical Research, Vol. 66, No. 12, pp. 4227-4232. (Original not seen, cited by Vanoni, 1975.)
- Vanoni, V. A. (editor) (1975), "Sedimentation Engineering", American Society of Civil Engineers, New York.

APPENDIX A

FIGURES

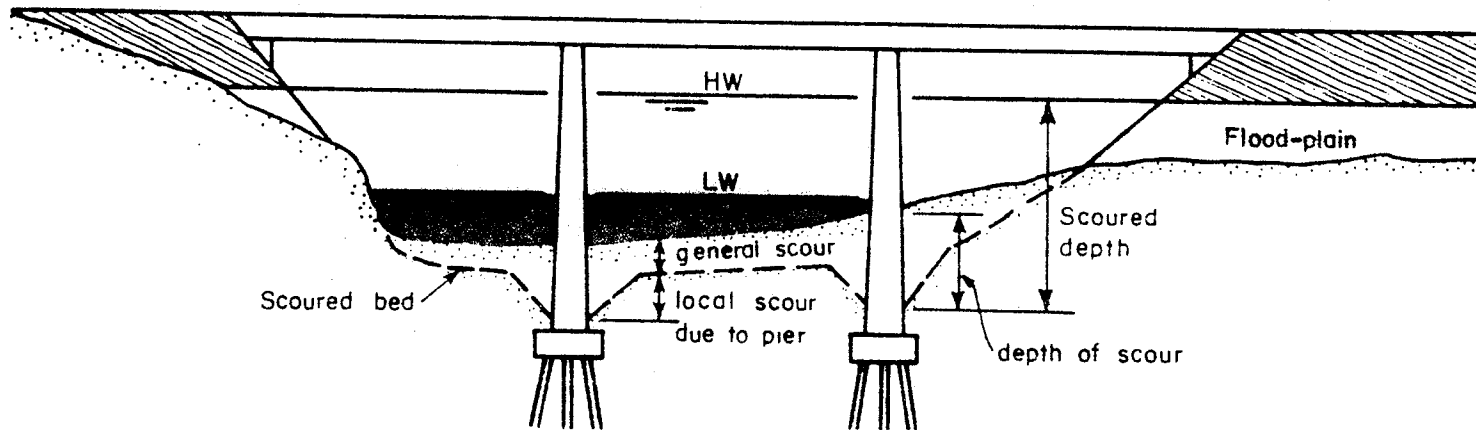


Fig. 2.1. Cross-Section at a Bridge Waterway Opening,
Illustrating Scour Terminology (After Neill, 1973)

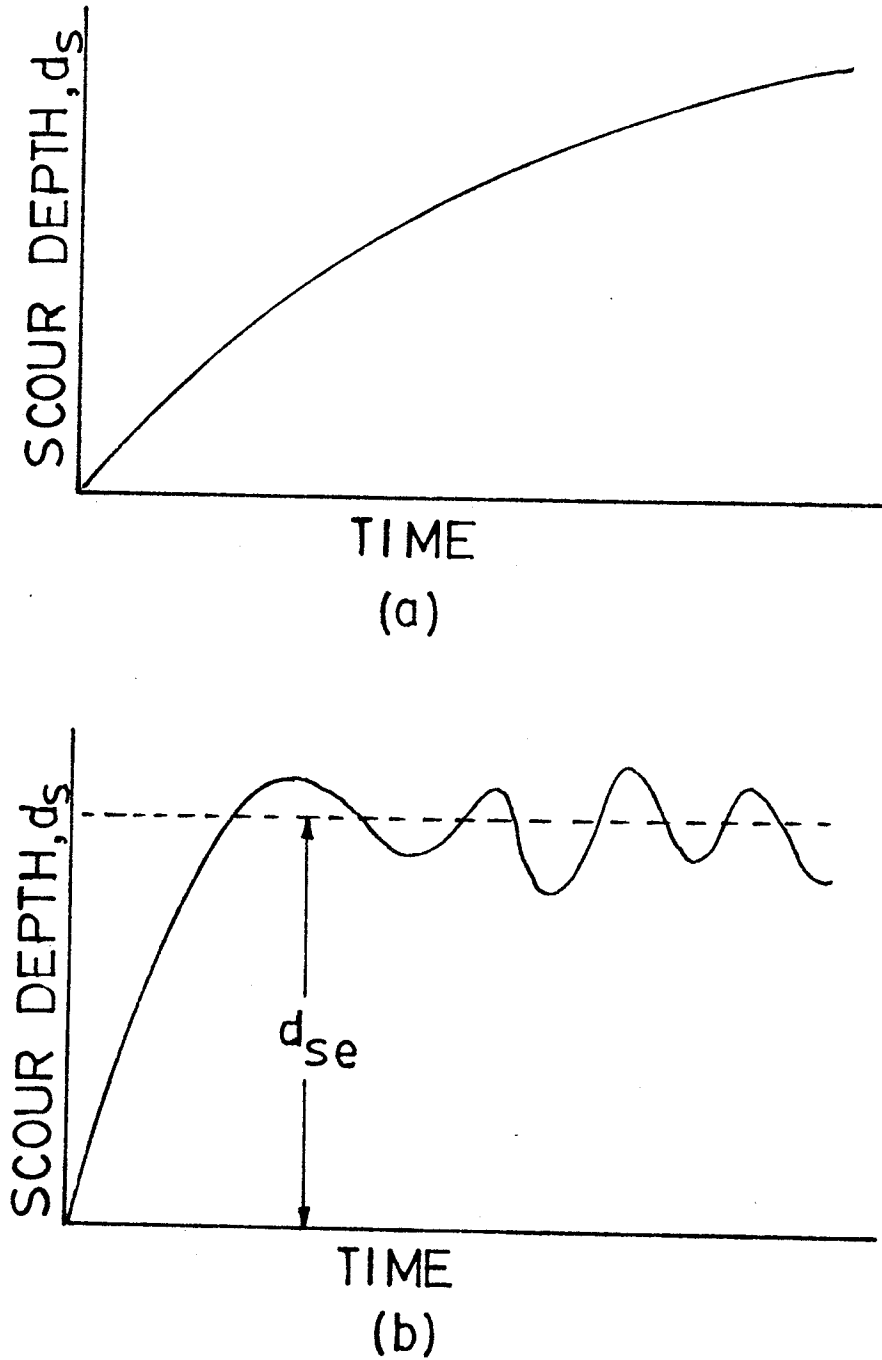


Fig. 2.2. Variation of Scour Depth with Time
(a) Clear-water Scour
(b) Scour with Continuous Sediment Supply
(After Shen et al, 1969)

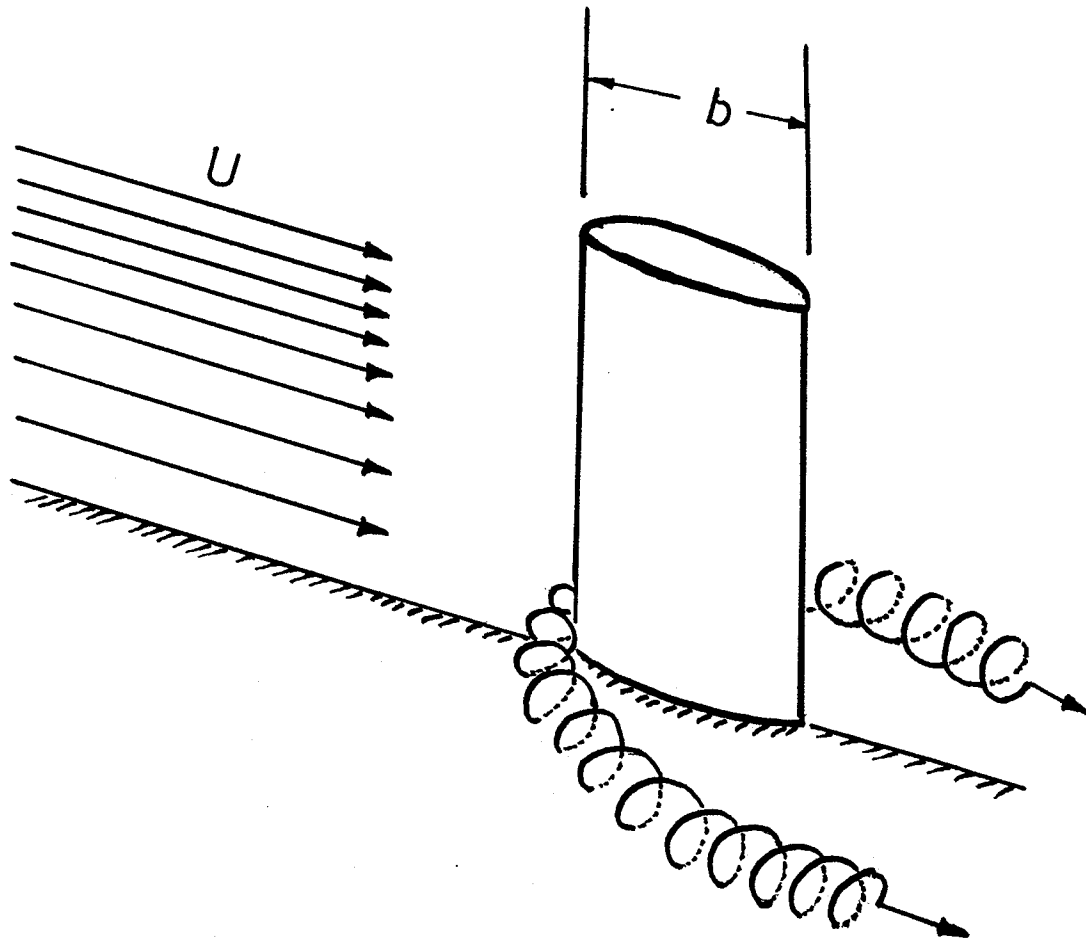


Fig. 3.1. Horseshoe-Vortex on a Flat Bed

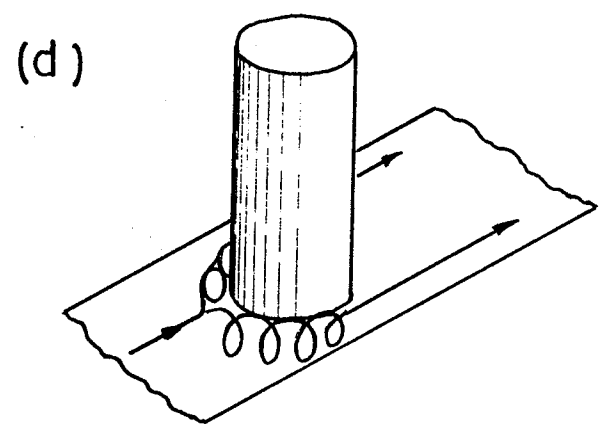
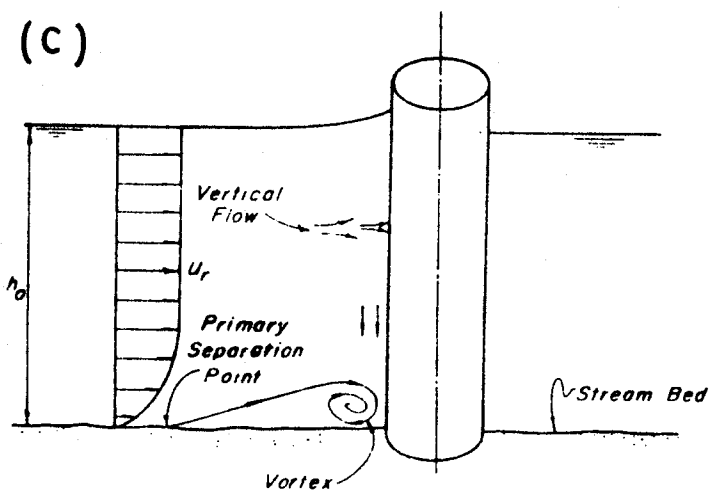
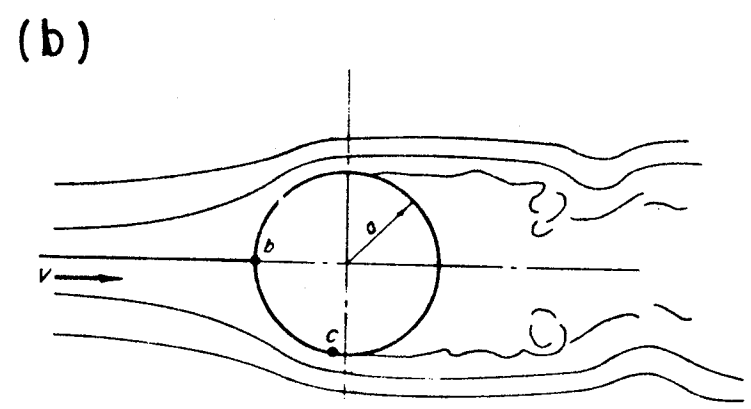
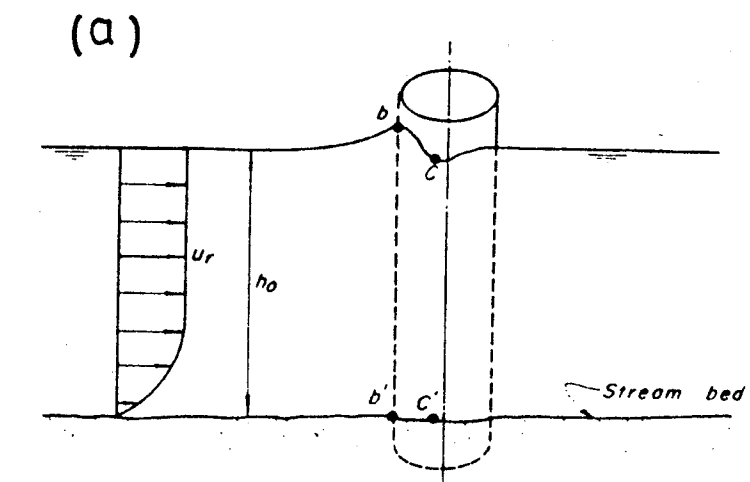


Fig. 3.2. Features of Flow Around a Blunt-Nosed Pier (After Shen et al, 1966 except (d))

(a) Elevation of Pier Before Scour Begins
 (b) Plan View of Flow Distribution Around the Pier
 (c) Features of Flow on the Stagnation Plane
 (d) Three-Dimensional Obstacle With the Horseshoe-Vortex (After Roper et al, 1967)

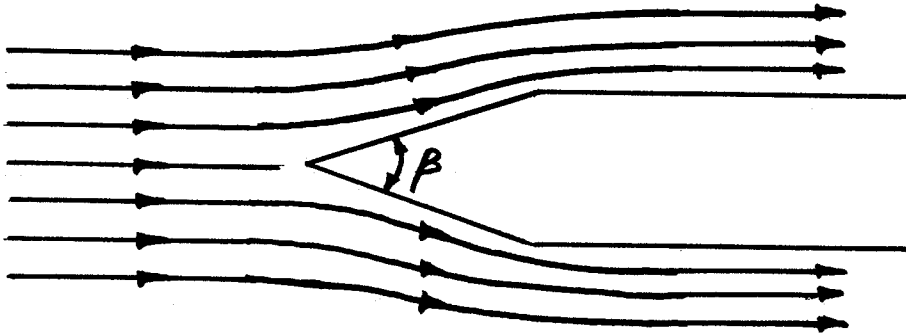


Fig. 3.3. Flow Around a Sharp-Nosed Pier
(After Shen et al, 1966)

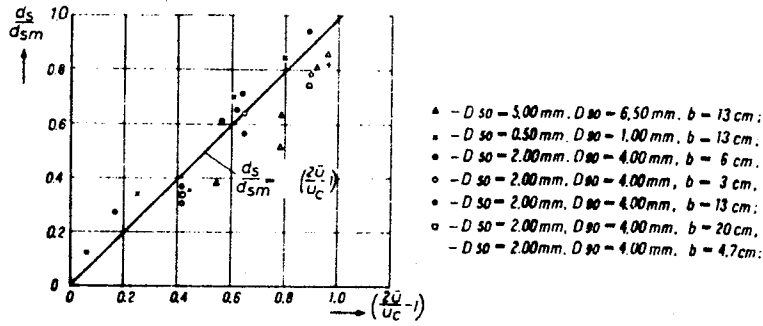


Fig. 5.1. Hincu's Experimental Results for Circular Piers
(After Breusers et al, 1977)

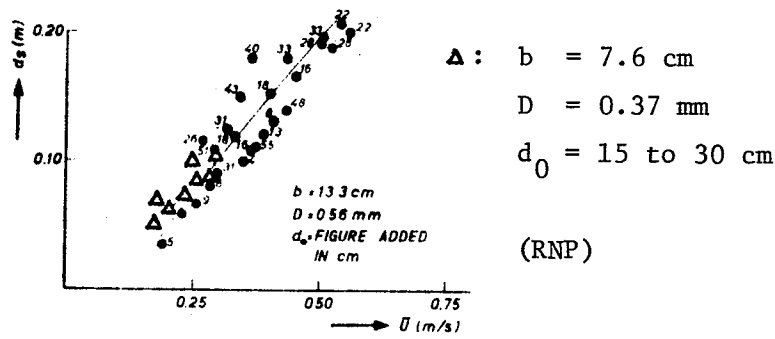


Fig. 5.2. Experimental Results for a Circular Pier Presented
by Alvarez and Bribiesca (After Breusers et al, 1977)

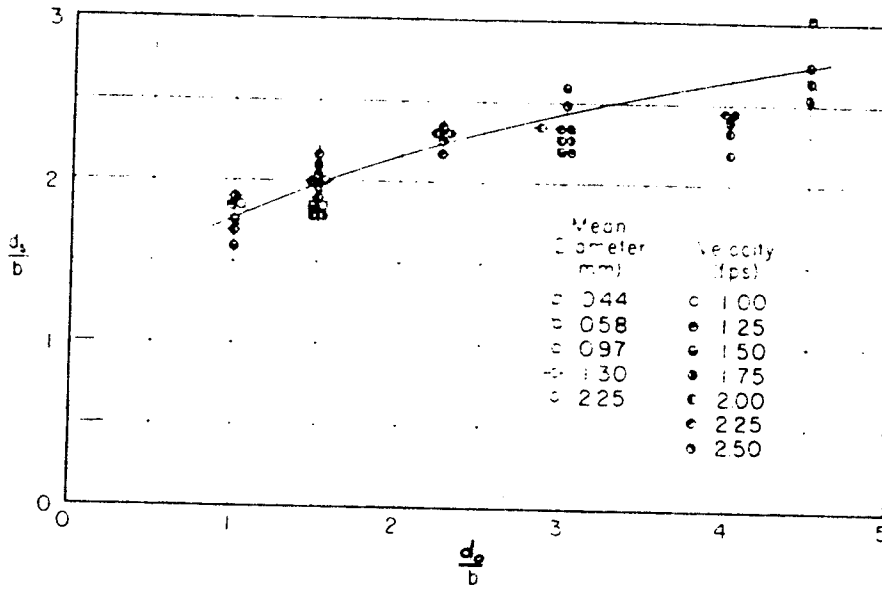


Fig. 5.3. Results of Equilibrium Scour Study
(After Laursen and Toch, 1956)

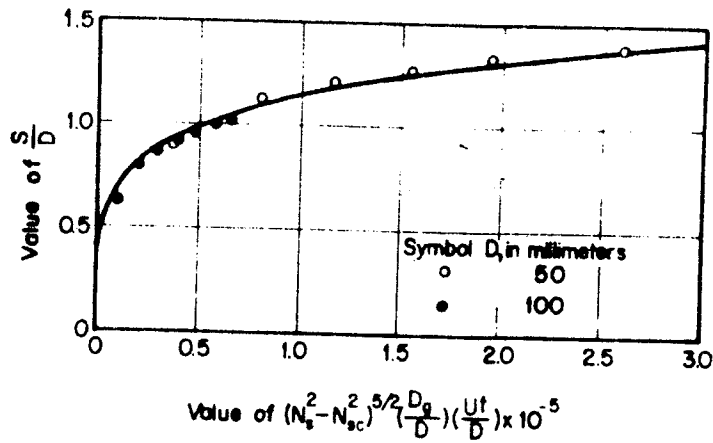
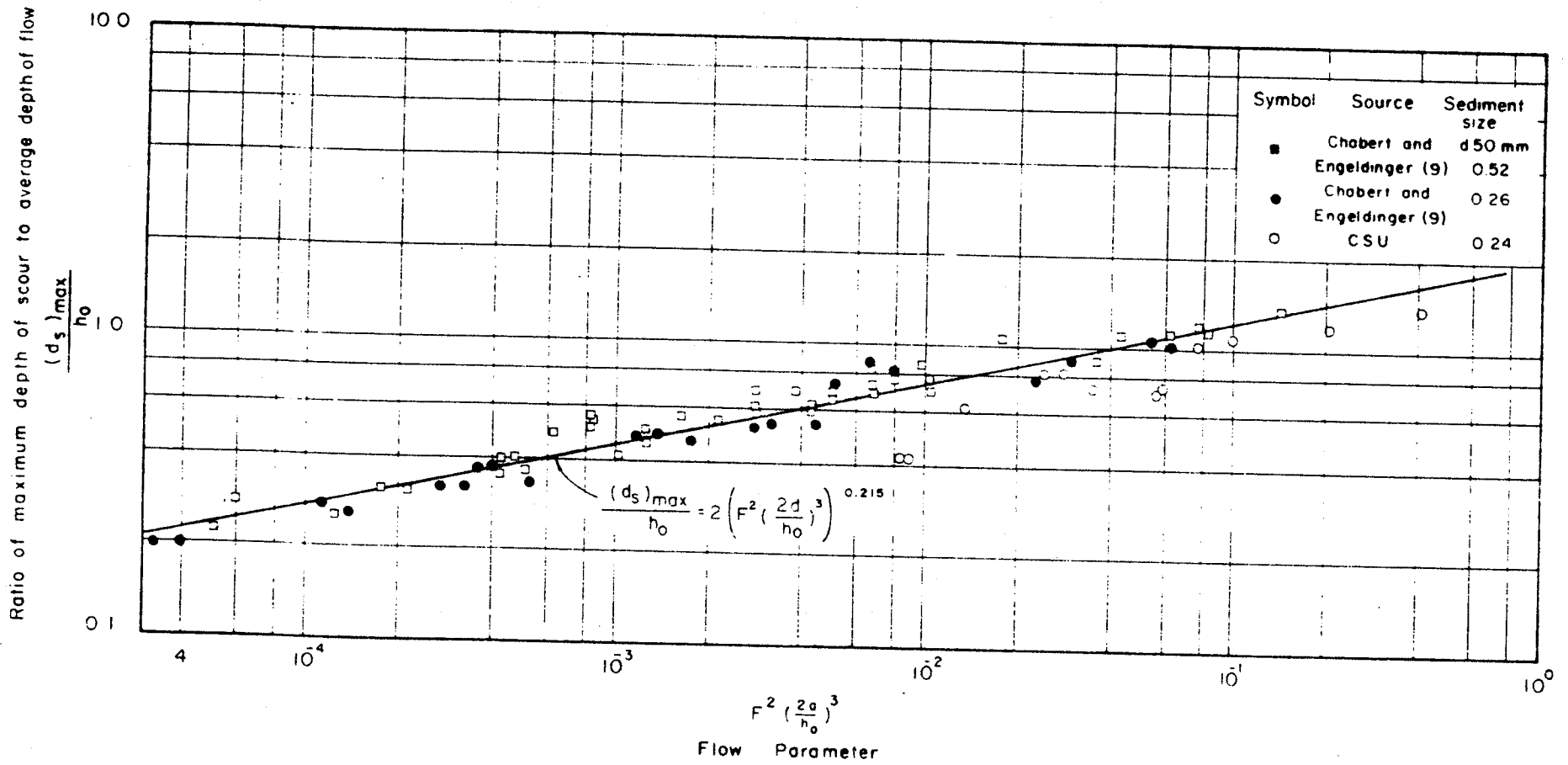


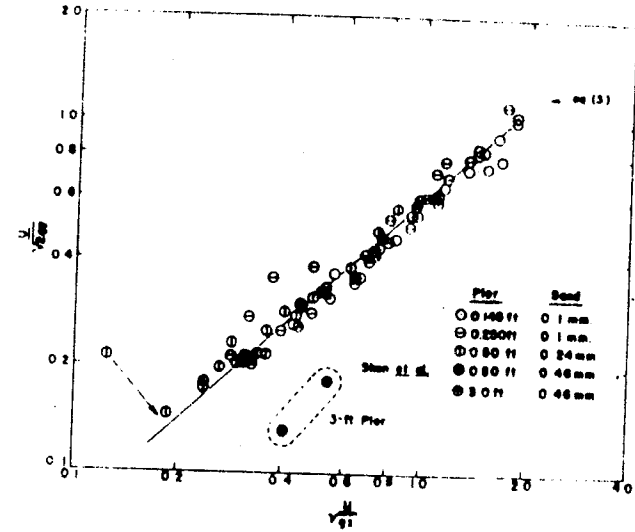
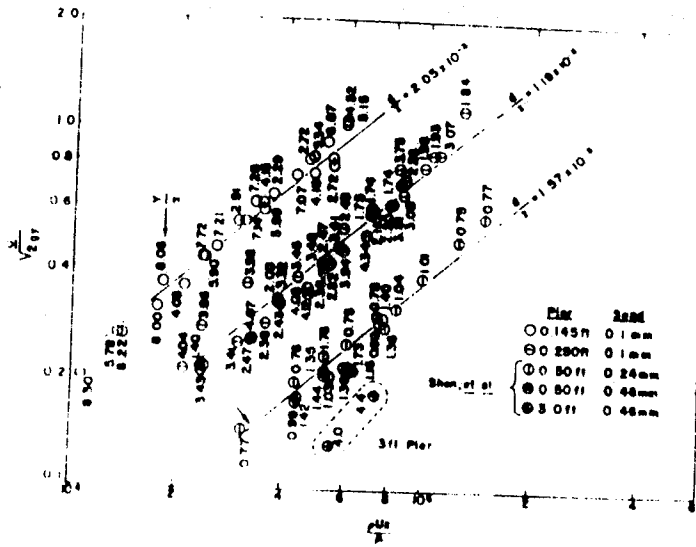
Fig. 5.4. Scour Depth Versus Time for a Vertical
Cylinder (After Carlsens, 1966)



$$(h_0 \equiv d_0, F \equiv Fr, a \equiv b/2)$$

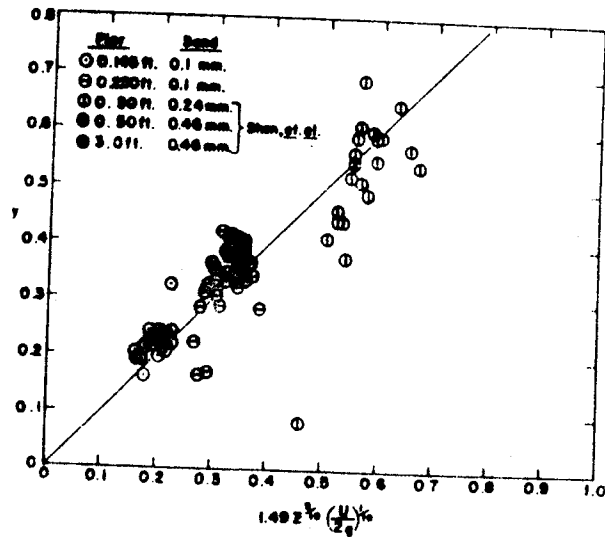
Fig. 5.5. Ratio of Maximum Depth of Scour to the Average Depth of Flow Versus a Flow Parameter (After Shen et al, 1966)

(a)



(c)

(b)



$$(y \equiv d_s, Y \equiv d_0, z \equiv b)$$

Fig. 5.6. (a) Euler-Reynold Relations
 (b) The Euler-Froude Function
 (c) The Scour Hole Depth Function
 (After Coleman, 1971)

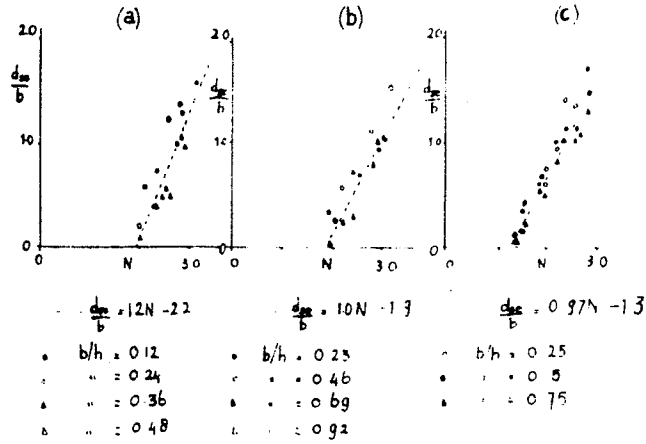
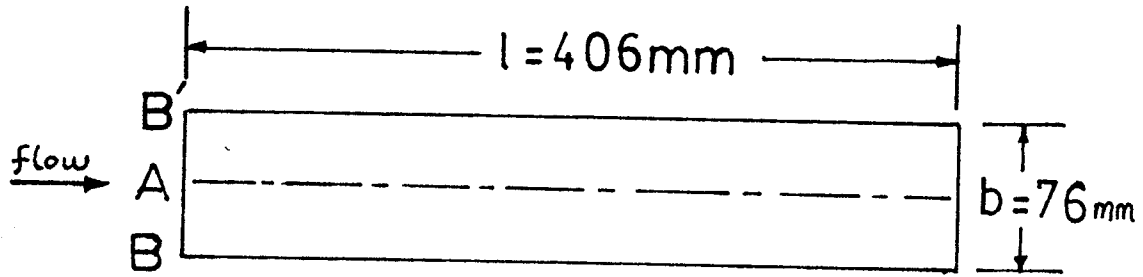
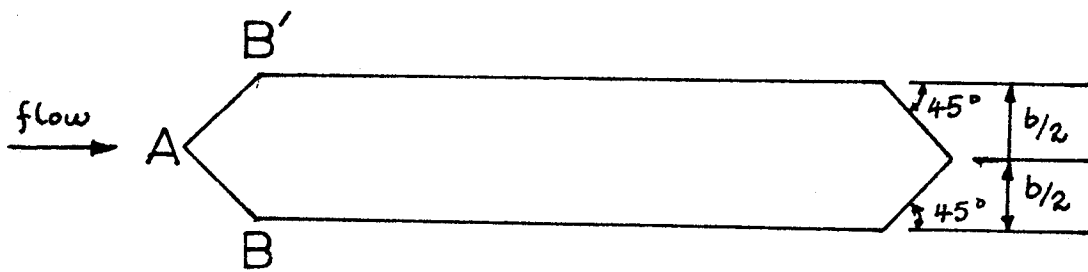


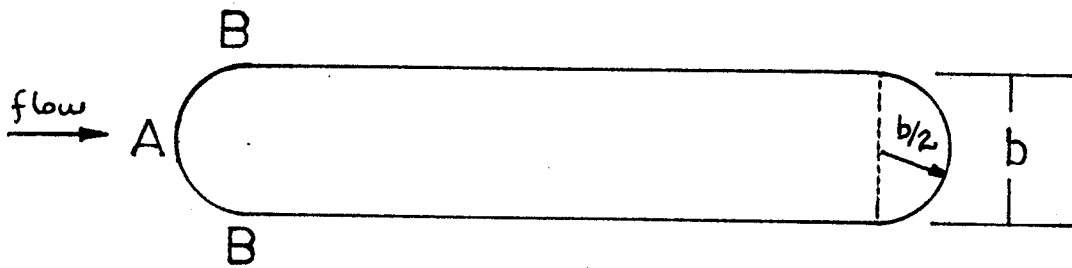
Fig. 5.7. Experimental Results of Baker [(a) and (b)] and Chabert and Engeldinger [(c)] for Clear-water Scour (After Baker, 1980)



(a)



(b)



(c)

Fig. 6.1. Geometrical Characteristics of Piers

(a) Square-Nosed Pier (SNP)

(b) Triangular-Nosed Pier (TNP)

(c) Round-Nosed Pier (RNP)

MECHANICAL ANALYSIS OF SOILS

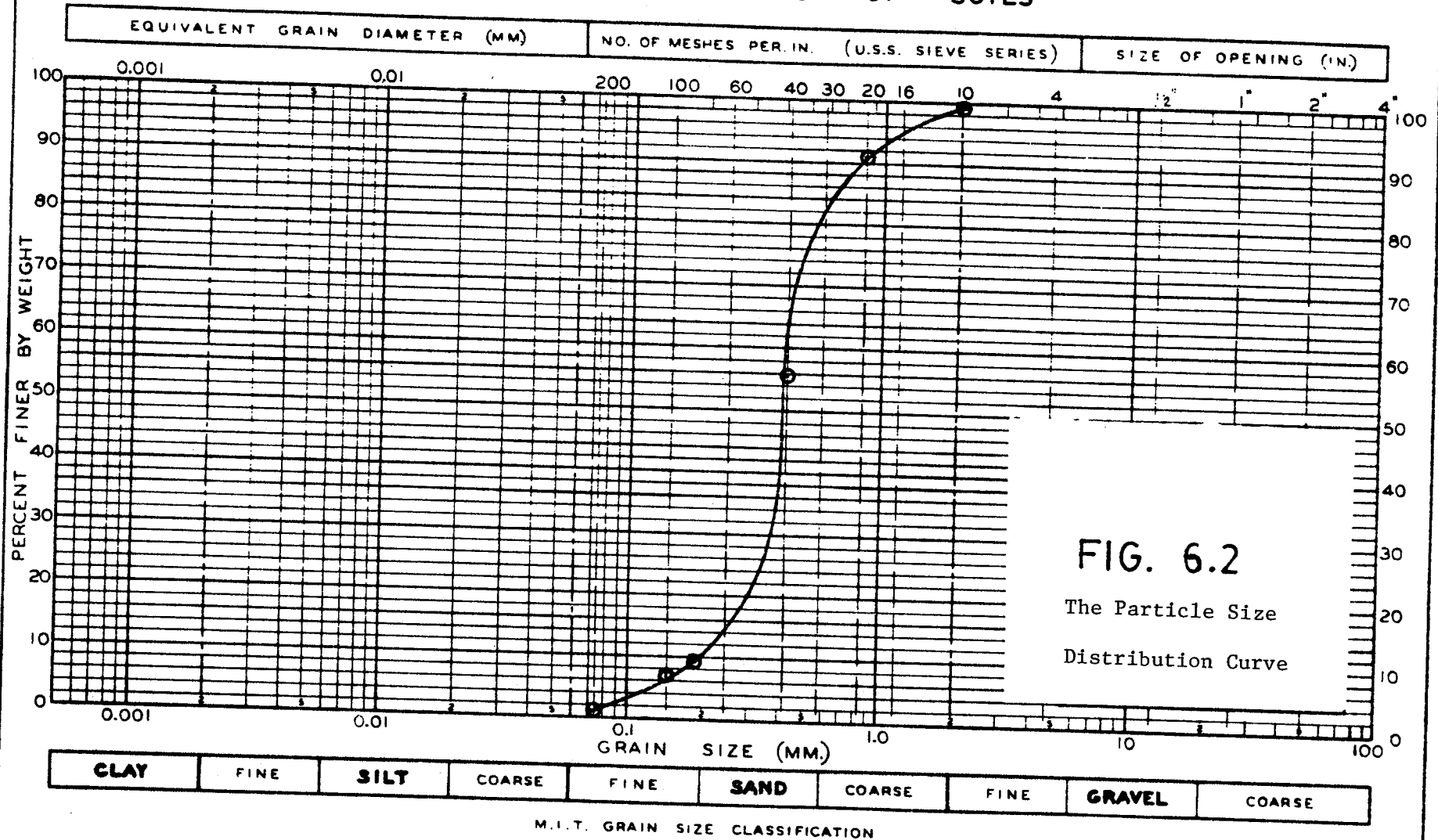


FIG. 6.2
The Particle Size
Distribution Curve

PROJECT: LOCAL SCOUR		SAMPLE NO. _____		SOIL MECHANICS LABORATORY DEPARTMENT OF CIVIL ENGINEERING UNIVERSITY OF MANITOBA FORT GARRY MANITOBA
PLOTTED: NDGM	DATE: MAY 23/80	REMARKS: D₅₀ = 0.37 mm		
CHECKED: _____	DATE: _____	G_s = 2.68		

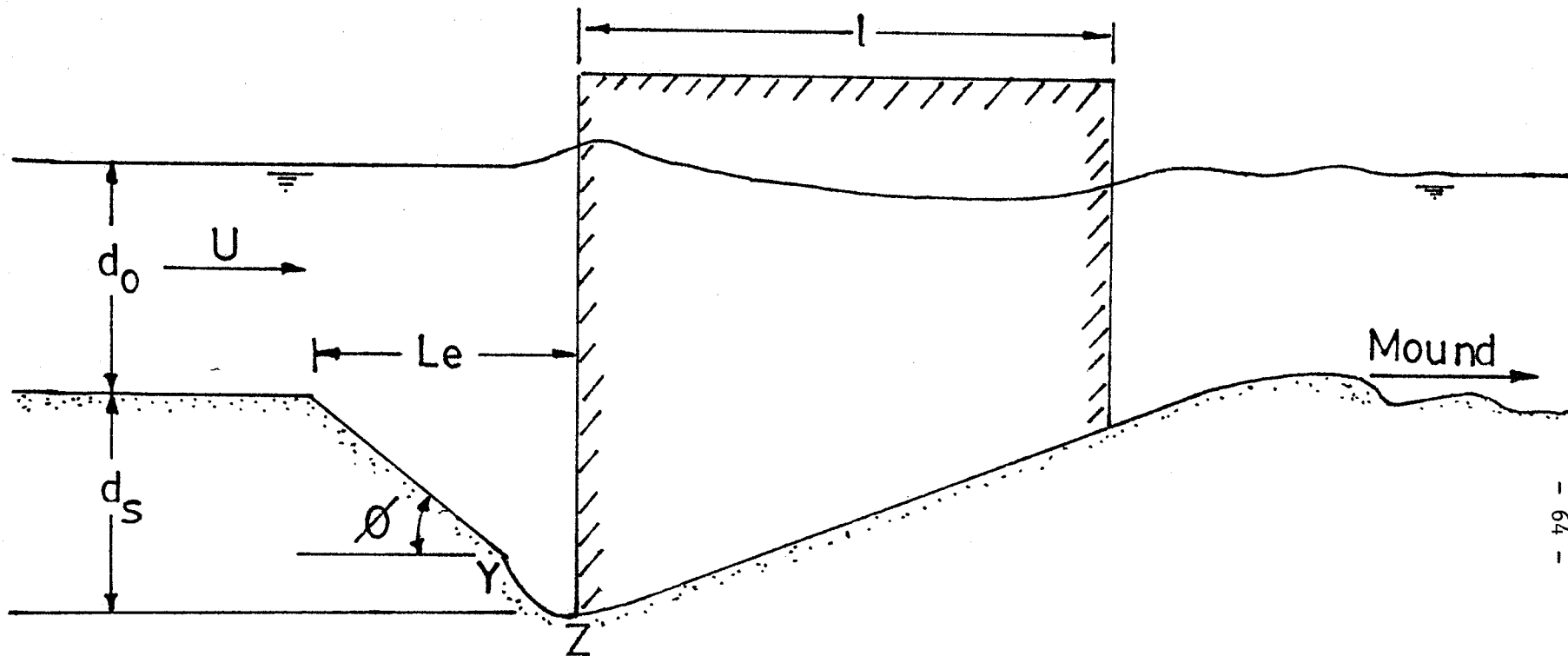


Fig. 6.3. Definition Sketch for Flow Around a Rectangular Pier

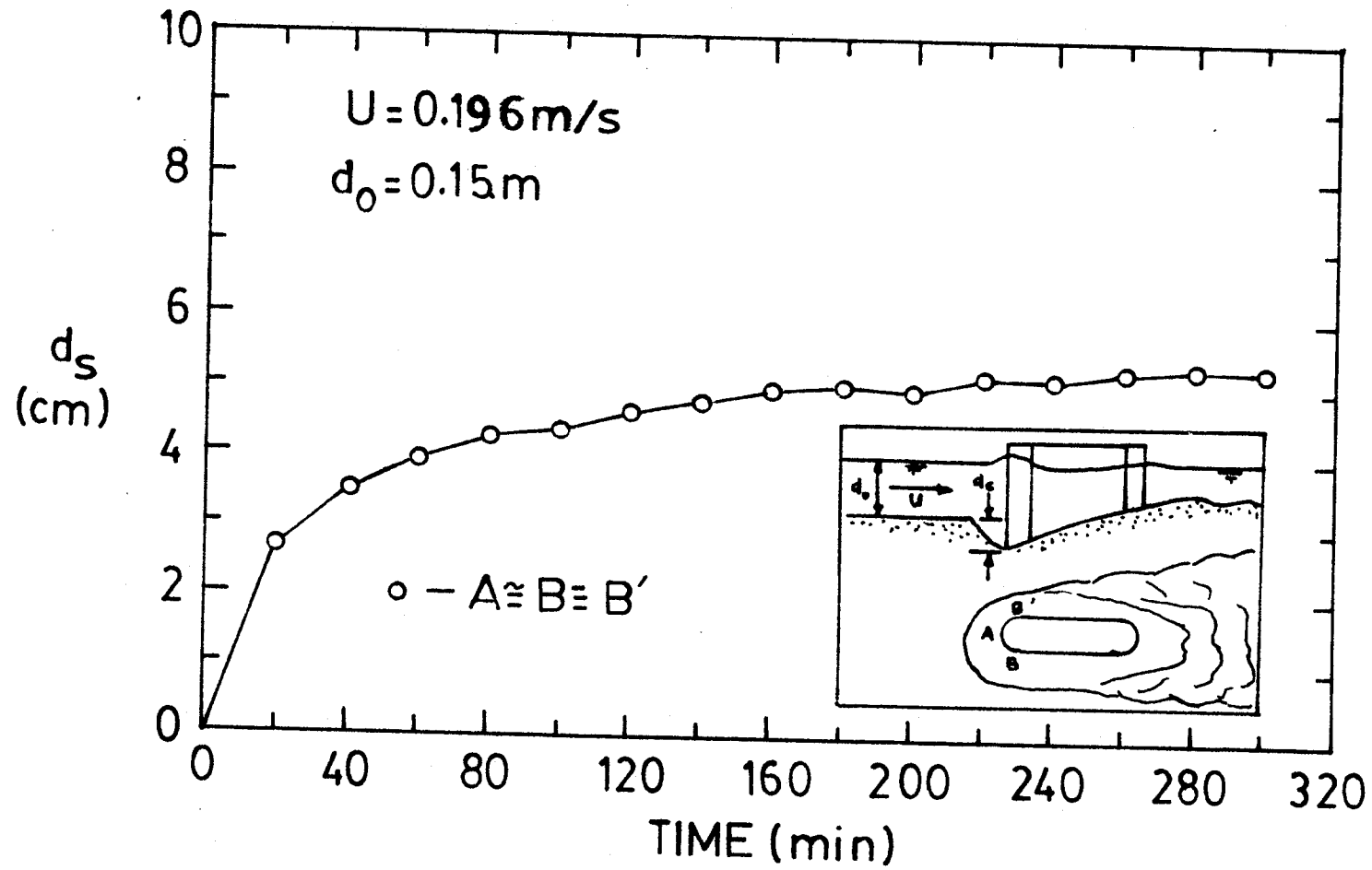


Fig. 6.4(a). The Variation of Scour Depth With Time:
 Round-Nosed Pier

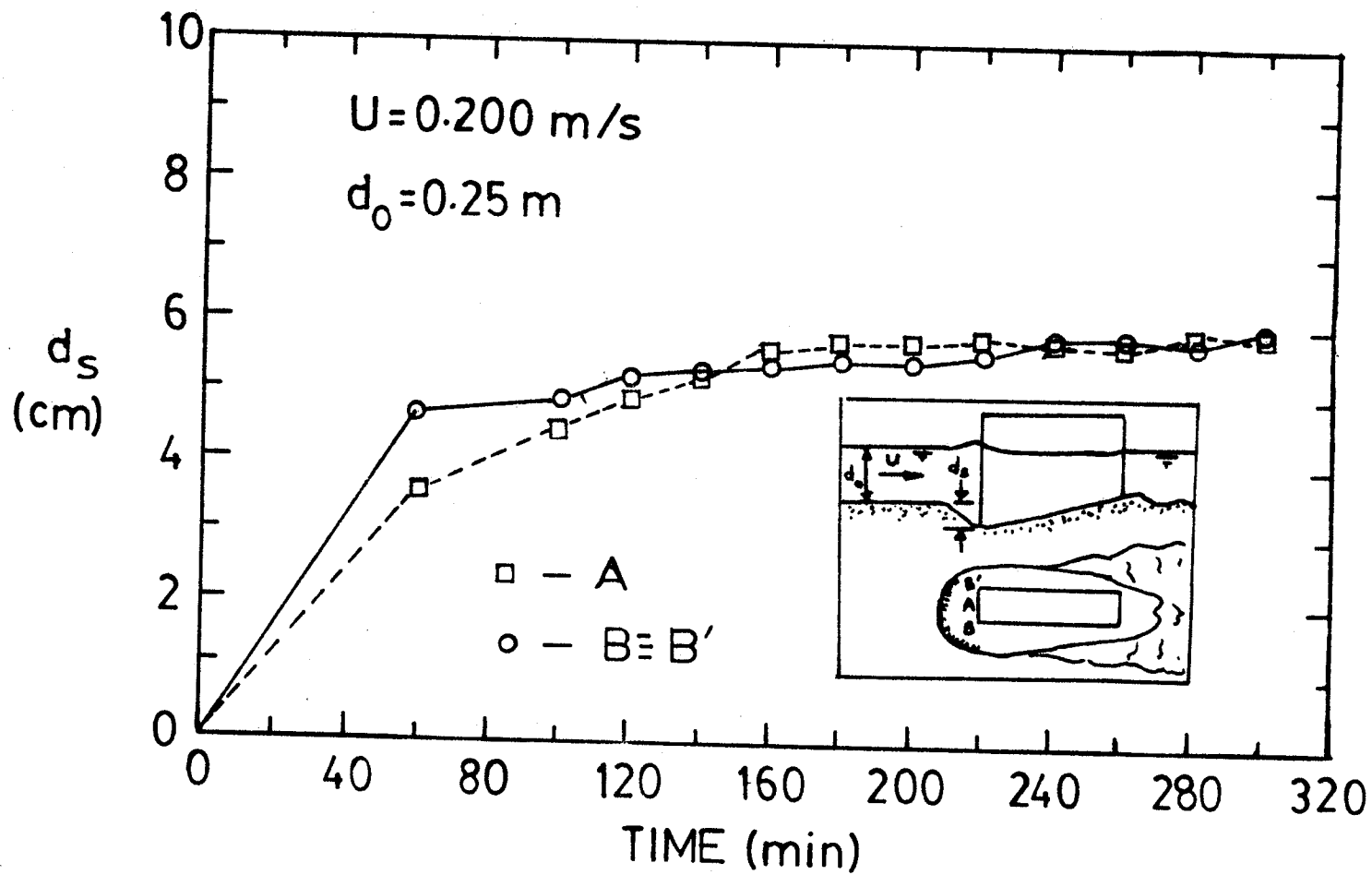


Fig. 6.4(b). The Variation of Scour Depth With Time:
 Triangular-Nosed Pier

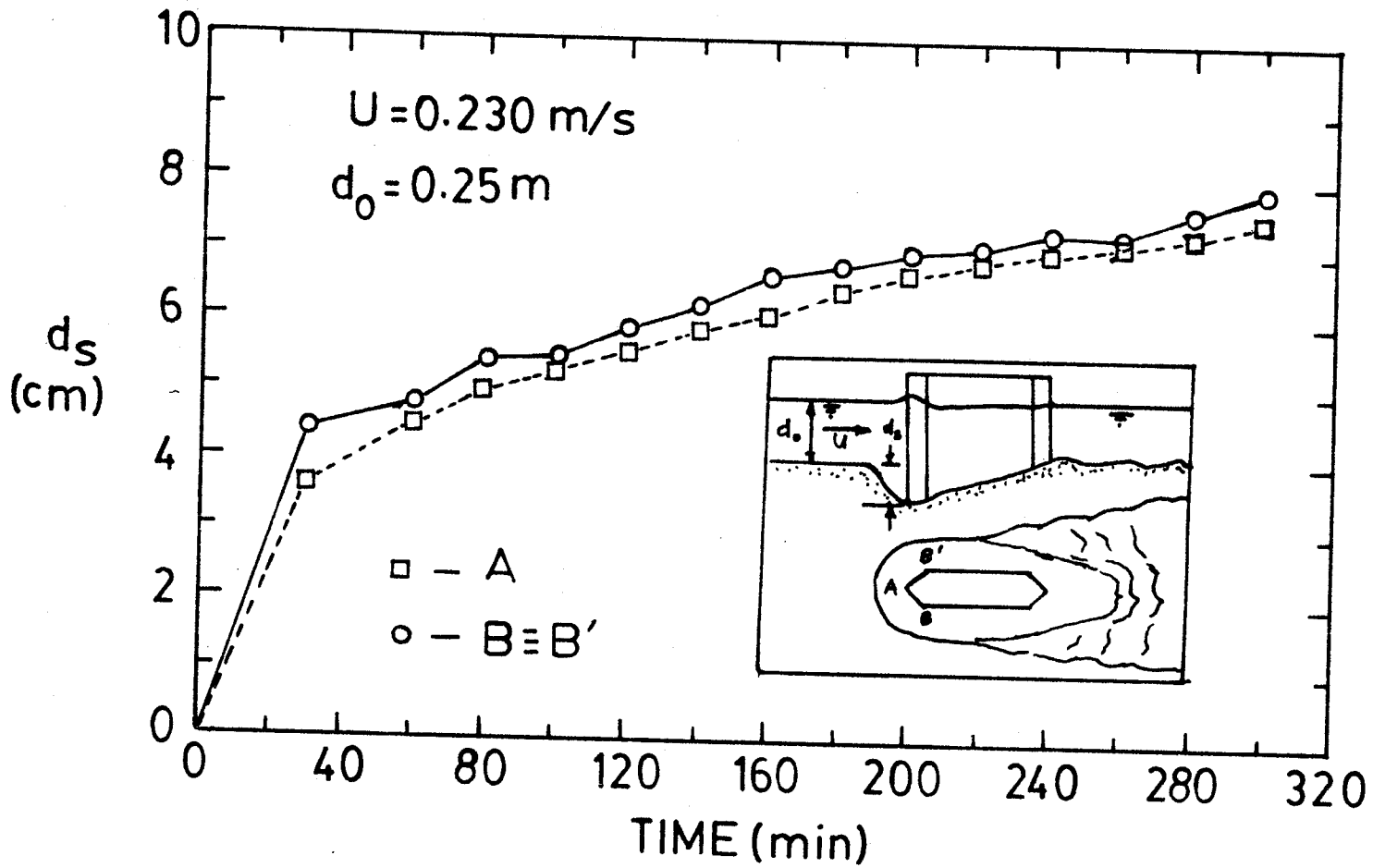


Fig. 6.4(c). The Variation of Scour Depth With Time:
 Triangular-Nosed Pier

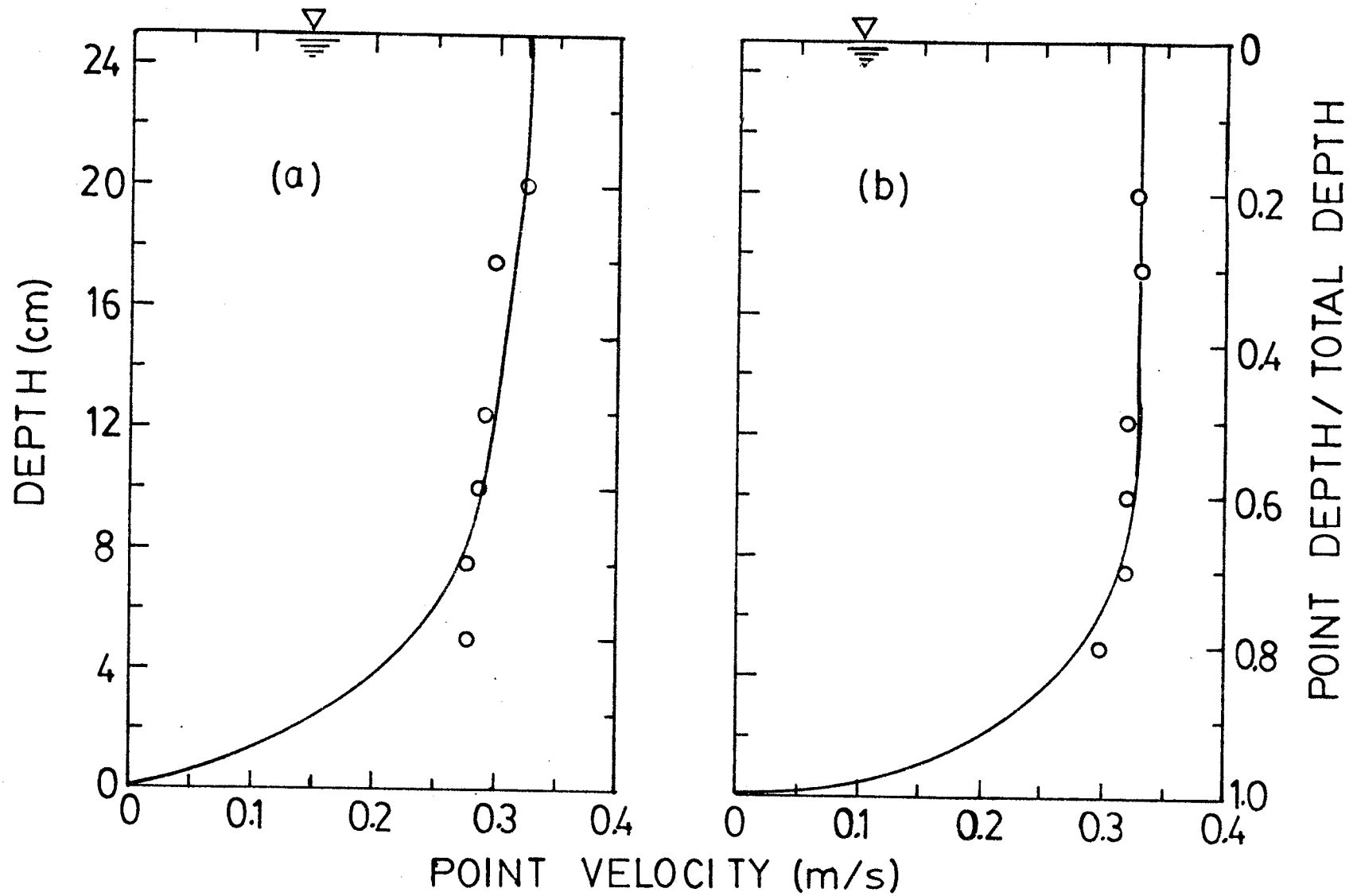


Fig. 7.1 Velocity Profile at the Threshold of Sediment Movement
 (a) on the Wood Bed (b) on the Sand Bed

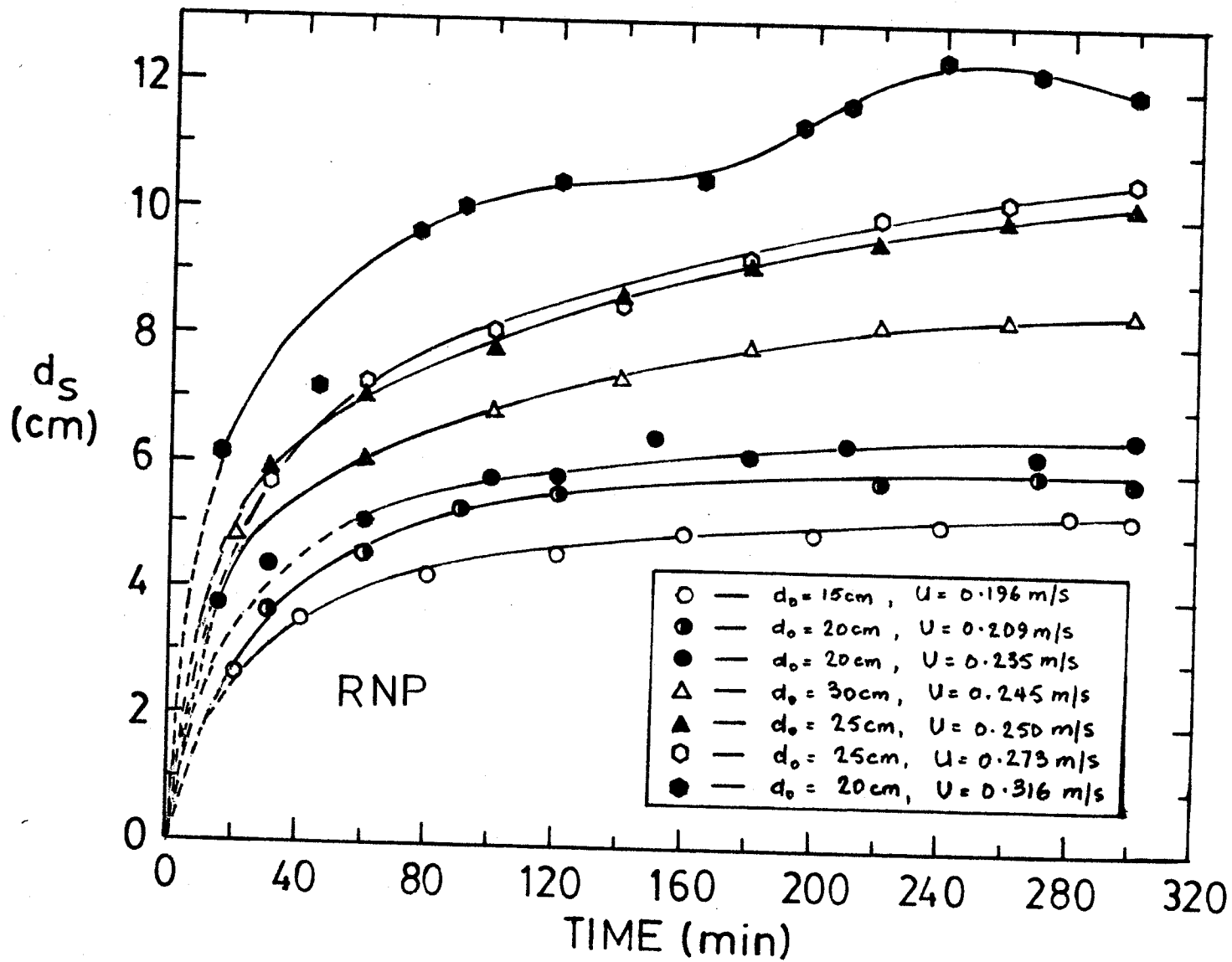


Fig. 7.2(a). The Variation of Scour Depth With Time for Different Flow Conditions: Round-Nosed Pier

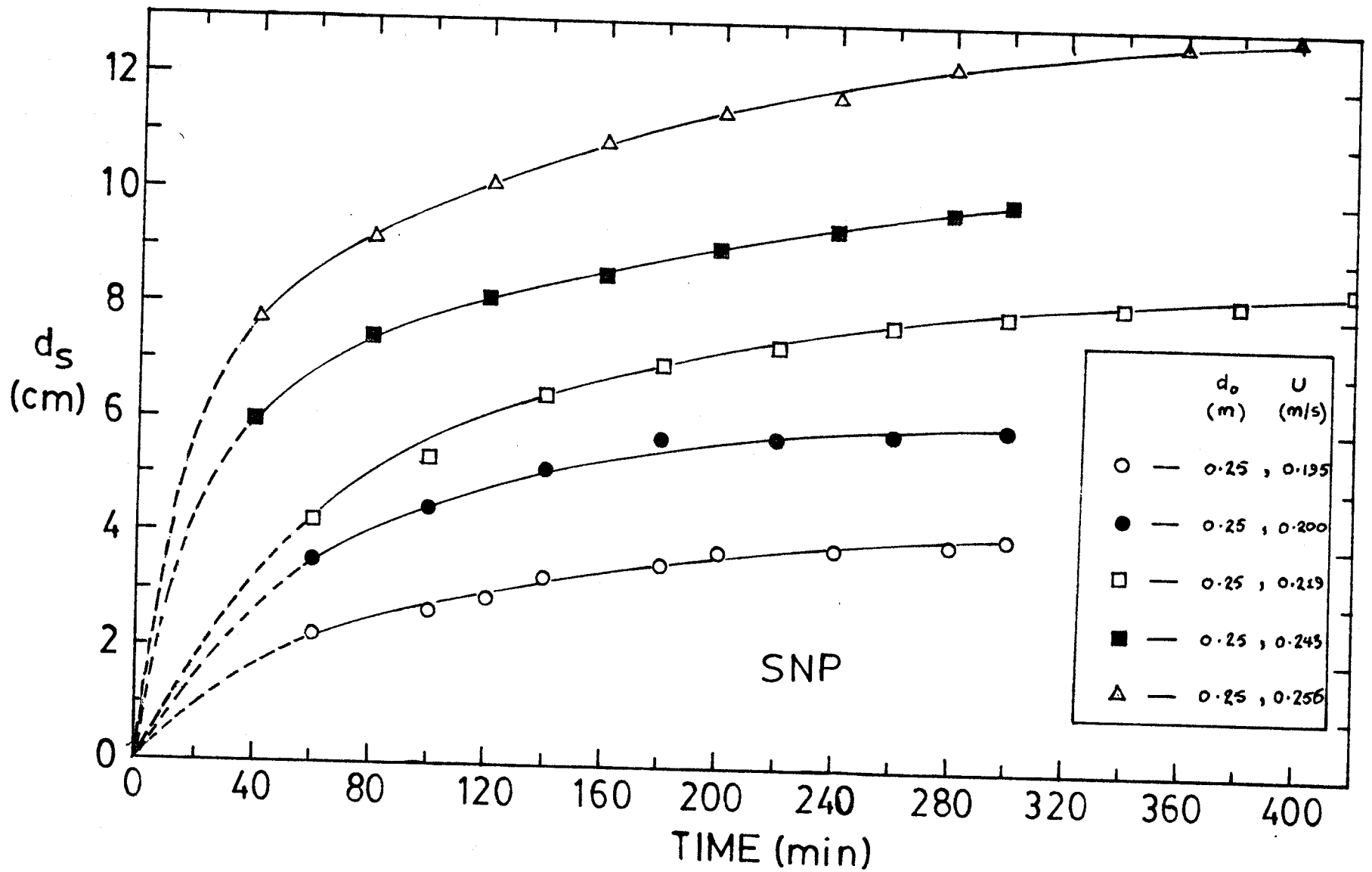


Fig. 7.2(b). The Variation of Scour Depth With Time for Different Flow Conditions: Square-Nosed Pier

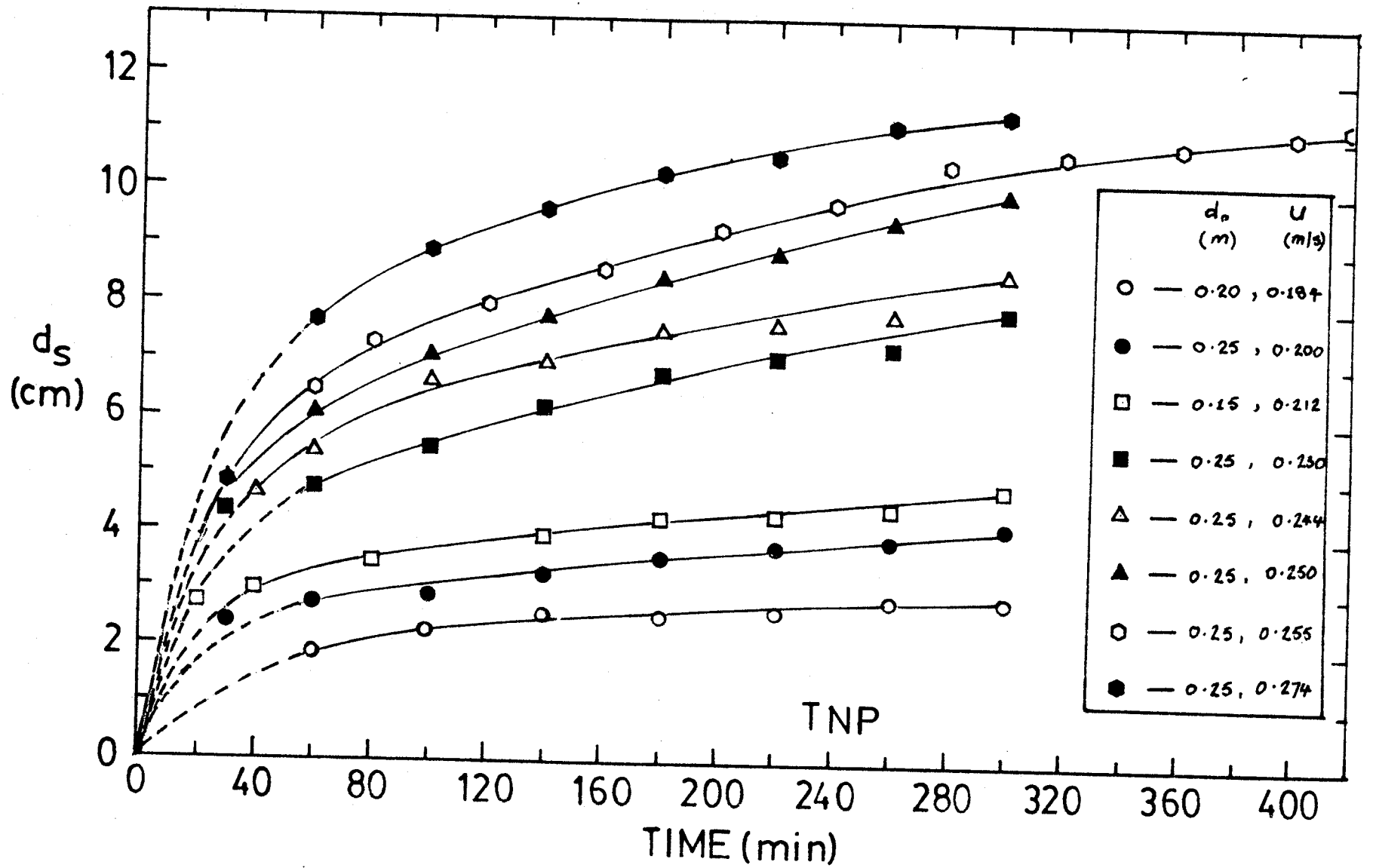


Fig. 7.2(c). The Variation of Scour Depth With Time for Different Flow Conditions: Triangular-Nosed Pier

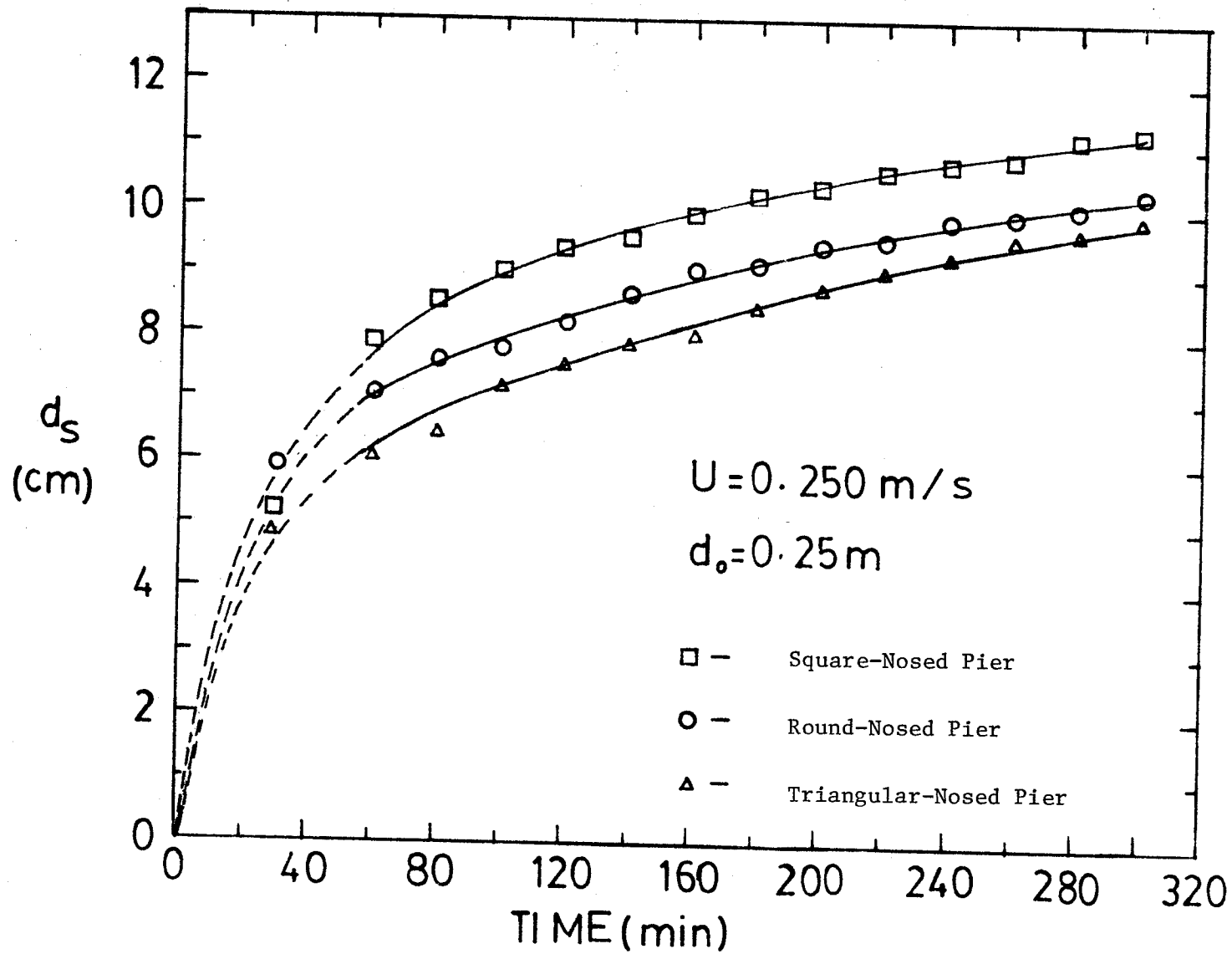


Fig. 7.3. The Influence of the Pier Shape

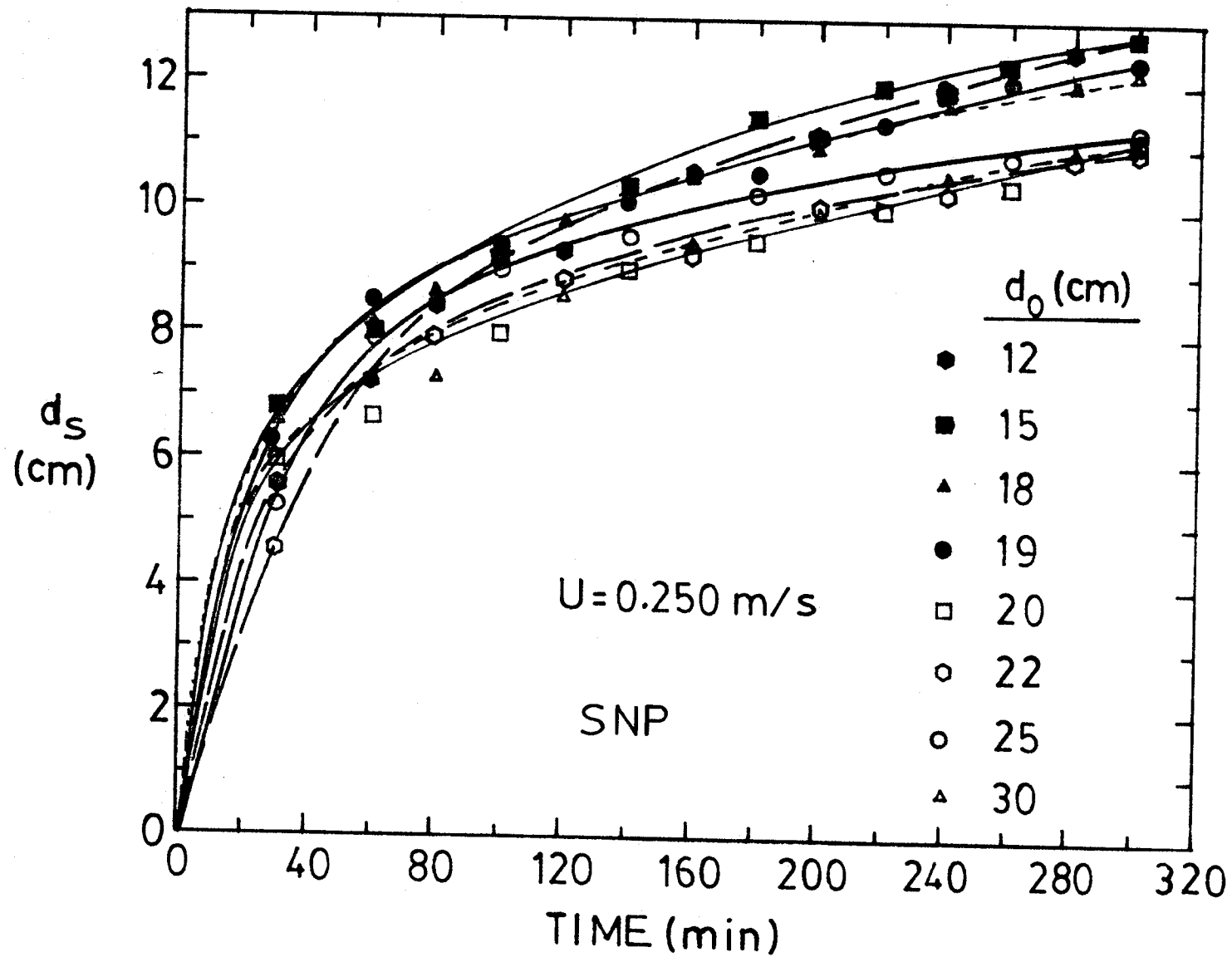


Fig. 7.4. The Variation of Scour Depth With Time for Different Flow Depths

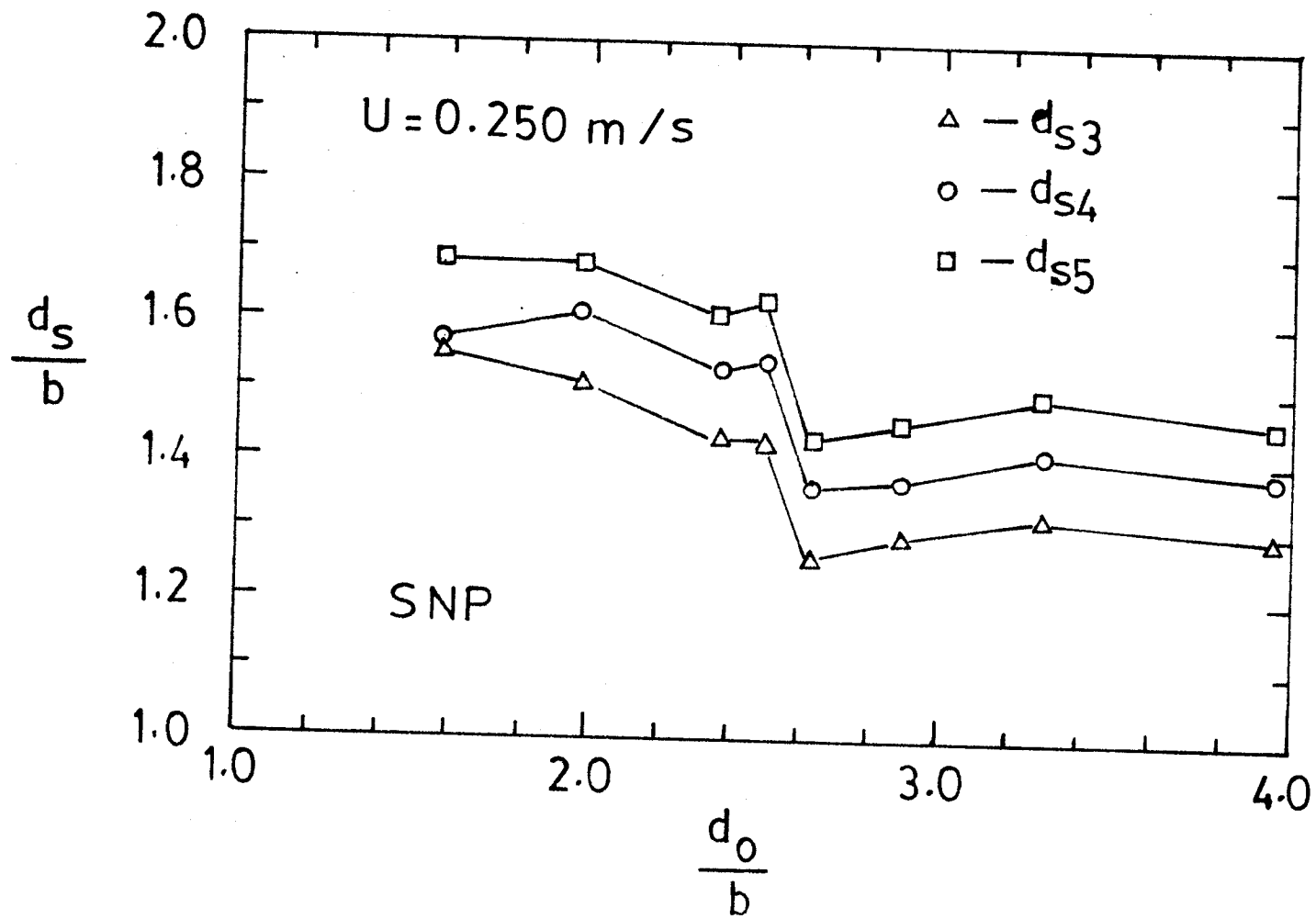


Fig. 7.5. The Influence of the Depth of Flow

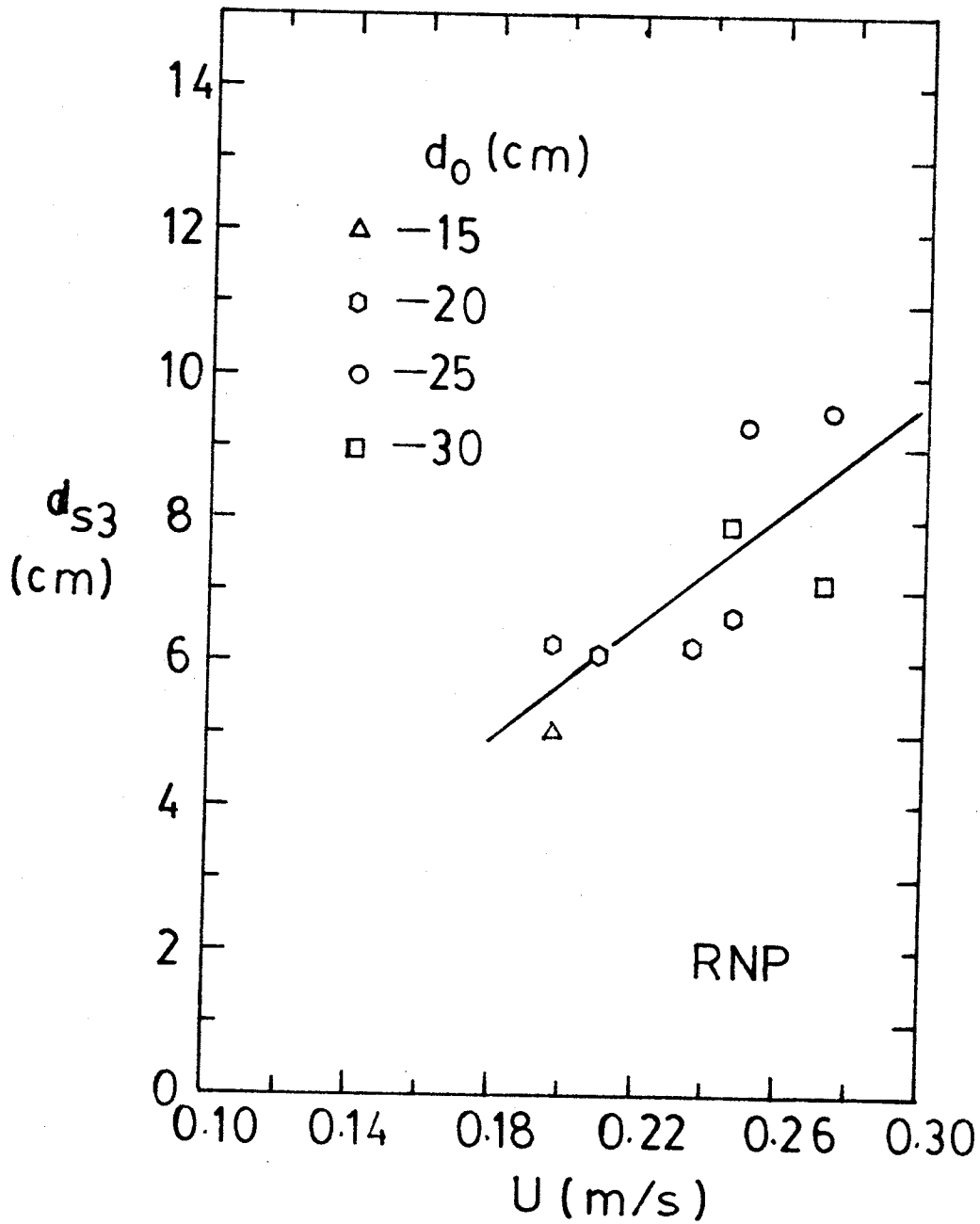


Fig. 7.6(a). The Influence of Velocity: 3-Hour Scour Depth for the Round-Nosed Pier

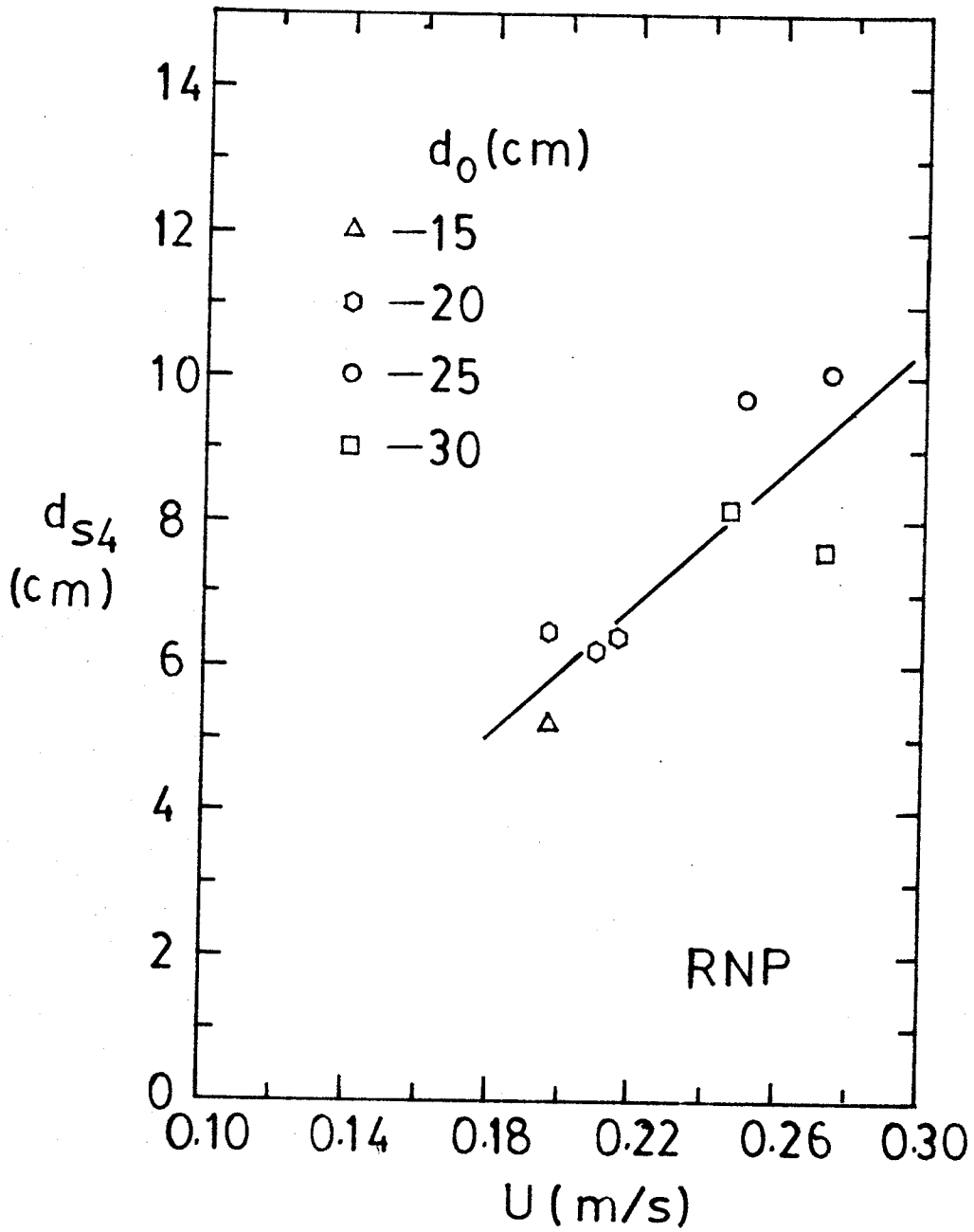


Fig. 7.6(b). The Influence of Velocity: 4-Hour Scour Depth for the Round-Nosed Pier

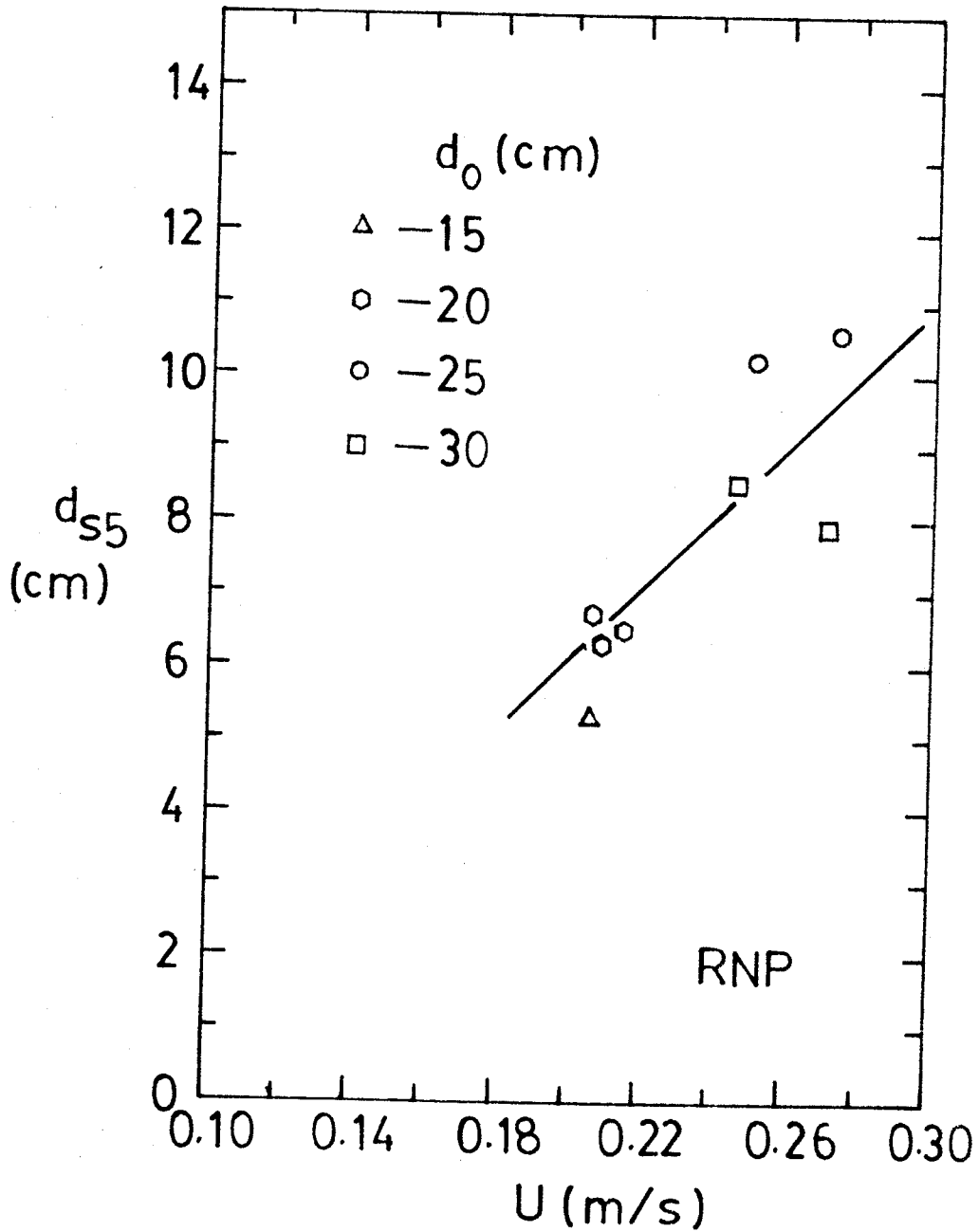


Fig. 7.6(c). The Influence of Velocity: 5-Hour Scour Depth for the Round-Nosed Pier

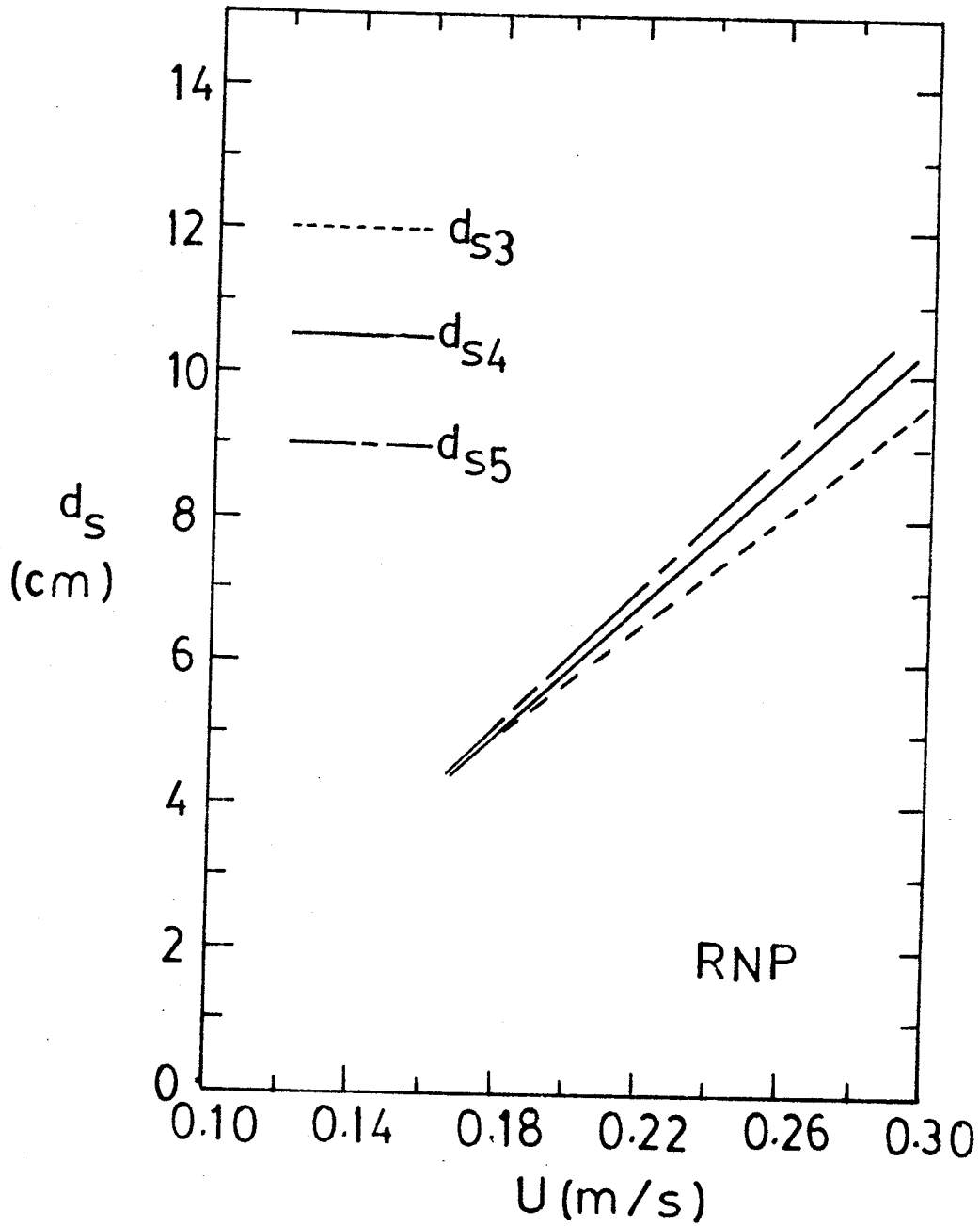
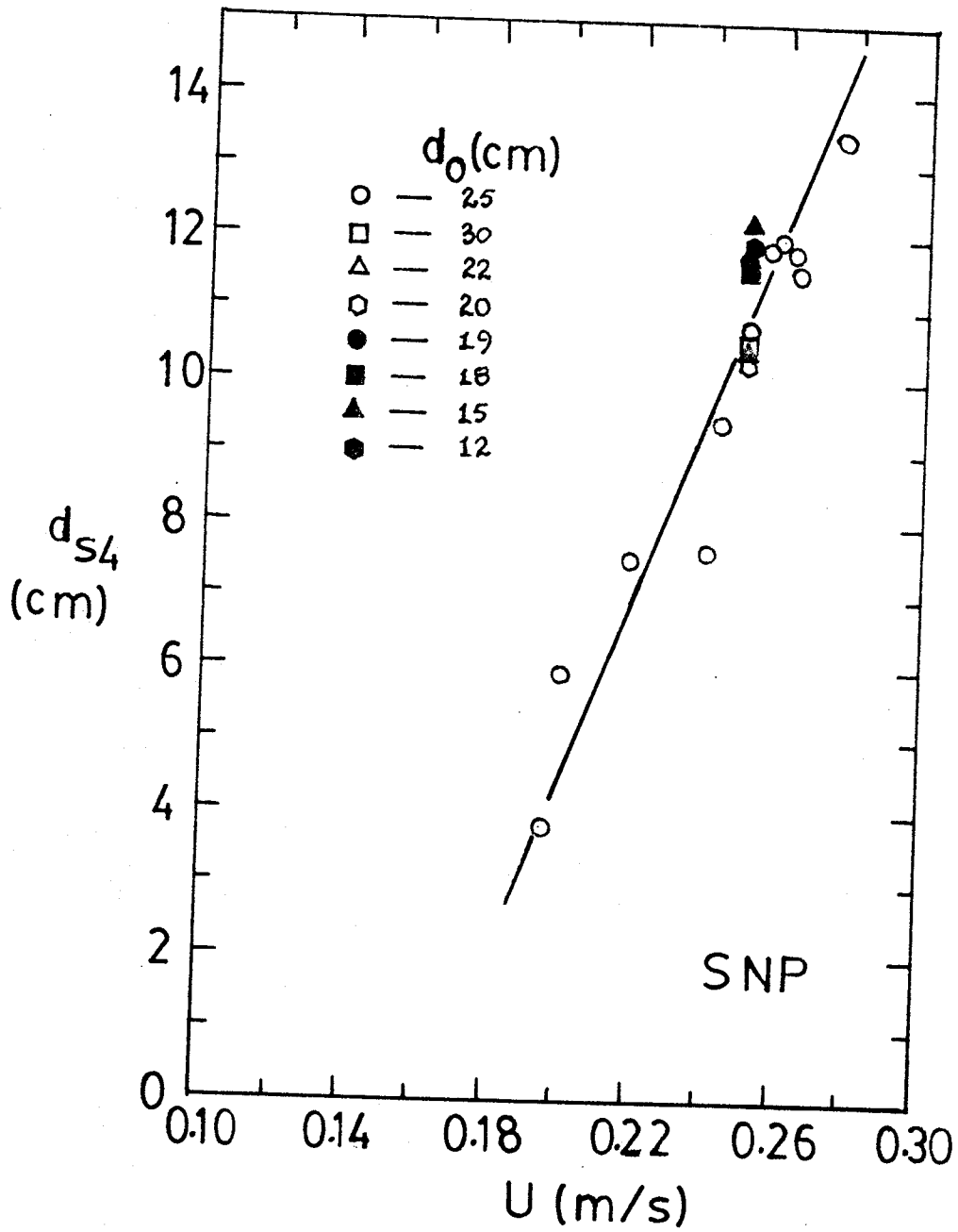


Fig. 7.6(d): The Influence of Velocity: Comparison of the 3-Hour, 4-Hour, and 5-Hour Scour Depths for the Round-Nosed Pier



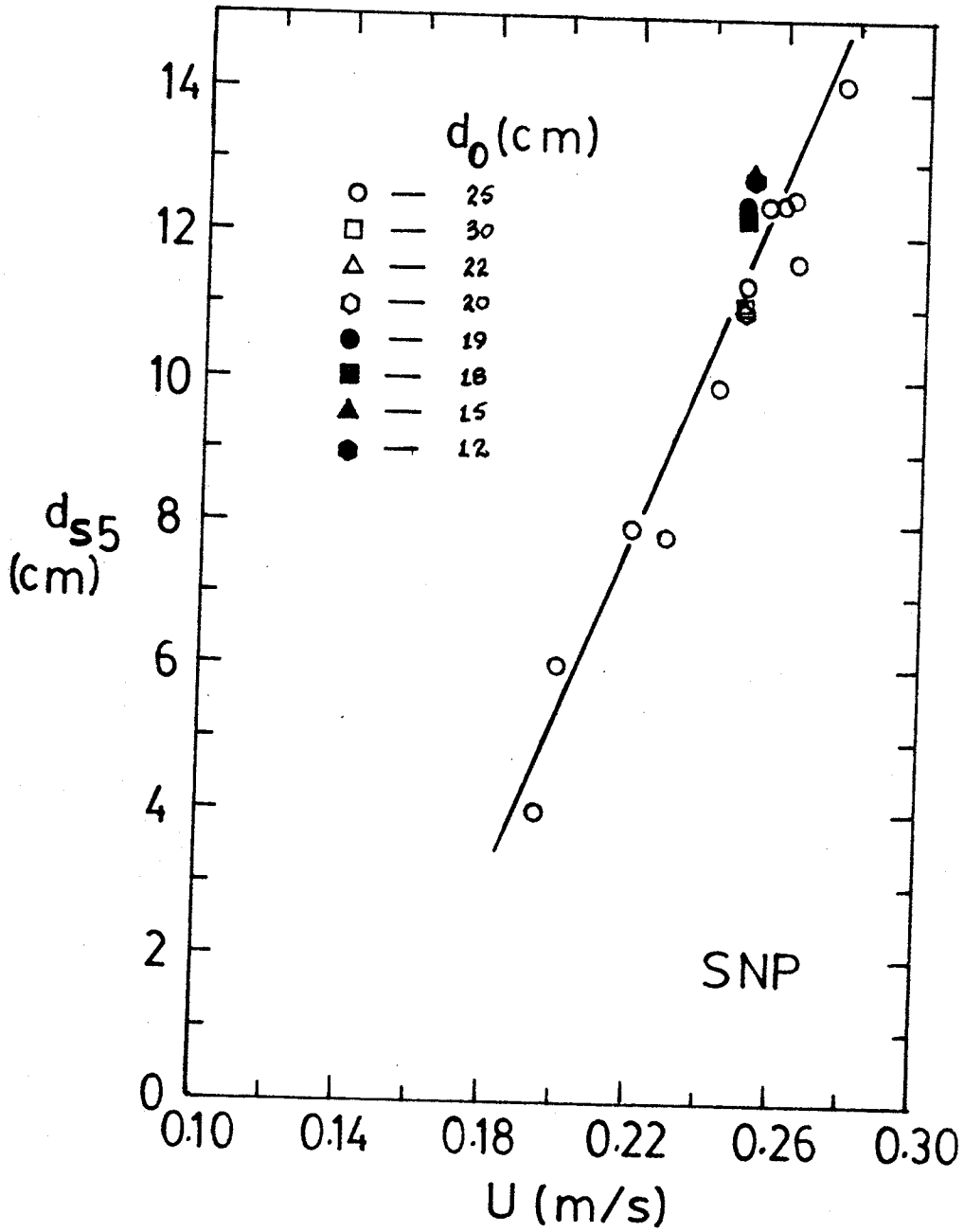


Fig. 7.7(c). The Influence of Velocity: 5-Hour Scour Depth for the Square-Nosed Pier

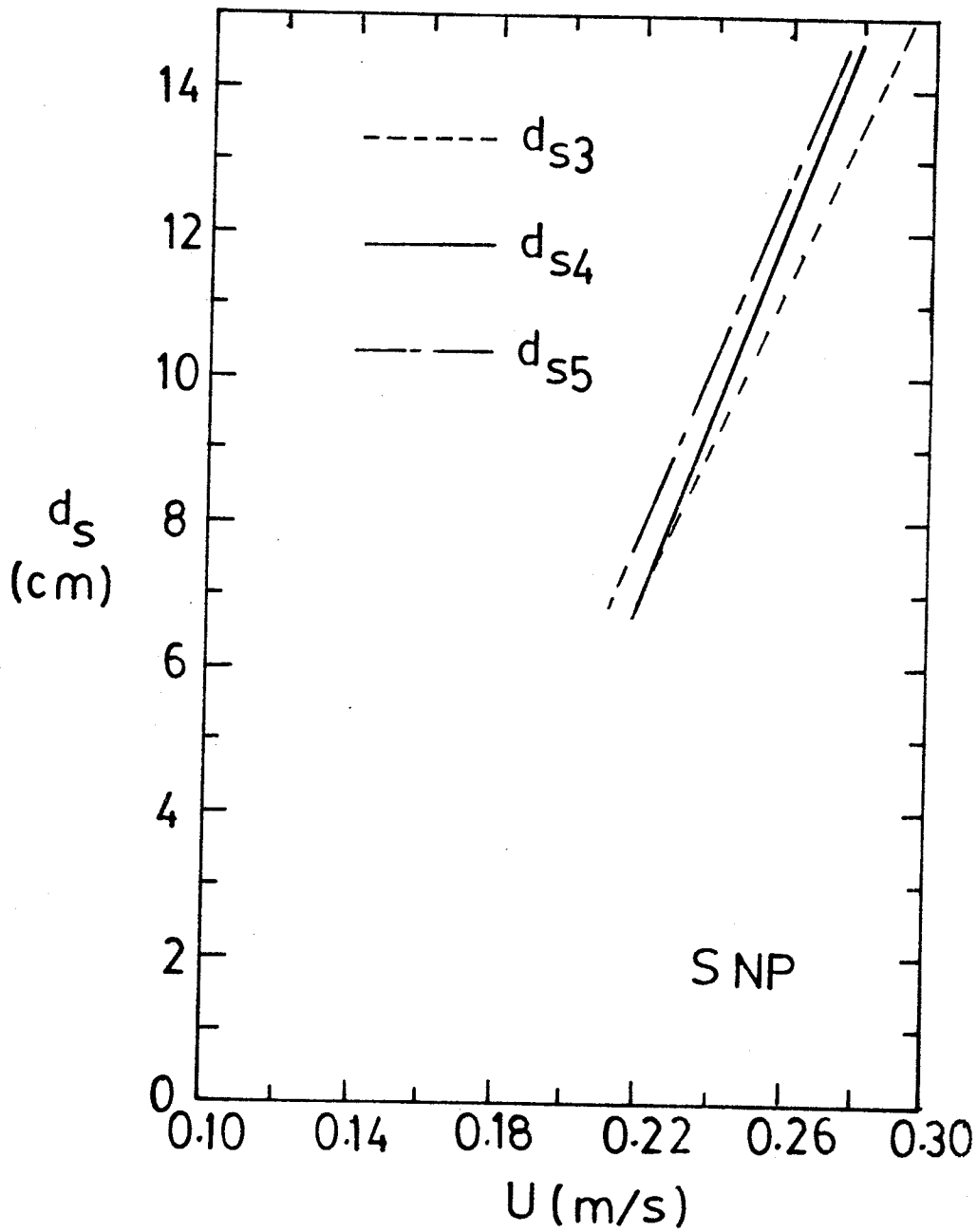


Fig. 7.7(d). The Influence of Velocity: Comparison of the 3-Hour, 4-Hour, and 5-Hour Scour Depths for the Square-Nosed Pier

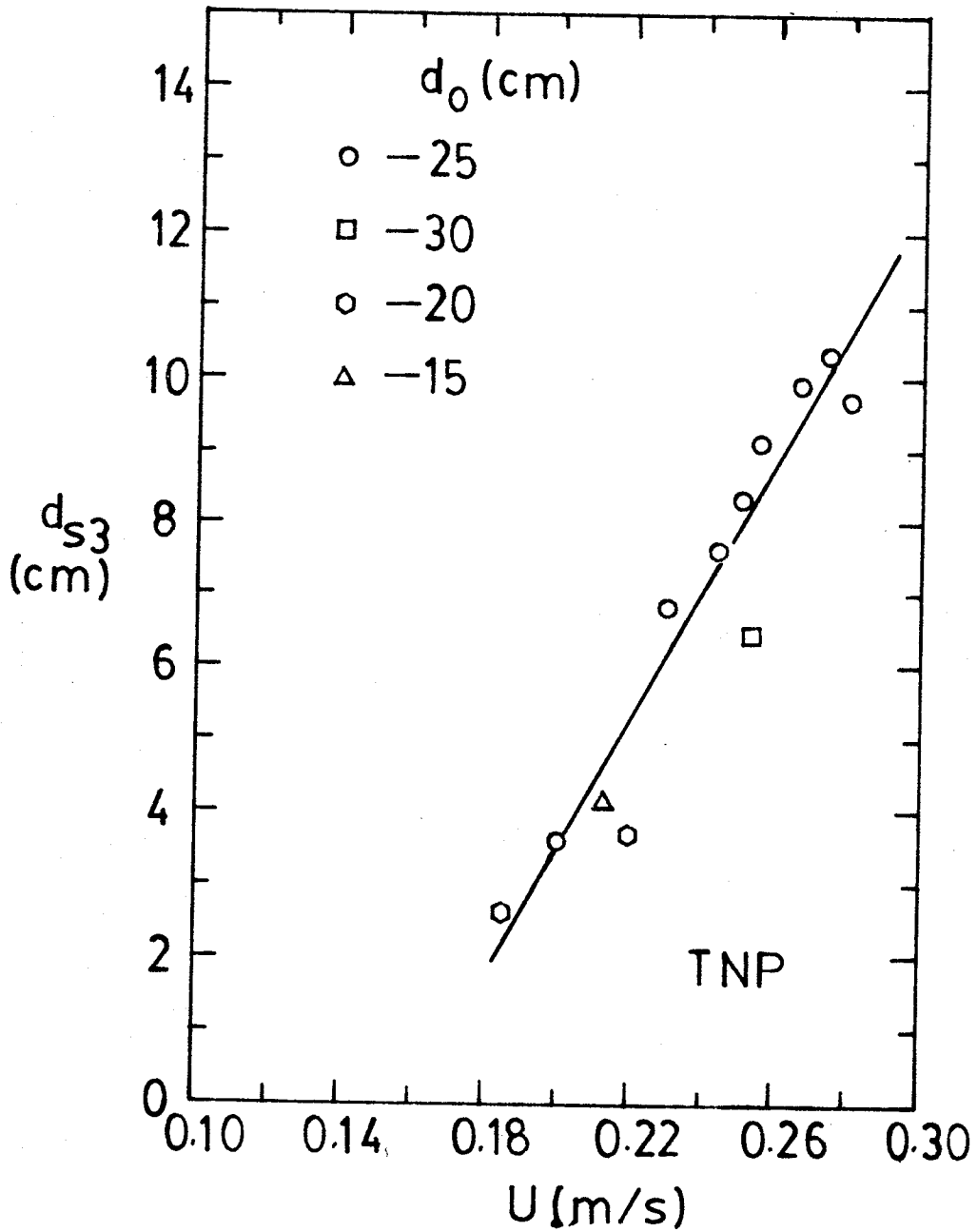


Fig. 7.8(a). The Influence of Velocity: 3-Hour Scour Depth for the Triangular-Nosed Pier

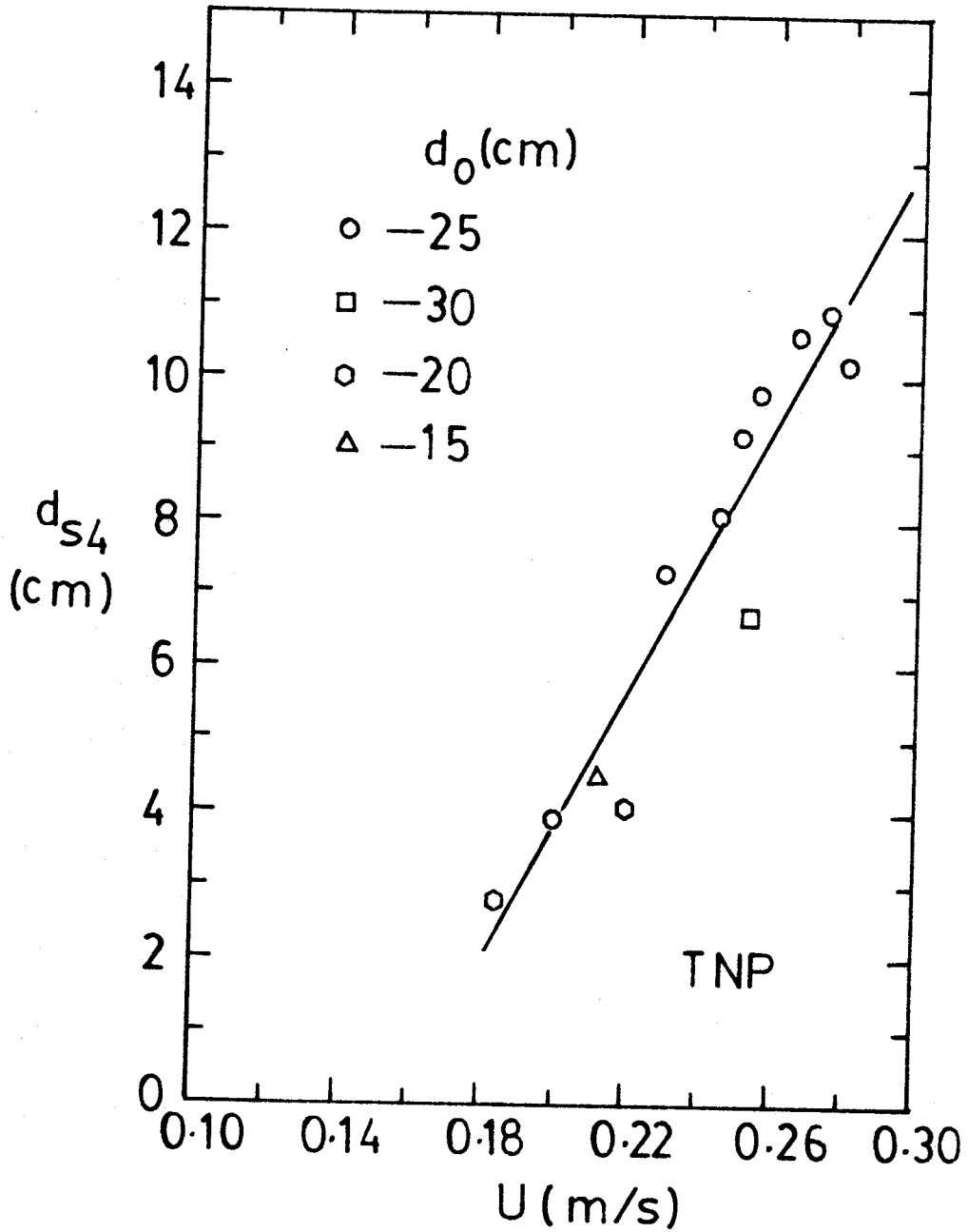


Fig. 7.8(b). Influence of Velocity: 4-Hour Scour Depth
for the Triangular-Nosed Pier

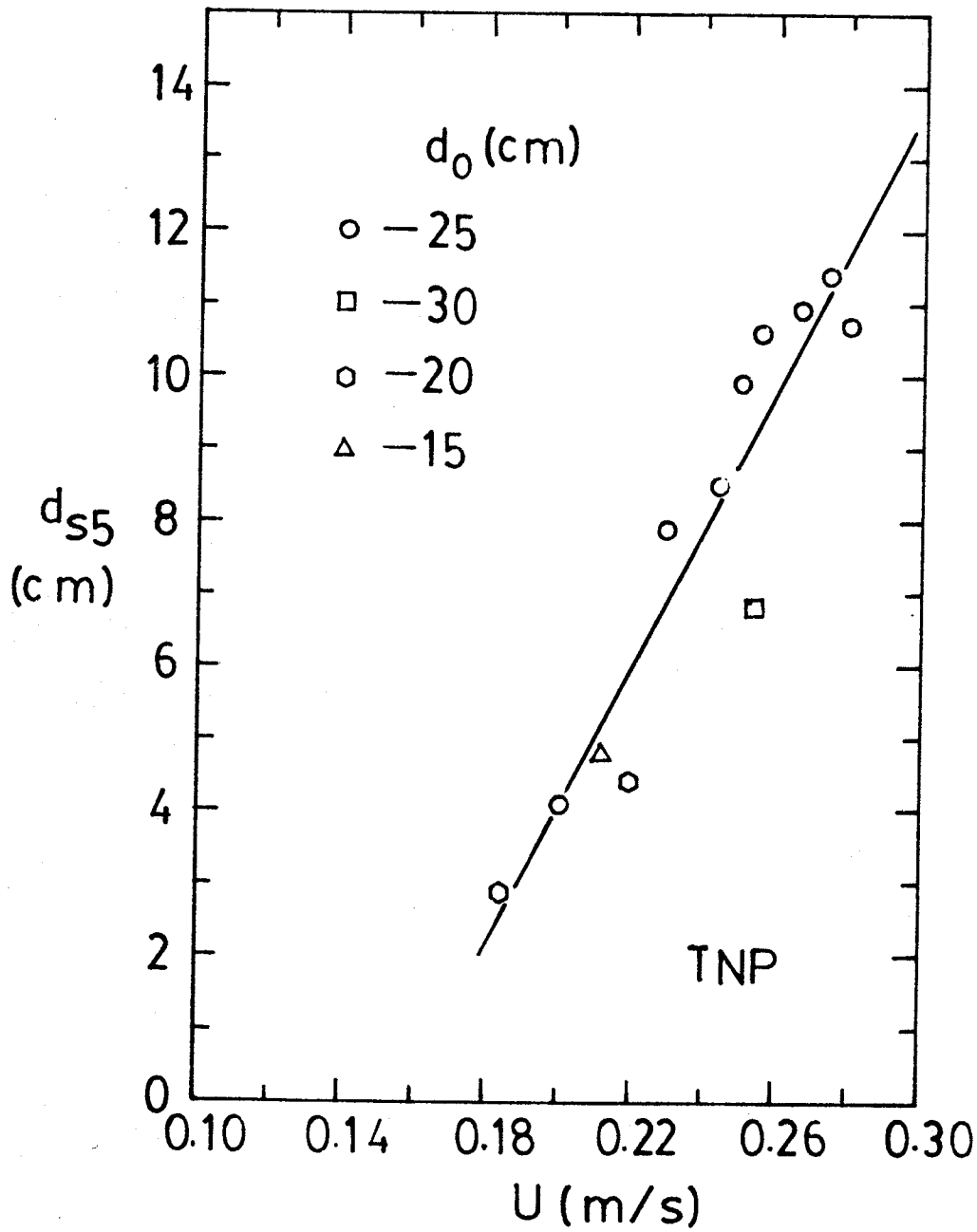


Fig. 7.8(c). The Influence of Velocity: 5-Hour Scour Depth for the Triangular-Nosed Pier

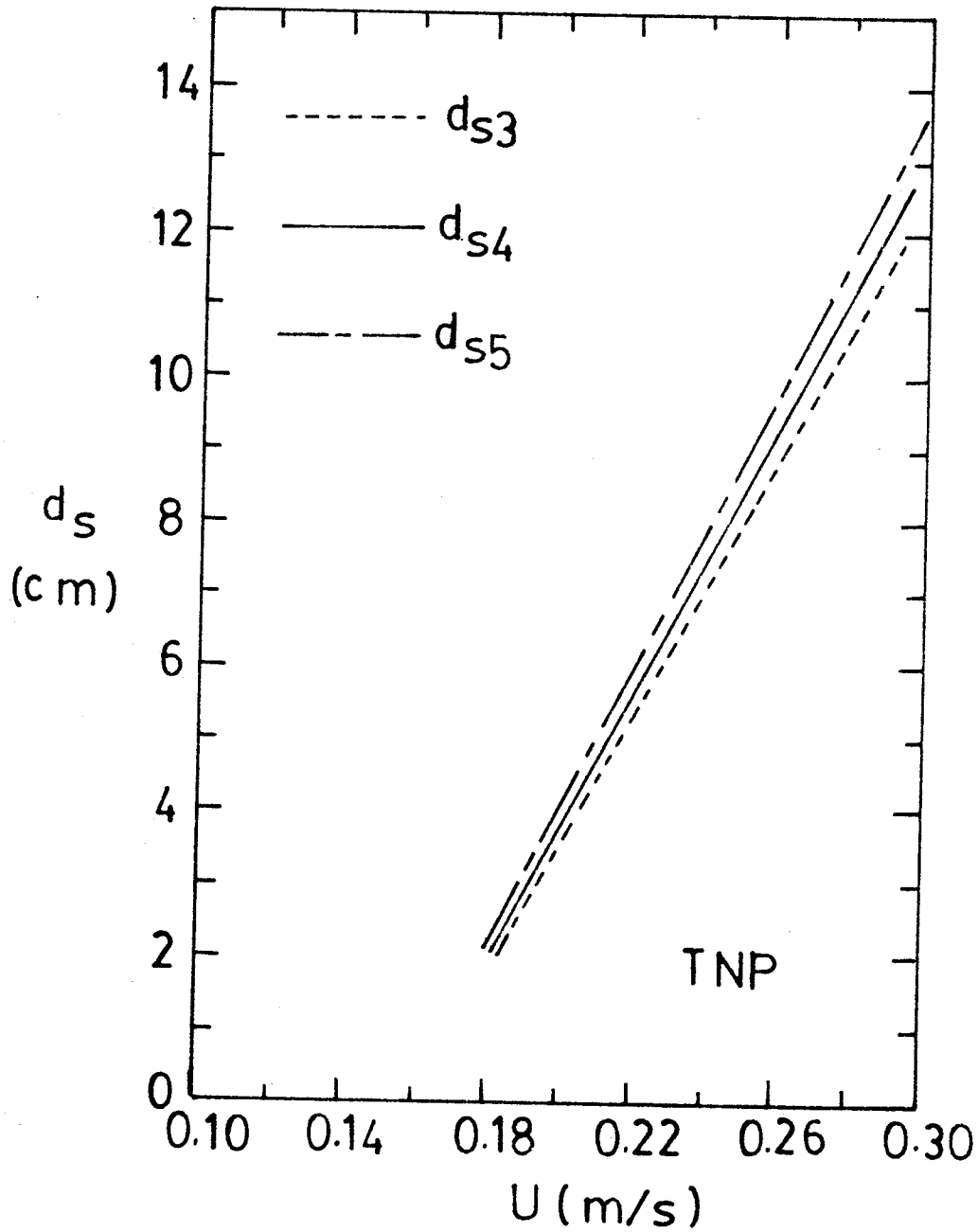


Fig. 7.8(d). The Influence of Velocity: Comparison of the 3-Hour, 4-Hour, and 5-Hour Scour Depths for the Triangular-Nosed Pier

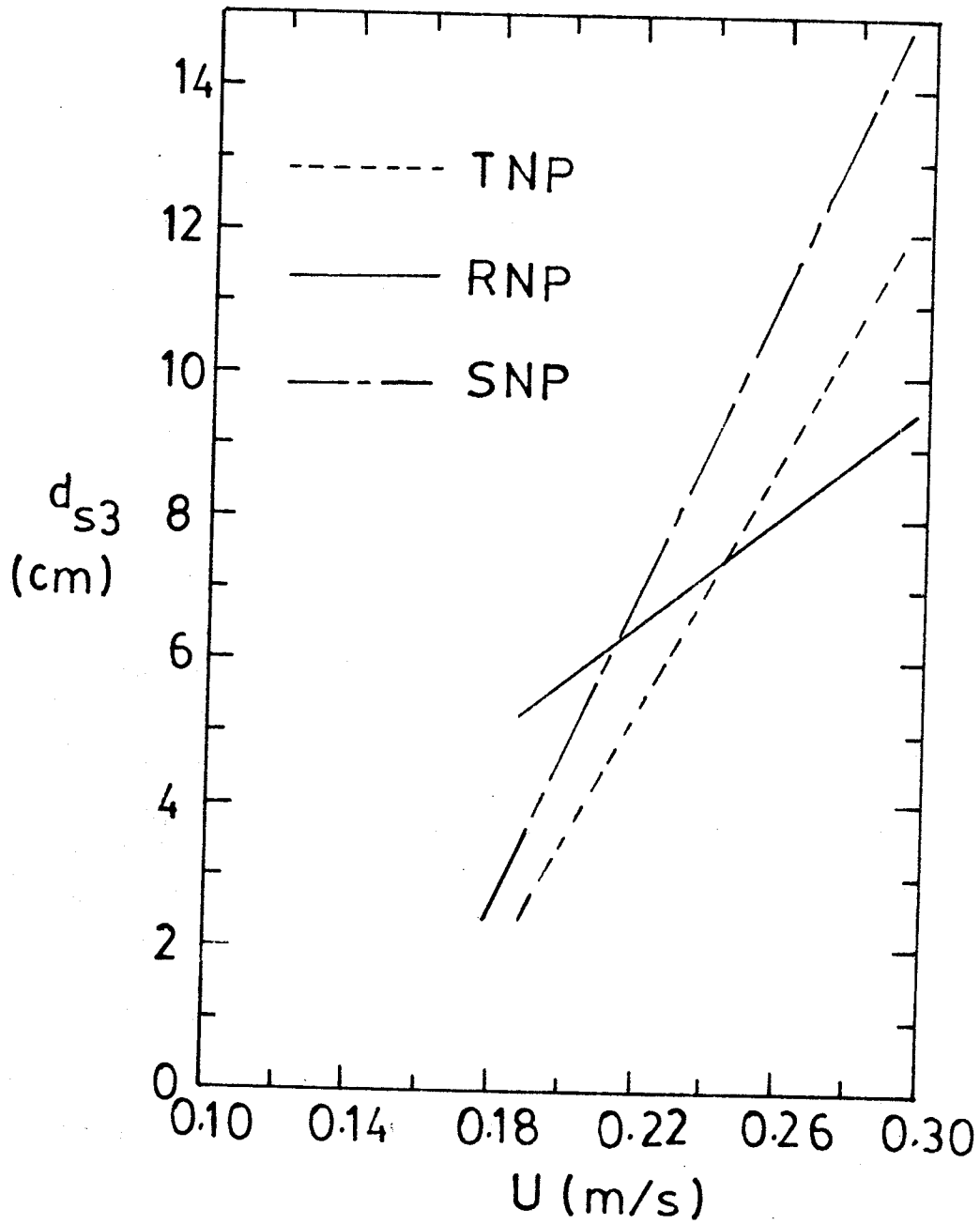


Fig. 7.9(a). Comparison of the Linear Regression Lines for the Different Pier Shapes: 3-Hour Scour Depth

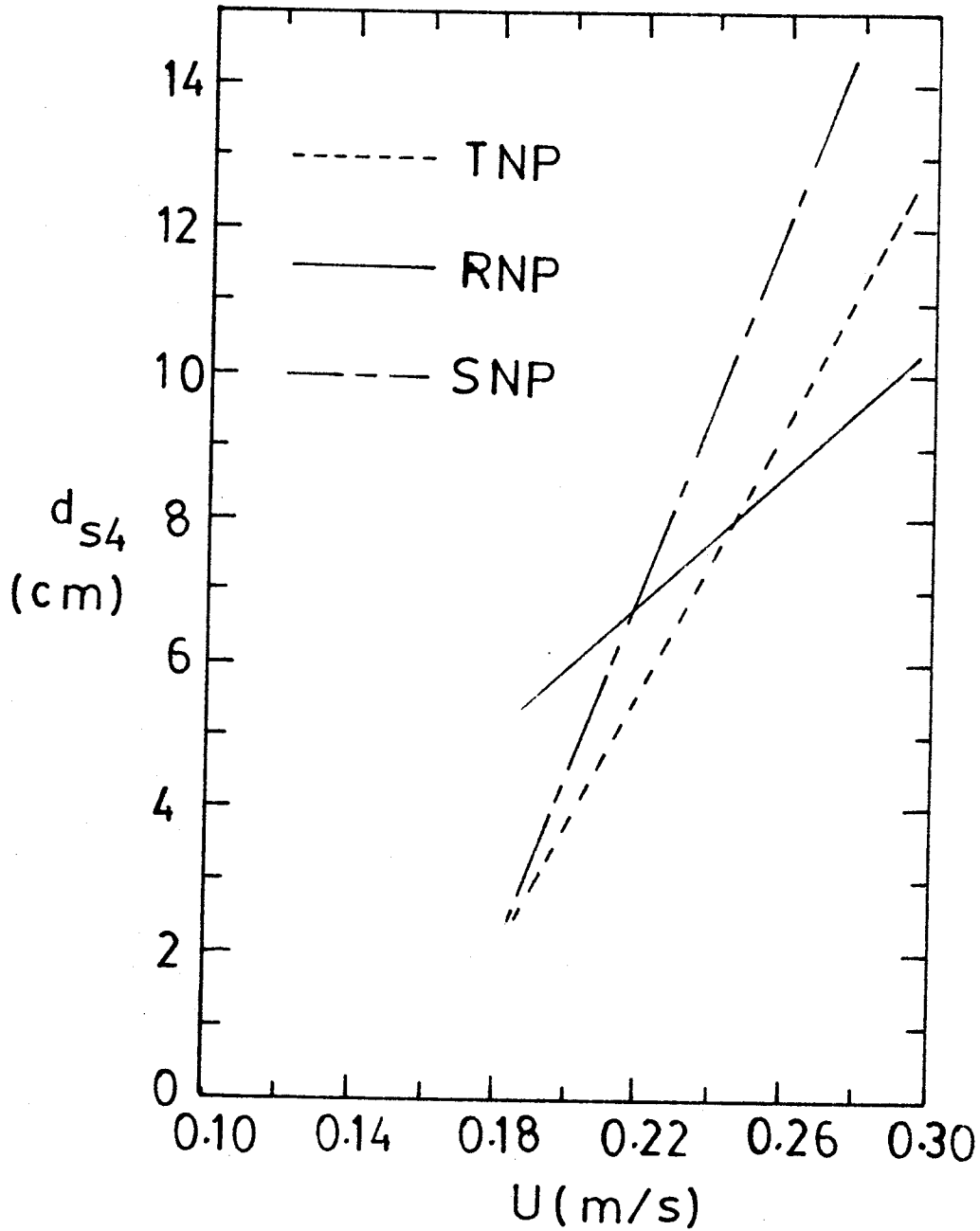


Fig. 7.9(b). Comparison of the Linear Regression Lines for the Different Pier Shapes: 4-Hour Scour Depth

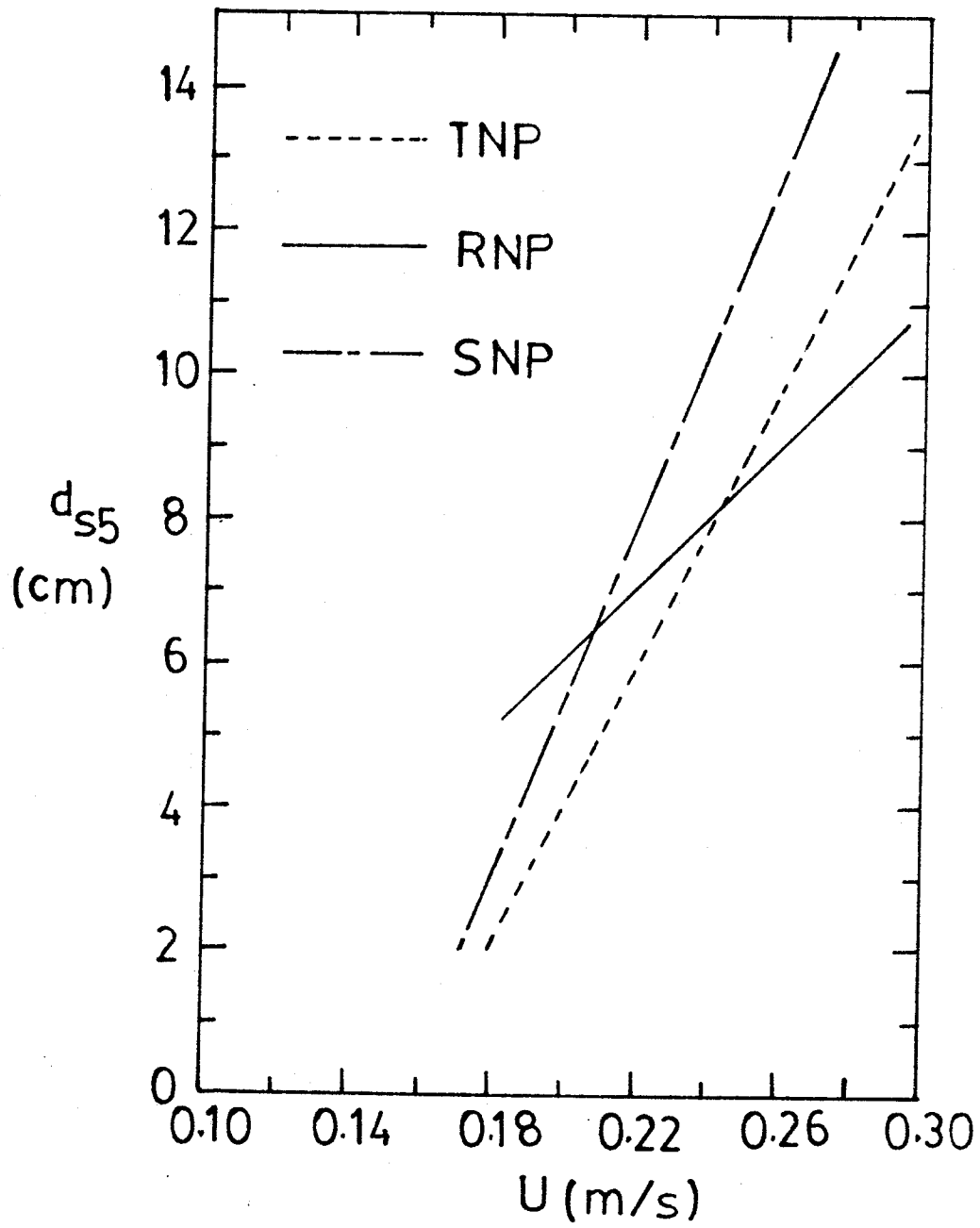


Fig. 7.9(c). Comparison of the Linear Regression Lines for the Different Pier Shapes: 5-Hour Scour Depth

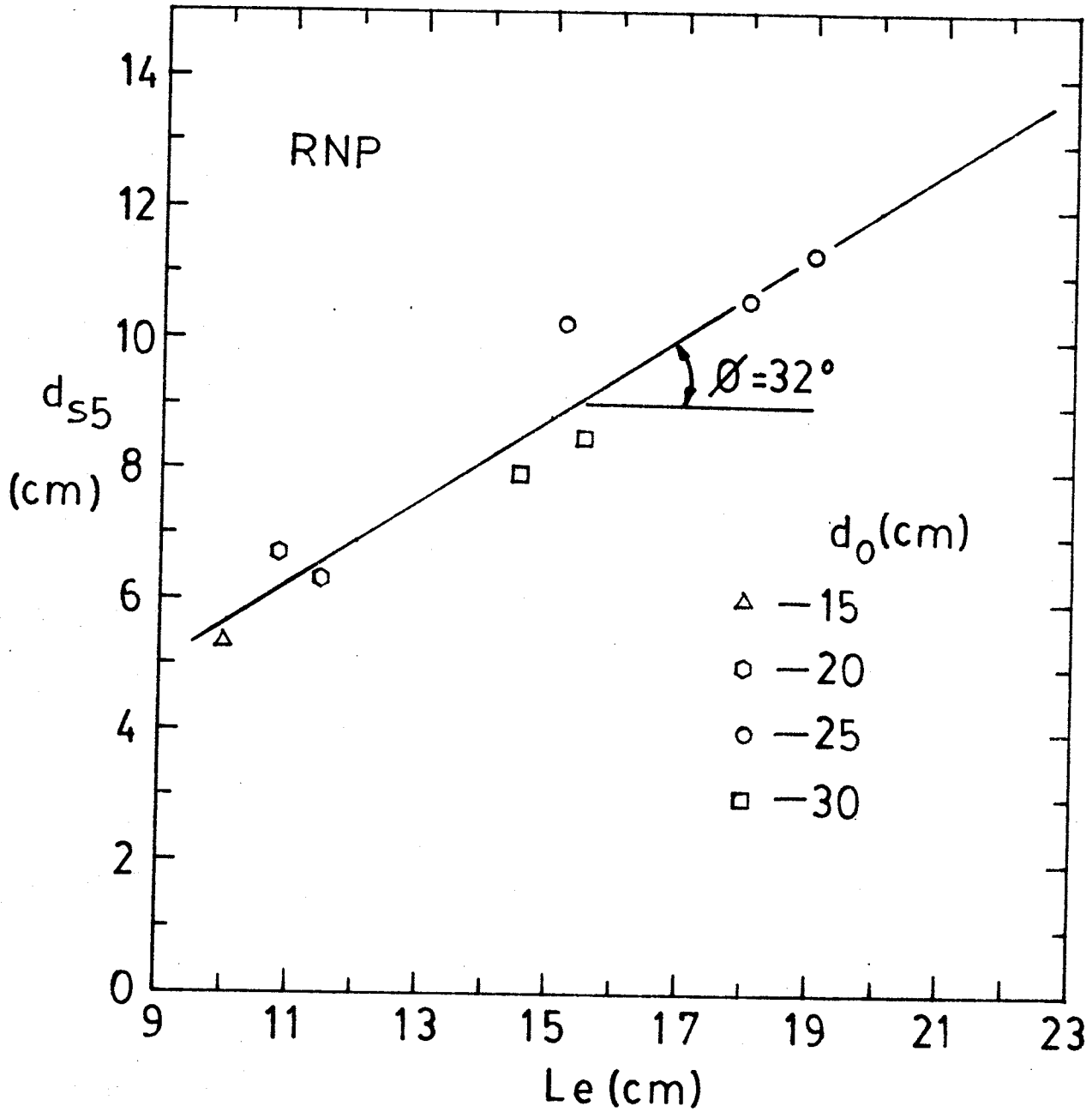


Fig. 7.10(a). 5-Hour Scour Depth Versus the Longitudinal Extent of Scour: Round-Nosed Pier

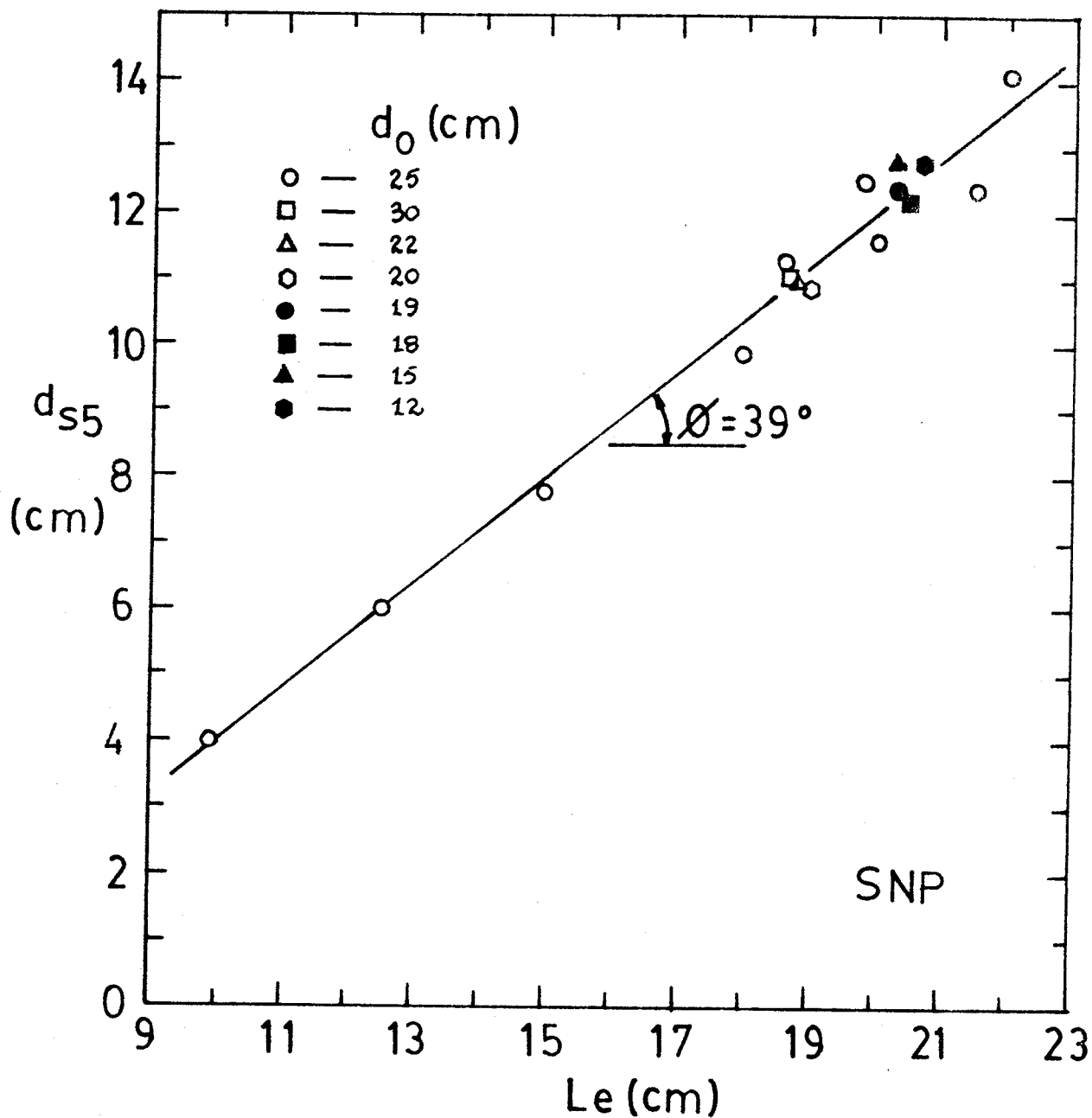


Fig. 7.10(b). 5-Hour Scour Depth Versus the Longitudinal Extent of Scour: Square-Nosed Pier

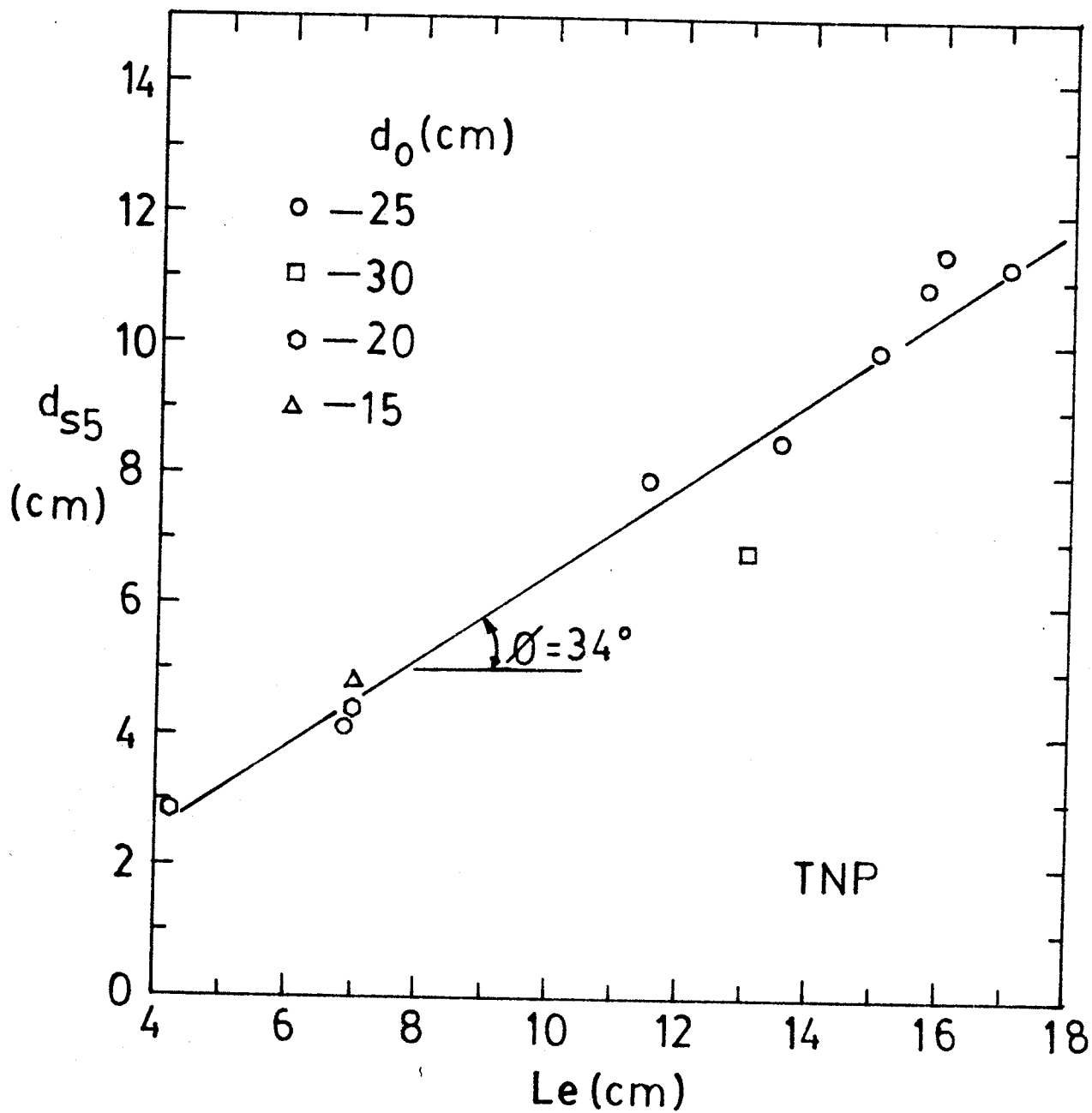
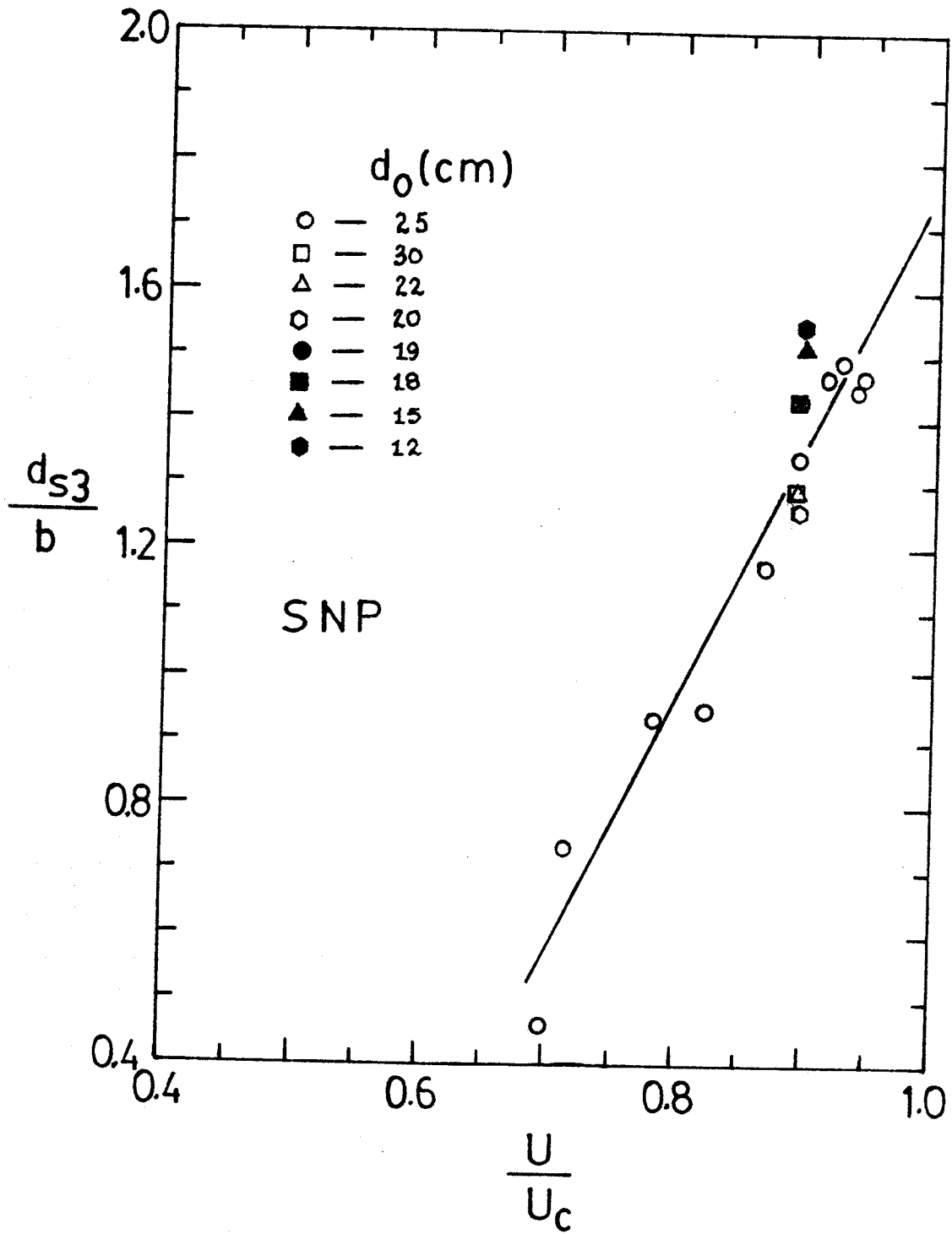


Fig. 7.10(c) 5-Hour Scour Depth Versus the Longitudinal Extent of Scour: Triangular-Nosed Pier



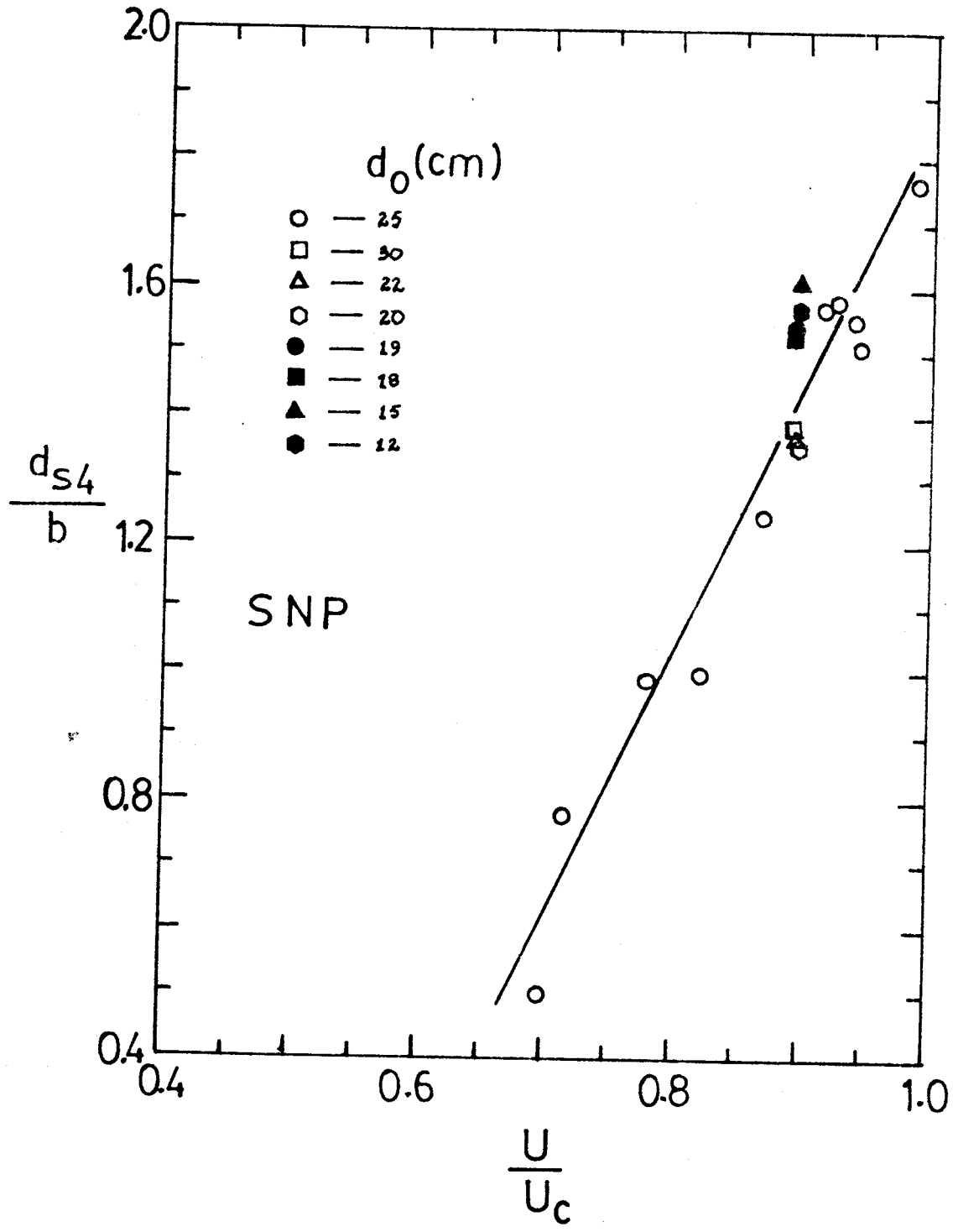


Fig. 7.11(b). Influence of the Mean Approach Flow Velocity:
4-Hour Scour Depth for the Square-Nosed Pier

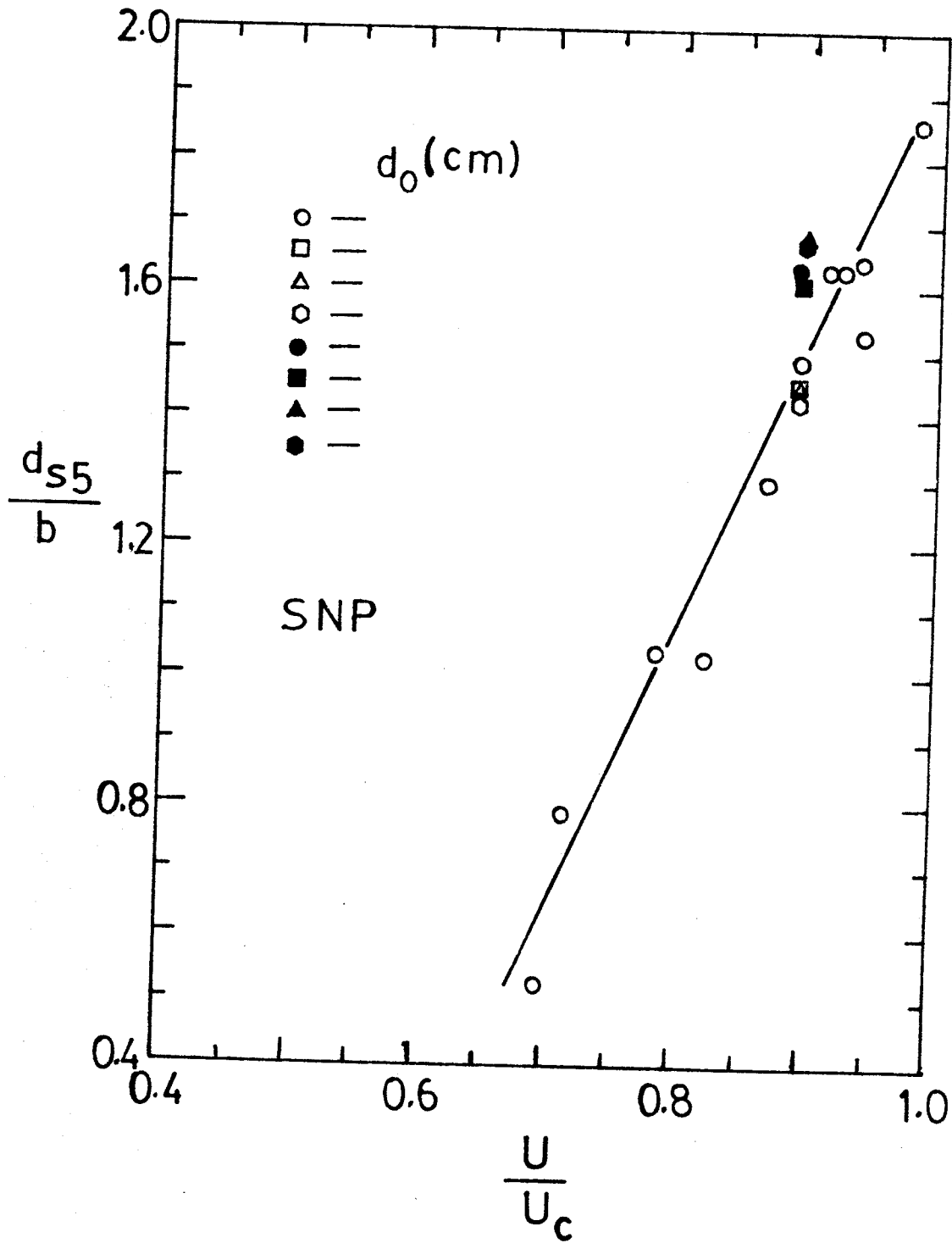


Fig. 7.11(c). Influence of the Mean Approach Flow Velocity:
5-Hour Scour Depth for the Square-Nosed Pier

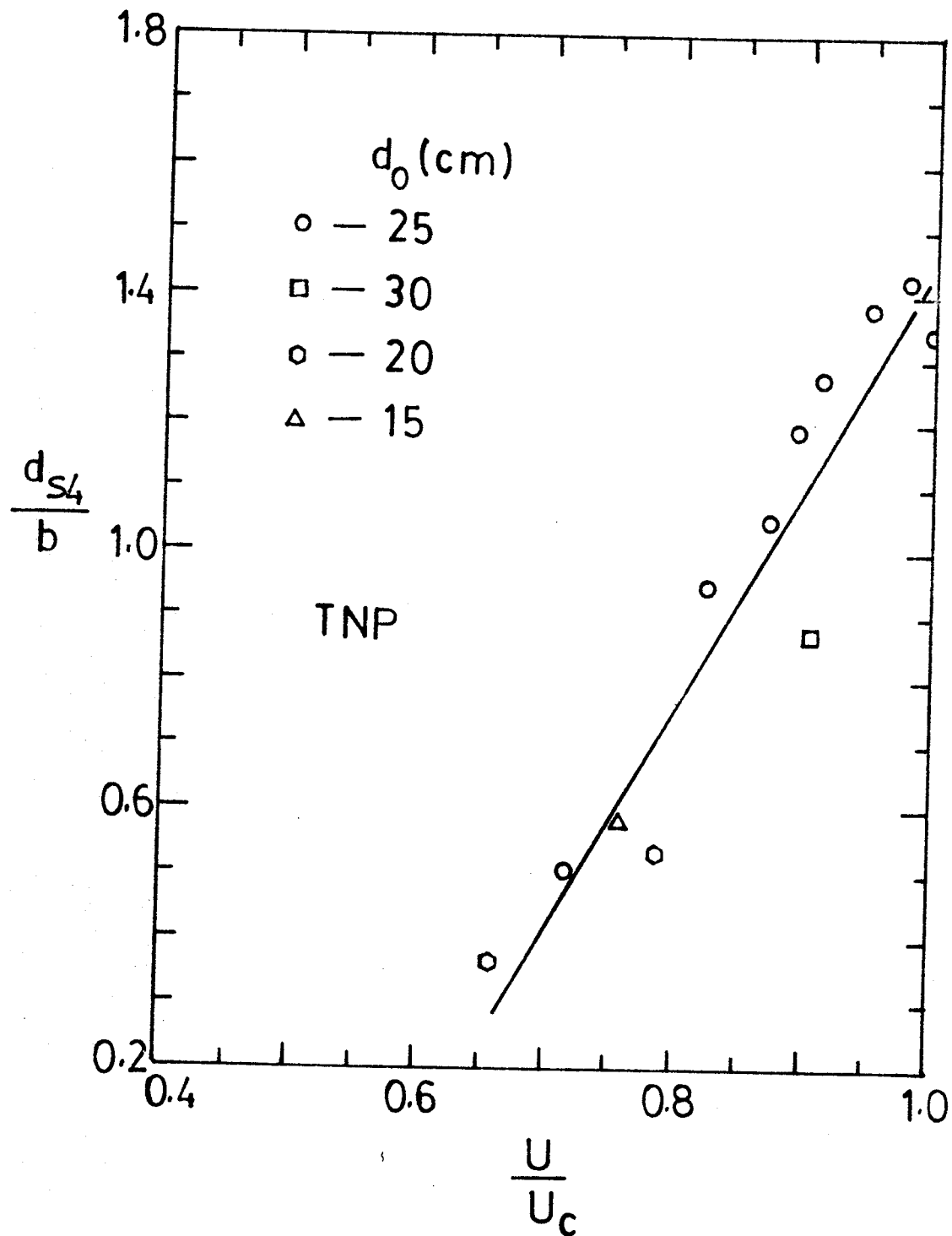


Fig. 7.12. Influence of the Mean Approach Flow Velocity:
4-Hour Scour Depth for the Triangular-Nosed Pier

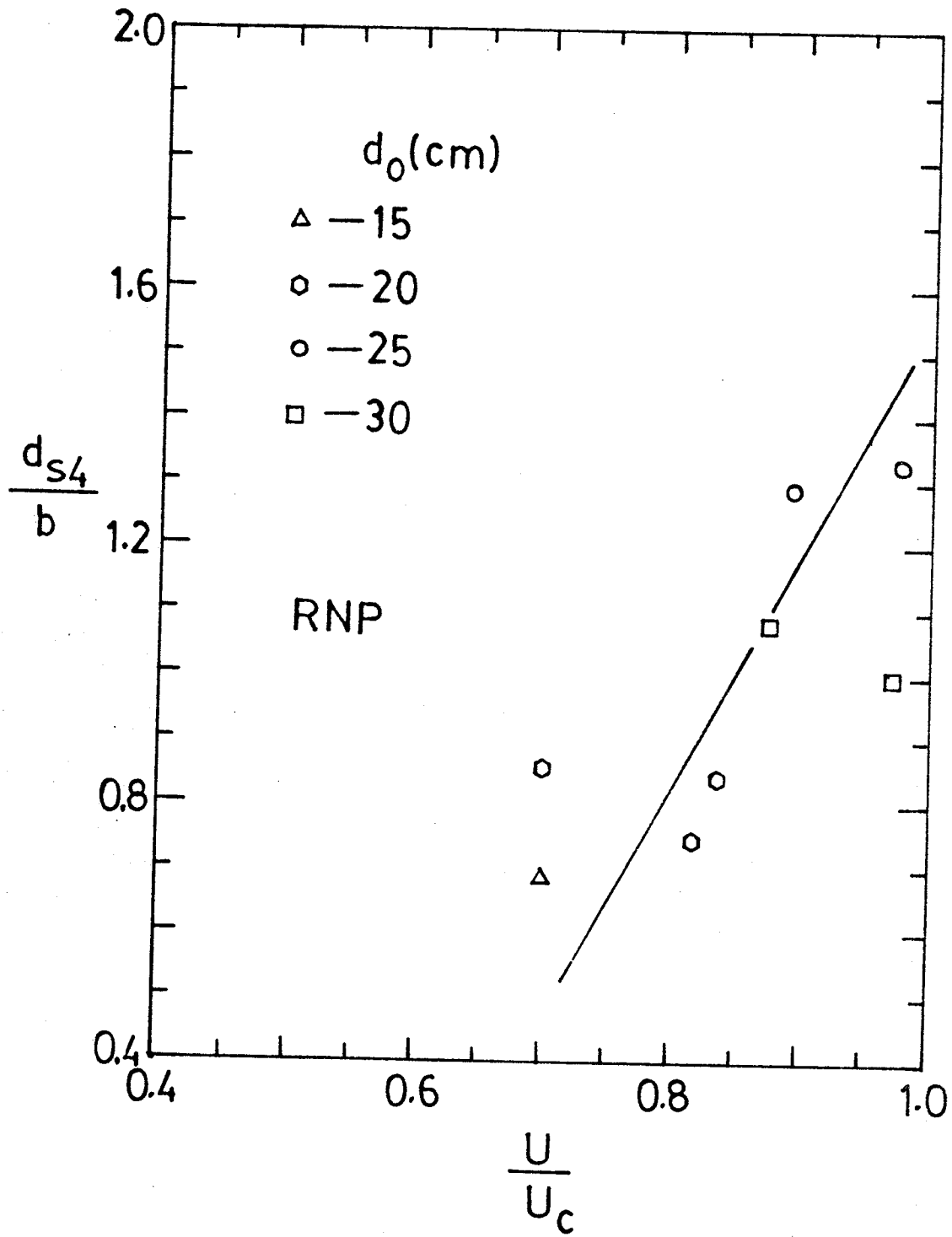


Fig. 7.13. Influence of the Mean Approach Flow Velocity:
4-Hour Scour Depth for the Round-Nosed Pier

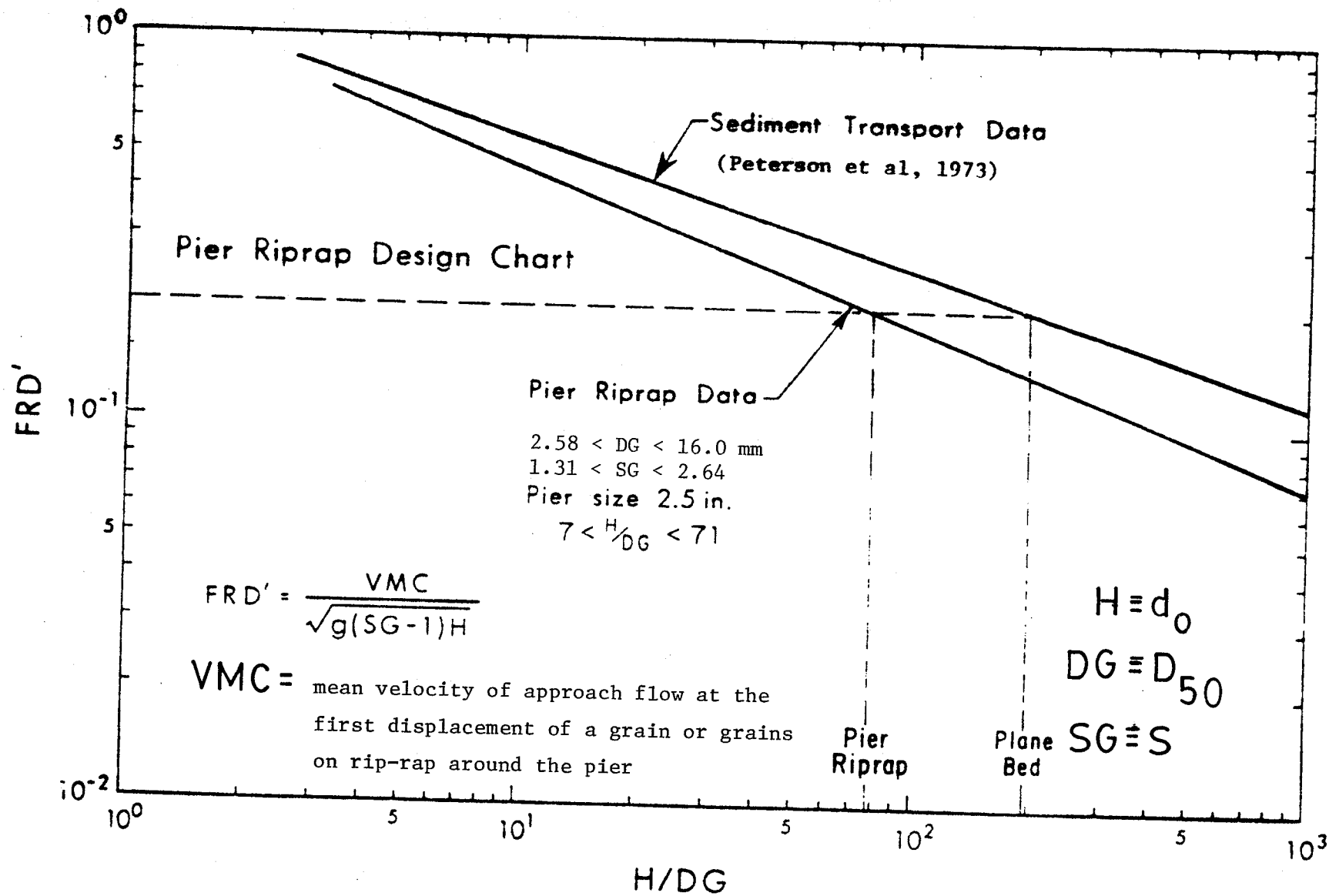


Fig. 8.1. Recommended Design Curve for Pier Rip-Rap (After Quazi and Peterson, 1973)

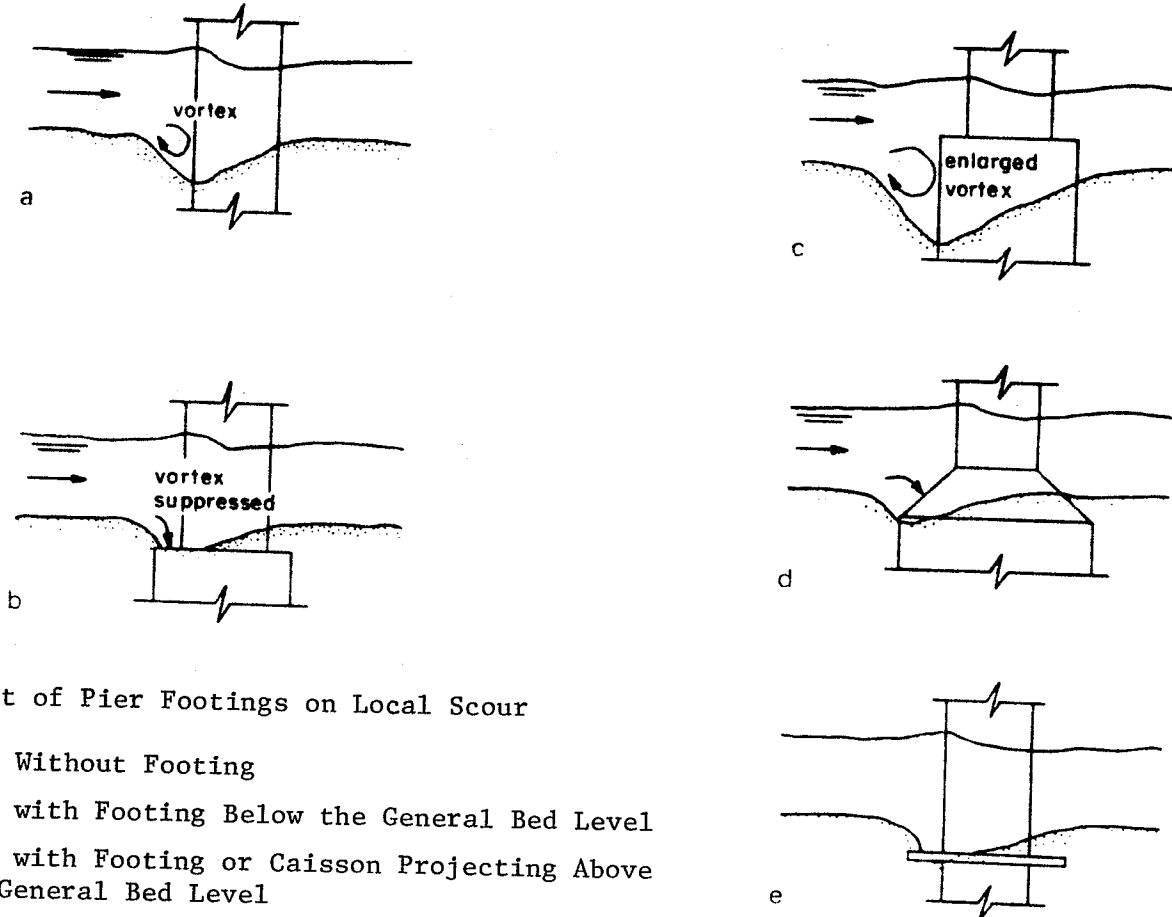


Fig. 8.2. The Effect of Pier Footings on Local Scour

- (a) Pier Without Footing
- (b) Pier with Footing Below the General Bed Level
- (c) Pier with Footing or Caisson Projecting Above the General Bed Level
- (d) Pier with Conical Transition Between Shaft and Footing
- (e) Collar Instead of Footing

(After Neill, 1973)

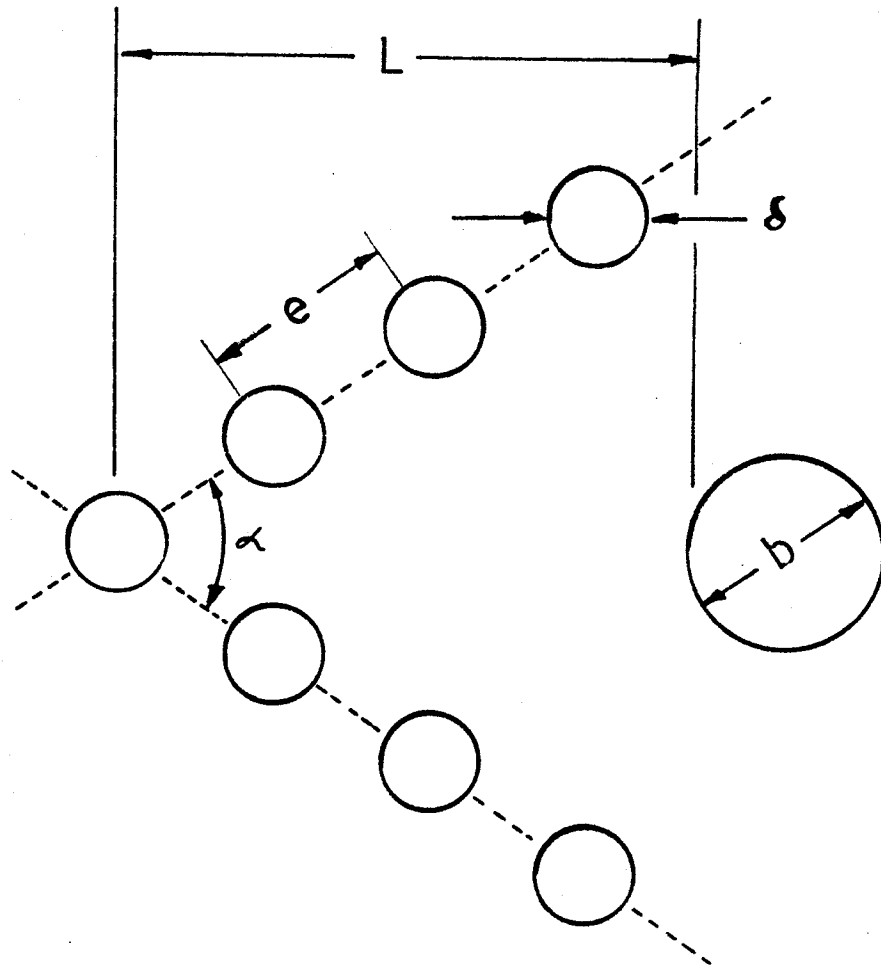


Fig. 8.3. Piles Placed Upstream of Pier
(After Breusers et al, 1977)

APPENDIX B

TABLES

TABLE 7.1 SUMMARY OF COLLECTED DATA FOR THE ROUND-NOSED PIER

(Note: $b = 0.076\text{m}$, $U_c = 0.280\text{m/s}$)

TEST No.	d_0 (m)	$\frac{d_0}{b}$	U (m/s)	ρ (kg/m^3)	$v \times 10^6$ (m^2/s)	d_{s3} (m)	d_{s4} (m)	d_{s5} (m)	Le (m)	$\frac{U}{U_c}$	$\frac{d_{s3}}{b}$	$\frac{d_{s4}}{b}$	$\frac{d_{s5}}{b}$	Fr $(\frac{U}{\sqrt{gd_0}})$	ϕ
RN004	0.20	2.63	0.196	997	1.03	0.063	0.065	0.067	0.108	0.700	0.829	0.855	0.882	0.140	41°
RN010	0.15	1.97	0.196	997	0.969	0.050	0.052	0.053	0.100	0.700	0.658	0.684	0.697	0.162	41°
RN001	0.20	2.63	0.209	997	1.03	0.061	0.062	0.063	0.115	0.746	0.803	0.816	0.829	0.149	-
RN002*	0.20	2.63	0.235	997	1.05	0.062	0.064	0.065	0.110	0.839	0.816	0.842	0.855	0.168	41°
RN009	0.30	3.95	0.245	997	0.969	0.079	0.082	0.085	0.155	0.875	1.04	1.08	1.12	0.143	37°
RN003**	0.20	2.63	0.246	997	0.992	0.066	-	-	0.100	0.879	0.868	-	-	0.176	39°
RN011	0.25	3.29	0.250	997	0.945	0.093	0.097	0.102	0.152	0.893	1.22	1.28	1.34	0.160	-
RN008	0.30	3.95	0.272	997	0.976	0.071	0.076	0.079	0.145	0.971	0.934	1.00	1.04	0.159	-
RN006	0.25	3.29	0.273	997	0.992	0.095	0.101	0.106	0.180	0.975	1.25	1.33	1.39	0.174	-
RN005†	0.20	2.63	0.316	997	1.00	0.115	0.119	0.121	0.185	1.13	1.51	1.57	1.59	0.226	41°

* 6-Hour Run

** 3-Hour Run

†5.5-Hour Run and $U > U_c$

TABLE 7.2 SUMMARY OF COLLECTED DATA FOR THE SQUARE-NOSED PIER

(Note: $b = 0.076\text{m}$, $U_c = 0.280\text{m/s}$)

TEST No.	d_0 (m)	$\frac{d_0}{b}$	U (m/s)	ρ (kg/m^3)	$v \times 10^6$ (m^2/s)	d_{s3} (m)	d_{s4} (m)	d_{s5} (m)	Le (m)	$\frac{U}{U_c}$	$\frac{d_{s3}}{b}$	$\frac{d_{s4}}{b}$	$\frac{d_{s5}}{b}$	Fr $(\frac{U}{\sqrt{gd_0}})$	ϕ
SN004	0.25	3.29	0.195	996	0.953	0.035	0.038	0.040	0.099	0.696	0.461	0.500	0.526	0.124	39°
SN010	0.25	3.29	0.200	996	0.937	0.056	0.059	0.060	0.125	0.714	0.737	0.776	0.789	0.128	39°
SN006*	0.25	3.29	0.219	996	0.937	0.071	0.075	0.079	0.165	0.782	0.934	0.987	1.04	0.140	37°
SN002	0.25	3.29	0.230	997	0.945	0.072	0.076	0.078	0.150	0.821	0.947	1.00	1.03	0.147	40°
SN007	0.25	3.29	0.243	997	0.937	0.089	0.094	0.099	0.180	0.867	1.17	1.24	1.30	0.155	39°
SN013	0.30	3.95	0.250	996	0.929	0.098	0.105	0.110	0.187	0.893	1.29	1.38	1.45	0.145	-
SN012	0.25	3.29	0.250	996	0.937	0.102	0.107	0.113	0.186	0.893	1.34	1.41	1.49	0.160	40°
SN018	0.22	2.89	0.250	996	0.945	0.098	0.104	0.110	0.188	0.893	1.29	1.37	1.45	0.170	-
SN014	0.20	2.63	0.250	996	0.921	0.096	0.103	0.109	0.190	0.893	1.26	1.36	1.43	0.178	37°
SN019	0.19	2.50	0.250	996	0.945	0.109	0.117	0.124	0.203	0.893	1.43	1.54	1.63	0.183	40°

* 7-Hour Run

Continued...

(continued)

TABLE 7.2 SUMMARY OF COLLECTED DATA FOR THE SQUARE-NOSED PIER

(Note: $b = 0.076\text{m}$, $U_c = 0.280\text{m/s}$)

TEST No.	d_0 (m)	$\frac{d_0}{b}$	U (m/s)	ρ (kg/m^3)	$v \times 10^6$ (m^2/s)	d_{s3} (m)	d_{s4} (m)	d_{s5} (m)	Le (m)	$\frac{U}{U_c}$	$\frac{d_{s3}}{b}$	$\frac{d_{s4}}{b}$	$\frac{d_{s5}}{b}$	Fr $(\frac{U}{\sqrt{gb_0}})$	ϕ
SN017	0.18	2.37	0.250	996	0.921	0.109	0.116	0.122	0.205	0.893	1.43	1.53	1.61	0.188	40°
SN015	0.15	1.97	0.251	996	0.929	0.115	0.122	0.128	0.203	0.896	1.51	1.61	1.68	0.207	43°
SN016	0.12	1.58	0.251	996	0.921	0.118	0.119	0.128	0.207	0.896	1.55	1.57	1.68	0.231	-
SN011*	0.25	3.29	0.256	996	0.953	0.112	0.119	0.124	0.220	0.914	1.47	1.57	1.63	0.163	39°
SN009	0.25	3.29	0.259	996	0.945	0.113	0.120	0.124	0.215	0.925	1.49	1.58	1.63	0.165	38°
SN005	0.25	3.29	0.263	996	0.945	0.110	0.118	0.125	0.198	0.939	1.45	1.55	1.64	0.168	-
SN003	0.25	3.29	0.264	997	0.969	0.112	0.115	0.116	0.200	0.943	1.47	1.51	1.53	0.169	39°
SN008	0.25	3.29	0.276	997	0.945	0.125	0.134	0.141	0.220	0.986	1.64	1.76	1.86	0.176	44°

* 7-Hour Run

TABLE 7.3 SUMMARY OF COLLECTED DATA FOR THE TRIANGULAR-NOSED PIER
 (Note: $b = 0.077\text{m}$, $U_c = 0.280\text{m/s}$)

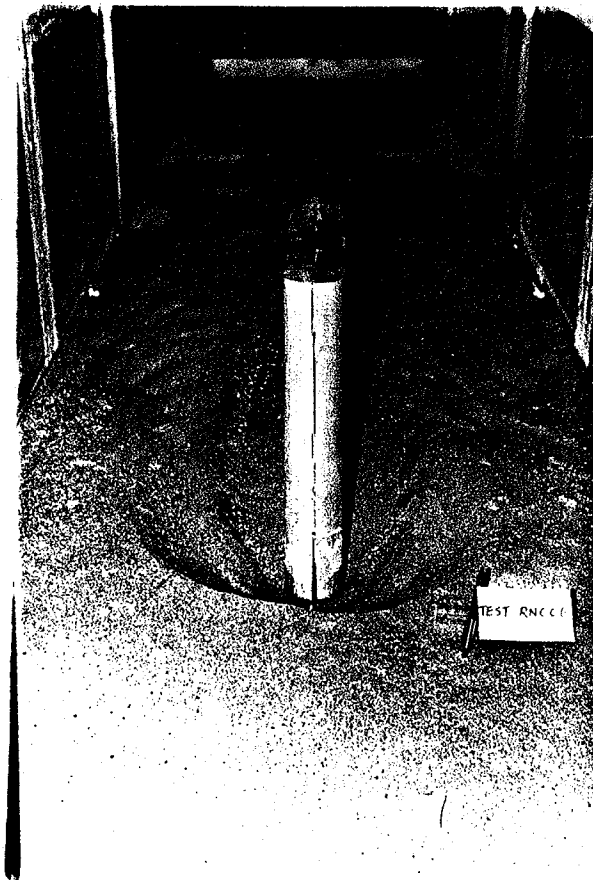
TEST No.	d_0 (m)	$\frac{d_0}{b}$	U (m/s)	ρ (kg/m^3)	$v \times 10^6$ (m^2/s)	d_{s3} (m)	d_{s4} (m)	d_{s5} (m)	Le (m)	$\frac{U}{U_c}$	$\frac{d_{s3}}{b}$	$\frac{d_{s4}}{b}$	$\frac{d_{s5}}{b}$	Fr ($\frac{U}{\sqrt{g d_0}}$)	ϕ
TN007	0.20	2.60	0.184	997	0.976	0.026	0.028	0.029	0.042	0.657	0.338	0.364	0.377	0.131	43°
TN013	0.25	3.25	0.200	996	0.921	0.036	0.039	0.041	0.068	0.714	0.468	0.506	0.532	0.128	-
TN001	0.15	1.95	0.212	997	1.00	0.041	0.045	0.048	0.070	0.757	0.532	0.584	0.623	0.175	37°
TN003	0.20	2.60	0.220	997	0.969	0.037	0.041	0.044	0.070	0.786	0.481	0.532	0.571	0.157	39°
TN010	0.25	3.25	0.230	997	0.937	0.068	0.073	0.079	0.115	0.821	0.883	0.948	1.03	0.147	37°
TN008	0.25	3.25	0.244	996	0.937	0.076	0.081	0.085	0.135	0.871	0.987	1.05	1.10	0.156	33°
TN012	0.25	3.25	0.250	996	0.929	0.083	0.092	0.099	0.150	0.893	1.08	1.19	1.29	0.160	-
TN002	0.30	3.90	0.253	997	0.976	0.064	0.067	0.068	0.130	0.904	0.831	0.870	0.883	0.147	39°
TN011*	0.25	3.25	0.255	996	0.937	0.091	0.098	0.106	-	0.911	1.18	1.27	1.38	0.163	37°
TN009	0.25	3.25	0.266	996	0.945	0.099	0.106	0.109	0.157	0.950	1.29	1.38	1.42	0.170	37°
TN006	0.25	3.25	0.274	997	0.984	0.103	0.109	0.114	0.160	0.978	1.34	1.42	1.48	0.175	39°
TN005	0.25	3.25	0.280	997	0.969	0.097	0.103	0.107	0.170	1.00	1.26	1.34	1.39	0.179	34°

* 7-Hour Run

APPENDIX C

PLATES

(a)



(b)

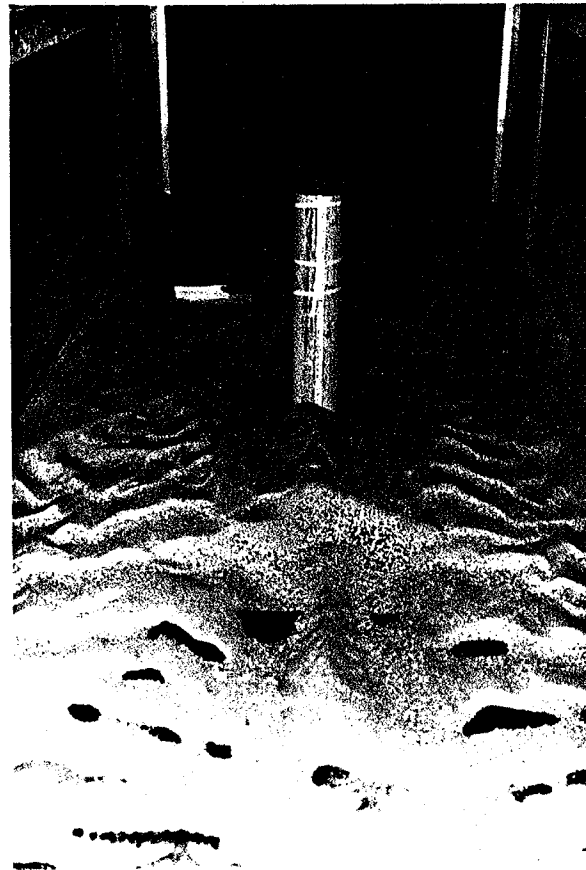
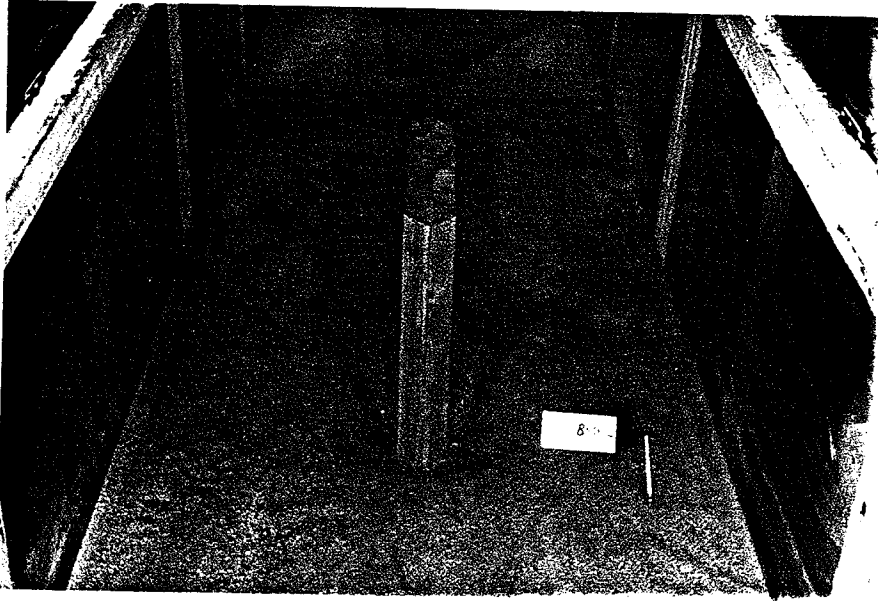
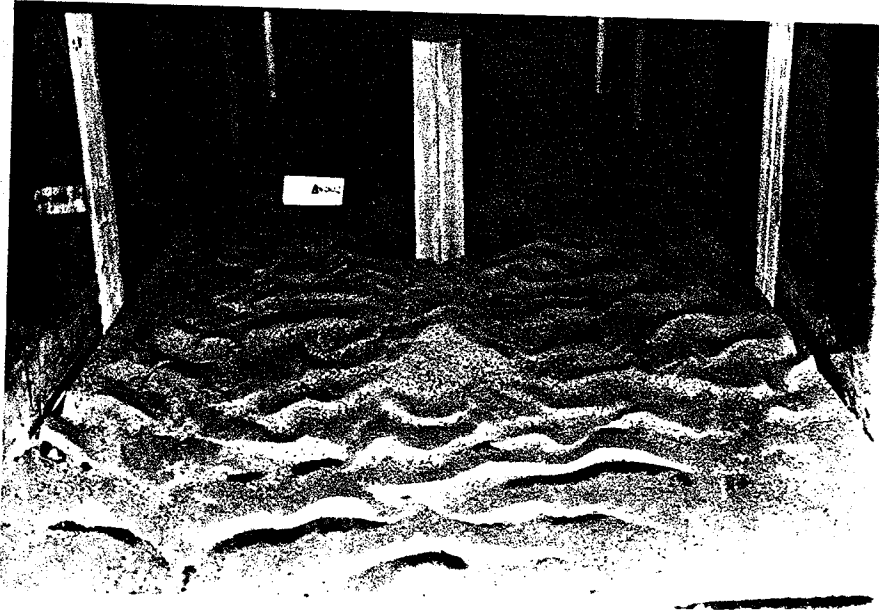


Plate 1. Views of the Scour Pattern (Test RN006)

(a) From Upstream (b) From Downstream



(a)



(b)



(c)

Plate 2. Views of the Scour Pattern (Test TN002)

- (a) From Upstream
- (b) From Downstream
- (c) Longitudinal Profile